



University of Kentucky  
**UKnowledge**

---

KWRRI Research Reports

Kentucky Water Resources Research Institute

---

8-1974


# Spatially Varied Subcritical and Supercritical Flow in Gullies

Digital Object Identifier: <https://doi.org/10.13023/kwrri.rr.74>

T. Y. Kao  
*University of Kentucky*

**Right click to open a feedback form in a new tab to let us know how this document benefits you.**

Follow this and additional works at: [https://uknowledge.uky.edu/kwrri\\_reports](https://uknowledge.uky.edu/kwrri_reports)

 Part of the [Earth Sciences Commons](#), and the [Environmental Sciences Commons](#)

---

## Repository Citation

Kao, T. Y., "Spatially Varied Subcritical and Supercritical Flow in Gullies" (1974). *KWRRI Research Reports*. 122.  
[https://uknowledge.uky.edu/kwrri\\_reports/122](https://uknowledge.uky.edu/kwrri_reports/122)

This Report is brought to you for free and open access by the Kentucky Water Resources Research Institute at UKnowledge. It has been accepted for inclusion in KWRRI Research Reports by an authorized administrator of UKnowledge. For more information, please contact [UKnowledge@lsv.uky.edu](mailto:UKnowledge@lsv.uky.edu).

Research Report No.

SPATIALLY VARIED SUBCRITICAL AND SUPERCRITICAL  
FLOW IN GULLIES

By

T.Y. Kao  
Principal Investigator

Project Number A-037-KY (Partial Completion Report)

Agreement Numbers: 14-31-0001-3517 (FY 1971)

14-31-0001-3817 (FY 1972)

Period of Project: August, 1971 - June, 1973

University of Kentucky Water Resources Institute  
Lexington, Kentucky

The work upon which this report is based was supported in part by funds provided by the United States Department of the Interior, Office of Water Resources Research, as authorized under the Water Resources Research Act of 1964

August 1974  
~~May 2, 1974~~

## ABSTRACT

The objective of this study was to investigate the phenomena of subcritical and supercritical spatially varied flow in rectangular expansions such as that in an erosion gully. Based on momentum and continuity principles, equations were developed to predict such flow phenomena. Computations of the water surface profiles for subcritical spatially varied flow were carried out by applying direct step numerical calculations. Because of the presence of standing waves, the method of characteristics was employed in the analytical analysis of the supercritical flow phenomena. Of primary importance in this study is the effect of varying amounts of lateral inflow rates. Other parameters varied during the experimental tests were the slope of the channel and the main channel discharge. Comparison of the analytical and experimental results indicated that for both subcritical and supercritical spatially varied flow, water surface profiles can be predicted with good accuracy.

---

KEY WORDS: open channel flow, transition flow, gullies flow, subcritical flow, supercritical flow, spatially varied flow, standing waves, method of characteristics

# TABLE OF CONTENTS

	Page
ACKNOWLEDGEMENTS . . . . .	iii
LIST OF FIGURES. . . . .	v
LIST OF TABLES . . . . .	vii
CHAPTER	
I INTRODUCTION. . . . .	1
Review of Previous Work . . . . .	2
Scope of the Present Study . . . . .	4
II ANALYTICAL ANALYSIS . . . . .	5
Dynamic Equation for Subcritical Spatially Varied Flow . . . . .	5
Theoretical Analysis for Supercritical Spatially Varied Flow . . . . .	10
Determination of Boundary Shear in Open Channel Flumes . . . . .	29
III EXPERIMENTAL FACILITY . . . . .	31
IV EXPERIMENTAL PROCEDURE. . . . .	38
V DATA ANALYSIS AND PRESENTATION. . . . .	40
Analysis of Subcritical Spatially Varied Flow . . . . .	40
Analysis of Supercritical Spatially Varied Flow . . . . .	42
VI CONCLUSIONS . . . . .	72
APPENDIX	
I REFERENCES. . . . .	75
II NOTATION. . . . .	77
III DIGITAL COMPUTER PROGRAMS . . . . .	79

# LIST OF FIGURES

Figure		Page
1	Definition Sketches for Subcritical Flow . .	6
2	Definition Sketches for Supercritical Flow. . . . .	12
3	Wave Pattern and Characteristic Curves for Supercritical Flow. . . . .	19
4	Main Channel with Experimental Converging - Diverging Apparatus . . . . .	32
5	Experimental Apparatus . . . . .	33
6	Uniform Lateral Inflow Plexiglas Flume . . .	36
7	Relationship Between Depth and Downstream Distance for Subcritical Flow; $Q = 0.368$ cfs . . . . .	47
8	Dimensionless Relationship Between Depth and Downstream Distance for Subcritical Flow; $Q = 0.368$ cfs . . . . .	48
9	Relationship Between Depth and Downstream Distance for Subcritical Flow; $Q = 0.211$ cfs . . . . .	49
10	Dimensionless Relationship Between Depth and Downstream Distance for Subcritical Flow; $Q = 0.211$ cfs . . . . .	50
11	Typical Cross Waves of Supercritical Spatially Varied Flow . . . . .	51
12	Relationship Between Depth and Downstream Distance for Supercritical Flow; $Q = 0.3632$ cfs, $S_o = 1\%$ . . . . .	64
13	Cross Wave Patterns for Supercritical Flow; $Q = 0.3632$ cfs, $S_o = 1\%$ . . . . .	65
14	Relationship Between Depth and Downstream Distance for Supercritical Flow; $Q = 0.3632$ cfs, $S_o = 4\%$ . . . . .	66

Figure		Page
15	Cross Wave Patterns for Supercritical Flow; $Q = 0.3632$ cfs, $S_o = 4\%$ . . . . .	67
16	Relationship Between Depth and Downstream Distance for Supercritical Flow; $Q = 0.1967$ cfs, $S_o = 1\%$ . . . . .	68
17	Cross Wave Patterns for Supercritical Flow; $Q = 0.1967$ cfs, $S_o = 1\%$ . . . . .	69
18	Cross Wave Patterns for Supercritical Flow; $Q = 0.1967$ cfs, $S_o = 4\%$ . . . . .	70
19	Cross Wave Patterns for Supercritical Flow; $Q = 0.1967$ cfs, $S_o = 4\%$ . . . . .	71
A-1	Flow Chart for Computer Program for Subcritical Flow. . . . .	80
A-2	Computer Program for Subcritical Flow. . . . .	81
A-3	Flow Chart for Computer Program for Supercritical Flow . . . . .	86
A-4	Computer Program for Supercritical Flow. . . . .	89

# LIST OF TABLES

Table		Page
I	Analytical Results for Subcritical Flow; $Q = 0.368$ cfs. . . . .	45
II	Analytical Results for Subcritical Flow; $Q = 0.211$ cfs. . . . .	46
III	Analytical Results for Supercritical Flow; $Q = 0.3632$ cfs, $q_* = 0.0$ cfs/ft, $S_o = 1\%$ . . . . .	52
IV	Analytical Results for Supercritical Flow; $Q = 0.3632$ cfs, $q_* = 0.0125$ cfs/ft, $S_o = 1\%$ . . . . .	53
V	Analytical Results for Supercritical Flow; $Q = 0.3632$ cfs, $q_* = 0.0236$ cfs/ft $S_o = 1\%$ . . . . .	54
VI	Analytical Results for Supercritical Flow; $Q = 0.3632$ cfs, $q_* = 0.0$ cfs/ft, $S_o = 4\%$ . . . . .	55
VII	Analytical Results for Supercritical Flow; $Q = 0.3632$ cfs, $q_* = 0.0125$ cfs/ft, $S_o = 4\%$ . . . . .	56
VIII	Analytical Results for Supercritical Flow; $Q = 0.3632$ cfs, $q_* = 0.0236$ cfs/ft, $S_o = 4\%$ . . . . .	57
IX	Analytical Results for Supercritical Flow; $Q = 0.1967$ cfs, $q_* = 0.0$ , $S_o = 1\%$ . . . . .	58
X	Analytical Results for Supercritical Flow; $Q = 0.1967$ cfs, $q_* = 0.0125$ cfs/ft, $S_o = 1\%$ . . . . .	59
XI	Analytical Results for Supercritical Flow; $Q = 0.1967$ cfs, $q_* = 0.0236$ cfs/ft, $S_o = 1\%$ . . . . .	60
XII	Analytical Results for Supercritical Flow; $Q = 0.1967$ cfs, $q_* = 0.0$ cfs/ft, $S_o = 4\%$ . . . . .	61

Table		Page
XIII	Analytical Results for Supercritical Flow; $Q = 0.1967$ cfs, $q_* = 0.0125$ cfs/ft, $S_o = 4\%$ . . . . .	62
XIV	Analytical Results for Supercritical Flow; $Q = 0.1967$ cfs, $q_* = 0.0236$ cfs/ft, $S_o = 4\%$ . . . . .	63



## CHAPTER I

### INTRODUCTION

Spatially varied or discontinuous flow can be defined as flow in which the discharge varies in the flow direction. There are basically two forms of spatially varied flow: flow with decreasing discharge and flow with increasing discharge.

Spatially varied flow with increasing discharge occurs in such places as side-channel spillways of dams; wash-water troughs in water and sewage treatment plants; and overland flow into rain gutters or gullies. In the case of a rain gully, not only is there increasing discharge, but the width also increases as the flow moves downstream.

A channel, whether artificial or natural, seldom has a straight, horizontal alignment. Most channels may vary in cross section as well as slope. Channel expansion occurs frequently at places where the flow emerges from a closed conduit, sluice gate, spillway or steep chute. Thus, the ability to predict accurately the profile of spatially varied flow in a channel expansion is of considerable importance.

## REVIEW OF PREVIOUS WORK

One of the first substantially correct differential equations describing spatially varied flow was established by Hinds (1) in 1926. His study dealt with the design of side-channel spillways. In his analysis, Hinds neglected the momentum due to the lateral inflow and the effect of friction. Favre (2) included a friction term in a similar study. In 1940, Camp (3) investigated rectangular channels with uniform lateral inflow. His main objective was analyzing lateral spillway channels as found in water and sewage treatment plants. Camp's equation is the same as Hinds' except for the inclusion of a friction term. Camp expressed the frictional resistance in terms of the Weisbach-Darcy friction factor,  $f$ . Li (4) obtained solutions for prismatic channels of various cross sections and slopes. He described the effect of friction in terms of the Chezy coefficient,  $C$ .

Yen and Wenzel (5) developed equations for steady spatially varied flow. These equations resulted from both momentum and energy approaches. In their study only channels with straight, horizontal alignment and longitudinally uniform cross section were considered.

A study dealing with supercritical flow passing through transitions was conducted by Ippen (6) in 1951. When the boundary alignment along the side walls is gradual,

small changes in depth resulted. For this reason Ippen neglected vertical acceleration, boundary - layer influences and nonuniformities in the velocity and pressure distributions. An analysis similar to Ippen's was made by Harrison (7). His analysis applied to the design of channels with a trapezoidal cross section.

The energy loss in a sudden expansion can be reduced by gradually enlarging the channel section or decreasing the angle of divergence (8). Rouse, Bhoota and Hsu (9) investigated high-velocity flow in abrupt and gradual expansions. The diverging section must be gradual enough to avoid separation at the entrance to the section. In order to eliminate a long diverging section, they suggested a continuous change in curvature which would allow the section to be shorter and reduce the chances of separation. Studies by Hom-ma and Shima (10) further indicate that separation may occur if an expansion is made to diverge too rapidly.

Standing waves are present in both subcritical and supercritical flow. Supercritical flow presents a problem because of the surface waves that appear as a consequence of the geometry of the lateral boundaries. In a symposium on high-velocity flow, Knapp (11) pointed out the presence of standing waves created in curved channels. Bagge and Herbich (12) analyzed, by using the method of characteristics, supercritical flow in a rectangular expansion.

They assumed frictionless flow and hydrostatic pressure distribution. Later, Herbich and Walsh (13) tested the equations of Bagge and Herbich for validity. They found the predicted profiles were generally lower than those measured, and attributed this to the neglect of friction. The United States Soil Conservation Service (14) has also made tests on supercritical flow through expansions in conjunction with the SAF stilling basin. The tests were made on transitions with straight flaring side walls and one percent channel slope.

#### SCOPE OF THE PRESENT STUDY

In this study subcritical and supercritical spatially varied transitional flow in a rectangular expansion is investigated. The lateral inflow is in the form of uniform sheet flow along the entire length of the diverging test section. Of primary importance are the effects of varying amounts of lateral inflow. The experimental results for both types of flow are compared with analytical solutions. Because of the high energy loss at the point of impact of the lateral inflow and the main flow, the momentum approach is utilized in the analysis rather than the energy approach.

CHAPTER II  
ANALYTICAL ANALYSIS

DYNAMIC EQUATION FOR SUBCRITICAL SPATIALLY VARIED FLOW

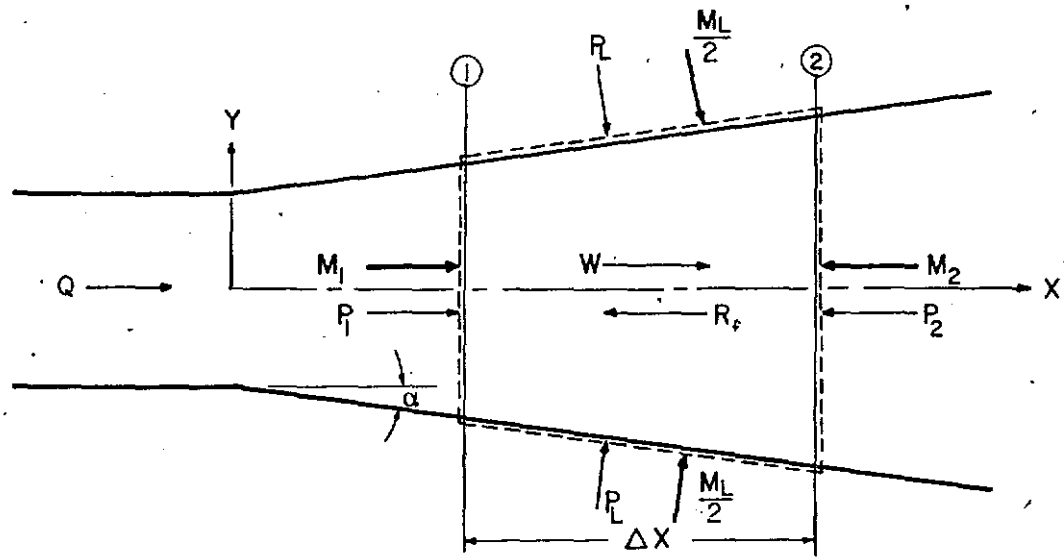
By use of momentum principles, an expression for the change in water depth with respect to distance is determined.

The depth,  $d$ , of the flow section is measured normal to the channel floor, which makes an angle  $\theta$  with the horizontal. Therefore, the channel slope,  $S_o$ , equals the tangent of the angle  $\theta$ . The lateral inflow,  $q_*$ , is defined as the uniform volumetric inflow per unit time per unit length along the sidewall. At the point where the lateral inflow joins the main flow,  $q_*$  has a velocity  $U$  which makes an angle  $\phi$  with the flow direction. In the case of vertical lateral inflow,  $\phi$  equals  $(\frac{\pi}{2} - \theta)$ .

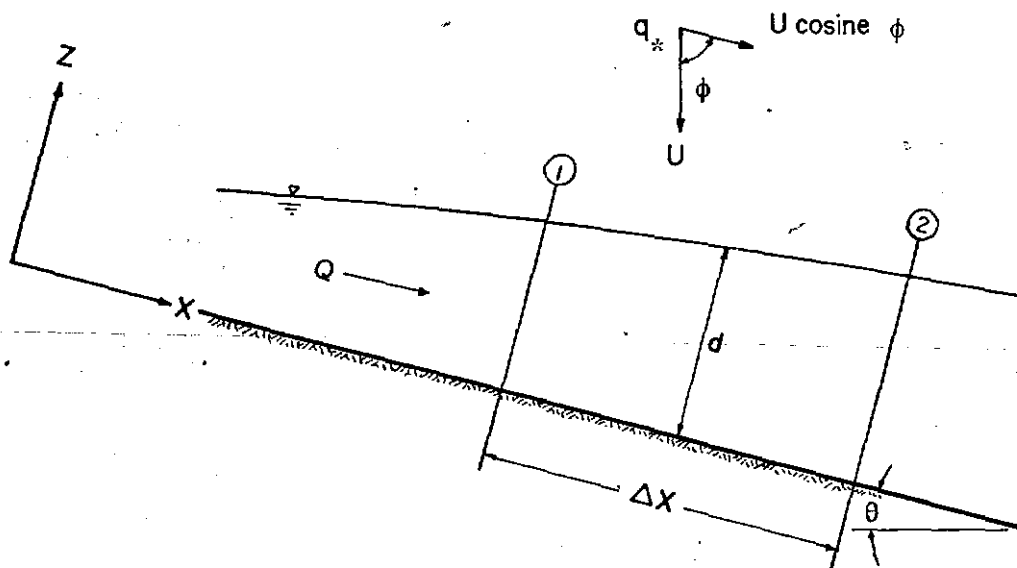
For the element of fluid between sections 1 and 2, as shown in Fig. 1 the summation of forces in the x-direction, including dynamic forces, equals zero. Mathematically, this can be expressed as:

$$M_1 + P_1 + 2P_{LX} + M_{LX} + W - R_f - M_2 - P_2 = 0 \quad (1)$$

where  $M_1$  and  $M_2$  are the momenta at sections 1 and 2 (per sec) respectively,  $P_1$  and  $P_2$  are the pressure forces at sections



TOP VIEW



FRONT VIEW

Fig. 1 - Definition Sketches for Subcritical Flow

1 and 2 respectively,  $P_{LX}$  is the x-component of the pressure force acting on the sidewall,  $M_{LX}$  is the x-direction momentum flux due to the lateral inflow,  $W$  is the force due to the weight of the fluid and  $R_f$  is the boundary resistance.

The change in water depth between sections 1 and 2 is  $\Delta d = d_2 - d_1$  and the corresponding distance in the x-direction is  $\Delta x = x_2 - x_1$ , where  $x_1$  and  $x_2$  are measured along the centerline from the beginning of the diverging test section.

Substituting the values of the forces, Eq. 1 becomes:

$$\begin{aligned} & \rho \beta V_1^2 B_1 d_1 + K \gamma B_1 d_1^2 \cos \theta + 2K \gamma \left( \frac{d_1 + d_2}{2} \right) \Delta x \cos \theta \sin \alpha \\ & + \rho q_* \Delta x U \cos \phi \cos \alpha + \left( \frac{A_1 + A_2}{2} \right) \Delta x \gamma \sin \theta \\ & - \frac{1}{2} (B_1 + 2d_1 + B_2 + 2d_2) \Delta x \tau - \rho \beta V_2^2 B_2 d_2 \\ & - K \gamma B_2 d_2^2 \cos \theta = 0 \end{aligned} \quad (2)$$

in which  $\rho$  is the mass density of the fluid,  $\beta$  is the momentum flux correction factor,  $V_1$  and  $V_2$  are the mean velocities at sections 1 and 2 respectively,  $B_1$  and  $B_2$  are the widths in the y-direction at sections 1 and 2 respectively,  $K$  is the pressure correction factor,  $\gamma$  is the specific weight of the fluid,  $\alpha$  is the divergent angle,  $A_1$  and  $A_2$  are the cross sectional areas at sections 1 and 2

respectively and  $\tau$  is the x-component boundary shear stress.

Since linear expansion is considered:

$$B_2 = B_1 + 2\Delta x \tan \alpha \quad (3)$$

Neglecting all higher order differentials and combining like terms in Eq. 2 will yield:

$$\begin{aligned} & (-\rho\beta V_2^2 B_1 - 2K\gamma B_1 d_1 \cos \theta) \Delta d \\ & + (\rho q_* U \cos \phi \cos \alpha + B_1 d_1 \gamma \sin \theta + 2K\gamma d_1^2 \cos \theta (\sin \alpha - \tan \alpha) \\ & - 2\rho\beta V_2^2 d_1 \tan \alpha - B_1 \tau - 2d_1 \tau) \Delta x \\ & + \rho\beta B_1 d_1 (V_1^2 - V_2^2) = 0 \end{aligned} \quad (4)$$

The continuity equation can be written as:

$$Q_2 = A_2 V_2 = Q_1 + q_* \Delta x \cos \phi \cos \alpha \quad (5)$$

with

$$A_2 = B_2 d_2 = B_1 d_1 + B_1 \Delta d + 2d_1 \Delta x \tan \alpha \quad (6)$$

Combining Eqs. 5 and 6 gives:

---


$$V_2^2 = \frac{Q_2^2}{A_2^2} = \frac{Q_1^2 + 2Q_1 q_* \Delta x \cos \phi \cos \alpha}{B_1^2 d_1^2 + 2B_1^2 d_1 \Delta d + 4B_1 d_1^2 \Delta x \tan \alpha} \quad (7)$$

For

$$V_1^2 = \frac{Q_1^2}{A_1^2} \quad (8)$$

we have



$$v_1^2 - v_2^2 = \frac{2Q_1^2 B_1 \Delta d + 4Q_1^2 d_1 \Delta x \tan \alpha - 2Q_1 A_1 q_* \Delta x \cos \phi \cos \alpha}{A_1^2 (A_1 + 2B_1 \Delta d + 4d_1 \Delta x \tan \alpha)} \quad (9)$$

Substituting Eq. 9 into Eq. 4 yields:

$$\begin{aligned} & \left( \frac{\rho \beta Q_1^2}{B_1 d_1^2} + 2 K \gamma B_1 d_1 \cos \theta \right) A_x \Delta d = \\ & (\rho q_* U \cos \phi \cos \alpha + B_1 d_1 \gamma \sin \theta + 2K\gamma d_1^2 \cos \theta (\sin \alpha - \tan \alpha) \\ & - \frac{2 \rho \beta d_1 Q_1^2 \tan \alpha}{B_1^2 d_1^2} - B_1 \tau - 2d_1 \tau) A_x \Delta x + \\ & \rho \beta B_1 d_1 \left\{ \frac{\Delta d}{A_1^2} (2Q_1^2 B_1) + \frac{\Delta x}{A_1^2} (4Q_1^2 d_1 \tan \alpha - \right. \\ & \left. 2 Q_1 A_1 q_* \cos \phi \cos \alpha) \right\} \quad (10) \end{aligned}$$

where

$$A_x = (A_1 + 2B_1 \Delta d + 4d_1 \Delta x \tan \alpha) \quad (11)$$

By neglecting all of the higher order terms included in the product of  $A_x \Delta d$  and  $A_x \Delta x$  terms, Eq. 10 can be simplified to yield:

$$\begin{aligned}
& \left\{ \gamma B_1 d_1 \left( 2K \cos \theta - \frac{\beta V_1^2}{g d_1} \right) \right\} \Delta d = \\
& \left\{ \gamma B_1 d_1 \left( \frac{q_* U \cos \phi \cos \alpha}{g B_1 d_1} + \sin \theta + 2K \frac{d_1}{B_1} \cos \theta (\sin \alpha - \tan \alpha) \right. \right. \\
& \left. \left. - \frac{\tau}{\gamma d_1} - \frac{2\tau}{\gamma B_1} - \frac{2\beta V_1 q_* \cos \phi \cos \alpha}{g B_1 d_1} + \frac{2\beta V_1^2 \tan \alpha}{g B_1} \right) \right\} \Delta x \quad (12)
\end{aligned}$$

For small angle  $\theta$

$$\sin \theta = \tan \theta = S_o \quad (13)$$

Solving for  $\frac{\Delta d}{\Delta x}$  from Eq. 12 gives:

$$\begin{aligned}
\frac{\Delta d}{\Delta x} = & \left\{ \frac{q_* U \cos \phi \cos \alpha}{g A_1} + S_o + 2K \frac{d_1}{B_1} \cos \theta (\sin \alpha - \tan \alpha) \right. \\
& \left. - \frac{\tau}{\gamma d_1} - \frac{2\tau}{\gamma B_1} - \frac{2\beta V_1 q_* \cos \phi \cos \alpha}{g A_1} + \frac{2\beta V_1^2 \tan \alpha}{g B_1} \right\} \div \\
& \left\{ 2K \cos \theta - \frac{\beta V_1^2}{g d_1} \right\} \quad (14)
\end{aligned}$$

which relates the change in water depth to an incremental change in distance in the downstream direction.

#### THEORETICAL ANALYSIS FOR SUPERCRITICAL SPATIALLY VARIED FLOW

By applying the basic principles of the conservation of momentum and mass, differential equations involving the partial derivatives of the velocity components and water depth with respect to the coordinate system defined in

Figure 2 are derived. Due to the complex nature of the flow system, exact solutions to the equations are not possible. Therefore, a finite difference technique is employed to obtain information concerning the flow properties of the entire flow field. The specific method used in the solution procedure is known as the method of characteristics. For this method to be applicable, irrotational flow is assumed for the entire flow region except in the relatively thin boundary layer in the immediate vicinity of the channel floor.

A few other basic assumptions are also made. It is assumed that (1) the pressure distribution is hydrostatic, (2) the velocity distribution in the z-direction is uniform (flow to be irrotational), except in the boundary layer and (3) horizontal momentum component introduced by the lateral inflow,  $q_*$ , as it enters the main flow vertically is very small compared with that due to the supercritical main channel flow, and thus, can be neglected.

The continuity equation for all points except at the sidewall is:

$$d \frac{\partial u}{\partial x} + u \frac{\partial d}{\partial x} + d \frac{\partial v}{\partial y} + v \frac{\partial d}{\partial y} = 0 \quad (15)$$

at the sidewall, Eq. 15 becomes:

$$d \frac{\partial u}{\partial x} + u \frac{\partial d}{\partial x} + d \frac{\partial v}{\partial y} + v \frac{\partial d}{\partial y} - \frac{q_1 + q_2}{\delta x \delta y} = 0 \quad (15')$$

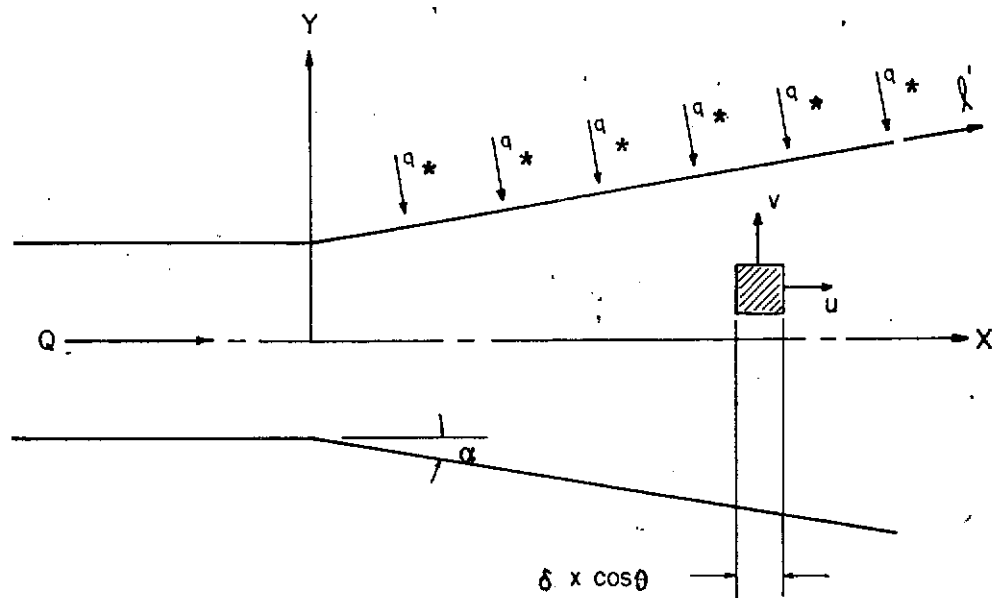
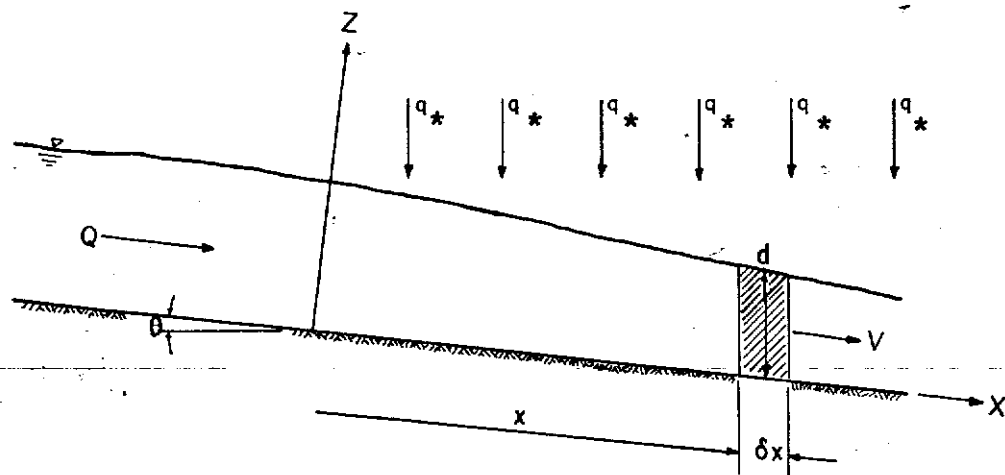
TOP VIEWFRONT VIEW

Fig. 2 - Definition Sketches for Supercritical Flow

where  $q_1$  and  $q_2$  are two portions of the lateral inflow between two adjacent points along the sidewall. The first portion,  $q_1$ , represents the lateral inflow over the distance covered by the y-direction projection of the segment between points  $i-(NP + 1)$  and  $i-NP$  on the sidewall. The distance covered by the projection of line  $i-NP$  to  $i$  is used to compute the magnitude of  $q_2$ . The vertical depth of the flow is  $d$ , and  $\alpha$  is the divergent angle of the test section. With  $\delta x$  and  $\delta y$  representing incremental changes in distance in the independent x-y coordinate system,  $u$  and  $v$  are the velocity components in the two directions respectively.

Writing the momentum equation in the x-direction for a fluid element, which does not include the sidewall, results in:

$$\frac{\partial d}{\partial x} = \tan \theta - \frac{u}{g} \frac{\partial u}{\partial x} - \frac{v}{g} \frac{\partial u}{\partial y} \quad (16)$$

At the sidewall, this equation becomes:

$$\begin{aligned} \frac{\partial d}{\partial x} = \tan \theta - \frac{u}{g} \frac{\partial u}{\partial x} - \frac{v}{g} \frac{\partial u}{\partial y} - \frac{q_1}{2dg \delta y} \frac{\partial u}{\partial x} \\ - \frac{q_2}{dg} \frac{u}{\delta x \delta y} \end{aligned} \quad (16')$$

where  $\theta$  is the angle the channel floor makes with the horizontal and  $g$  is the acceleration due to gravity.

The y-direction momentum equation is:

$$\frac{\partial d}{\partial y} = - \frac{v}{g} \frac{\partial v}{\partial y} - \frac{u}{g} \frac{\partial v}{\partial x} \quad (17)$$

for everywhere except at the sidewall.

At the sidewall, Eq. 17 becomes:

$$\frac{\partial d}{\partial y} = -\frac{v}{g} \frac{\partial v}{\partial y} - \frac{u}{g} \frac{\partial v}{\partial x} - \frac{q_1}{2dg \delta y} \frac{\partial v}{\partial x} - \frac{q_2 v}{dg \delta x \delta y} \quad (17')$$

By substituting Eqs. 16 and 17 into Eq. 15 and simplifying it, gives:

$$(d - \frac{u^2}{g}) \frac{\partial u}{\partial x} - \frac{uv}{g} \frac{\partial u}{\partial y} - \frac{uv}{g} \frac{\partial v}{\partial x} + (d - \frac{v^2}{g}) \frac{\partial v}{\partial y} = -u \tan \theta \quad (18)$$

For conditions at the sidewall, substitute Eqs. 16' and 17' into Eq. 15' to obtain:

$$\begin{aligned} & (d - \frac{u^2}{g} - \frac{q_1 u}{2dg \delta y}) \frac{\partial u}{\partial x} + (-\frac{uv}{g}) \frac{\partial u}{\partial y} \\ & + (-\frac{uv}{g} - \frac{q_1 v}{2dg \delta y}) \frac{\partial v}{\partial x} + (d - \frac{v^2}{g}) \frac{\partial v}{\partial y} = \phi \end{aligned} \quad (18')$$

where

$$\phi = \frac{q_1 + q_2}{\delta x \delta y} - u \tan \theta + (u^2 + v^2) \frac{1}{dg} \frac{q_2}{\delta x \delta y} \quad (19)$$

The condition for irrotational flow is:

$$\frac{\partial u}{\partial y} - \frac{\partial v}{\partial x} = 0 \quad (20)$$

and the total differentials of u and v are:

$$\delta u = \frac{\partial u}{\partial x} \delta x + \frac{\partial u}{\partial y} \delta y \quad (21)$$

$$\delta v = \frac{\partial v}{\partial x} \delta x + \frac{\partial v}{\partial y} \delta y \quad (22)$$

Eqs. 18, 20, 21, and 22 may be written in matrix form as:

$$\begin{pmatrix} d - \frac{u^2}{g} & -\frac{uv}{g} & -\frac{uv}{g} & d - \frac{v^2}{g} \\ 0 & 1 & -1 & 0 \\ \delta x & \delta y & 0 & 0 \\ 0 & 0 & \delta x & \delta y \end{pmatrix} \begin{pmatrix} \frac{\partial u}{\partial x} \\ \frac{\partial u}{\partial y} \\ \frac{\partial v}{\partial x} \\ \frac{\partial v}{\partial y} \end{pmatrix} = \begin{pmatrix} -u \tan \theta \\ 0 \\ \delta u \\ \delta v \end{pmatrix}$$

or

$$(N) \quad \begin{pmatrix} \frac{\partial u}{\partial x} \\ \frac{\partial u}{\partial y} \\ \frac{\partial v}{\partial x} \\ \frac{\partial v}{\partial y} \end{pmatrix} = \begin{pmatrix} -u \tan \theta \\ 0 \\ \delta u \\ \delta v \end{pmatrix}$$

Applying Cramer's rule, the derivatives of  $u$  and  $v$  with respect to  $x$  and  $y$  can be expressed as:

$$\frac{\partial u}{\partial x} = \frac{|K_1|}{|N|}, \quad \frac{\partial u}{\partial y} = \frac{|K_2|}{|N|}, \quad \frac{\partial v}{\partial x} = \frac{|K_3|}{|N|}, \quad \frac{\partial v}{\partial y} = \frac{|K_4|}{|N|} \quad (23)$$

In supercritical transitional flow, discontinuity occurs as a result of the presence of standing waves. Mathematically, such a discontinuity can be described by one of the following conditions:

$$\frac{\partial u}{\partial x} = 0, \quad \frac{\partial u}{\partial y} = 0, \quad \frac{\partial v}{\partial x} = 0, \quad \frac{\partial v}{\partial y} = 0 \quad (24)$$

Equating the determinant of the N matrix with zero results in:

$$\frac{\delta y}{\delta x} = \frac{-uv \pm dg \sqrt{F^2 - 1}}{dg - u^2} \quad (25)$$

where F is the Froude number and equals

$$\frac{v}{\sqrt{gd}} \quad \text{and} \quad V = \sqrt{u^2 + v^2}$$

Equation 25 can be rewritten as

$$\frac{\delta y}{\delta x} = \frac{-uv + dg \sqrt{F^2 - 1}}{dg - u^2} \quad (26a)$$

which is the -c characteristic and

$$\frac{\delta y}{\delta x} = \frac{-uv - dg \sqrt{F^2 - 1}}{dg - u^2} \quad (26b)$$

which is the +c characteristic in the x-y plane.



To define the u-v relationship along the characteristic curves, the determinant of the  $K_3$  matrix is equated to zero.

Solving for  $\frac{\delta v}{\delta u}$  gives:

$$\frac{\delta v}{\delta u} = \frac{1}{(d - \frac{v^2}{g})} \left\{ -u \tan \theta \left( \frac{\delta y}{\delta u} \right) - (d - \frac{u^2}{g}) \left( \frac{\delta y}{\delta x} \right) \right\} \quad (27)$$

replacing  $\frac{\delta y}{\delta x}$  with the values from Eqs. 26a and 26b yields:

$$\frac{\delta v}{\delta u} = \frac{1}{(d - \frac{v^2}{g})} \left\{ -u \tan \theta \left( \frac{\delta y}{\delta u} \right) + \frac{uv}{g} - d \sqrt{F^2 - 1} \right\} \quad (28a)$$

along the -c characteristic and

$$\frac{\delta v}{\delta u} = \frac{1}{(d - \frac{v^2}{g})} \left\{ -u \tan \theta \left( \frac{\delta y}{\delta u} \right) + \frac{uv}{g} + d \sqrt{F^2 - 1} \right\} \quad (28b)$$

along the +c characteristic curves.

For conditions at the sidewall, the x-y relationships become:

$$\begin{aligned} \frac{\delta y}{\delta x} = & \left\{ -uv + dg \sqrt{F^2 - 1 + \frac{q_1^2 v^2}{16d^4 g^2 \delta y^2}} + \frac{q_1 u}{2d^2 g \delta y} \right. \\ & \left. + \frac{q_1 v}{4d \delta y} \right\} \div \left\{ dg - u^2 - \frac{q_1 u}{2d \delta y} \right\} \end{aligned} \quad (26a')$$

for the -c characteristic and

$$\frac{\delta y}{\delta x} = \left\{ -uv - dg \sqrt{F^2 - 1 + \frac{q_1^2 v^2}{16d^4 g^2 \delta y^2} + \frac{q_1 u}{2d^2 g \delta y}} \right. \\ \left. + \frac{q_1 v}{4d \delta y} \right\} \div \left\{ dg - u^2 - \frac{q_1 u}{2d \delta y} \right\} \quad (26b')$$

for the +c characteristic.

The compatibility relationships, as described in Eqs. 28a and 28b become:

$$\frac{\delta v}{\delta u} = \frac{1}{d - \frac{v^2}{g}} \left\{ \phi \frac{\delta y}{\delta u} - \left( d - \frac{u^2}{g} - \frac{q_1 u}{2dg \delta y} \right) \frac{\delta y}{\delta x} \right\} \quad (28')$$

#### COMPUTATIONAL PROCEDURES

Since there are four regions, each of which contains different flow conditions, it is necessary to describe the numerical computation procedures in four individual sections. Subdividing the first '-c' characteristic curve into (NP-1) equal y-direction increments, the entire flow field can be isolated into the following computation groups as depicted in Fig. 3. Because of the symmetric flow properties, only half of the test section is shown in Fig. 3.

(I) Region one contains points 0 through NP. Along this characteristic curve  $v \equiv 0$ , and at point 0  $u = u_0$  and  $d = d_0$ .

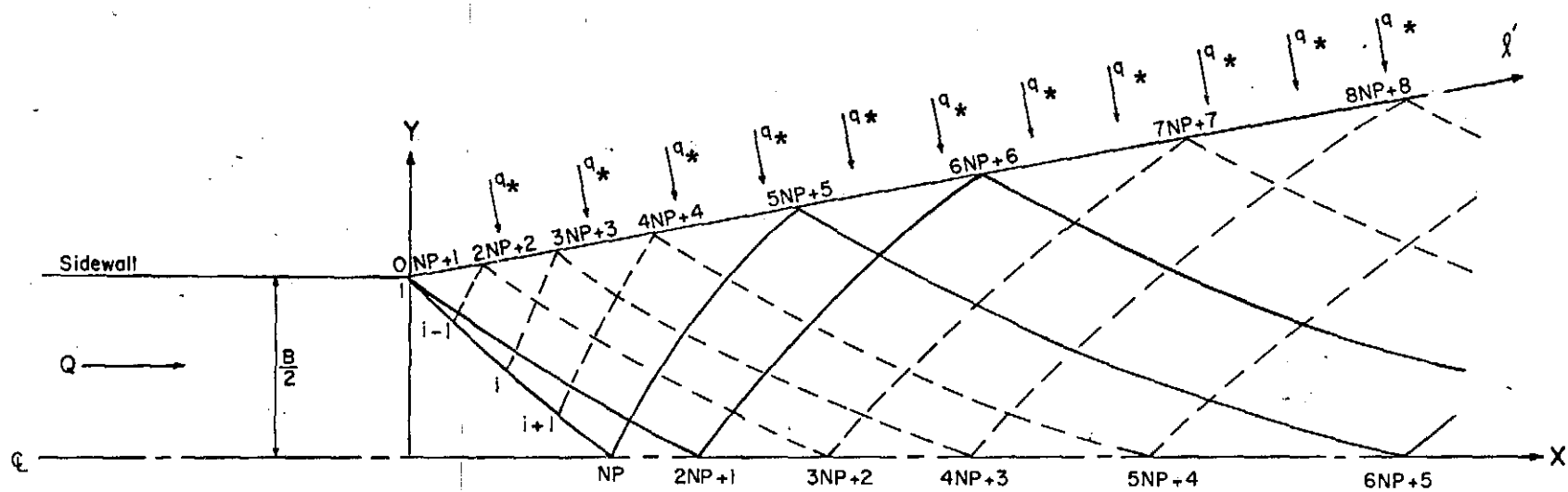


Fig. 3 - Wave Pattern and Characteristic Curves for Supercritical Flow

Based on these conditions, Eq. 28a may be written as:

$$\frac{\delta v}{\delta u} = \frac{1}{d_{i-1}} \left\{ -u_{i-1} \tan \theta \left( \frac{\delta y}{\delta u} \right) - d_{i-1} \sqrt{F_{i-1}^2 - 1} \right\} = 0 \quad (29)$$

or

$$\delta u = \frac{-u_{i-1} \tan \theta}{d_{i-1} \sqrt{F_{i-1}^2 - 1}} \delta y \quad (30)$$

Using Eq. 30 with a given  $\delta y$ ,  $\delta u$  can be computed such that

$$u_i = u_{i-1} + \delta u \quad (31)$$

The momentum equation along the negative characteristic line can be written as

$$\begin{aligned} & \rho (V'_{i-1})^2 d_{i-1} \cos \theta + \frac{1}{2} \rho g d_{i-1}^2 \cos \theta + \frac{1}{2} \rho g (d_{i-1} + \\ & d_i) \sqrt{(\delta x)^2 + (\delta y)^2} \sin \theta \cos \gamma - \rho (V'_i)^2 d_i \cos \theta \\ & - \frac{1}{2} \rho g d_i^2 \cos \theta = 0 \end{aligned} \quad (32)$$

where

$$\gamma = \tan^{-1} \left( \frac{\delta y}{\delta x} \right) \quad (33)$$

$$V'_{i-1} = \sqrt{(u_{i-1})^2 + (v_{i-1})^2} \cos \left( \gamma - \tan^{-1} \left( \frac{v_{i-1}}{u_{i-1}} \right) \right) \quad (34)$$

and

$$v_i' = \sqrt{(u_i')^2 + (v_i')^2} \cos \left( \gamma - \tan^{-1} \left( \frac{v_i'}{u_i'} \right) \right) \quad (34')$$

Solving for  $d_i$  from Eq. 32 results in:

$$\begin{aligned} d_i = \frac{1}{2} \left\{ - \left[ \frac{2}{g} (v_i')^2 - \tan \theta \cos \gamma \sqrt{(\delta x)^2 + (\delta y)^2} \right] \right. \\ \left. + \left\{ \left[ \frac{2}{g} (v_i')^2 - \tan \theta \cos \gamma \sqrt{(\delta x)^2 + (\delta y)^2} \right]^2 + \right. \right. \\ \left. \left. 4 d_{i-1} \left[ \frac{2}{g} (v_{i-1}')^2 + \tan \theta \cos \gamma \sqrt{(\delta x)^2 + (\delta y)^2} + d_{i-1} \right] \right\}^{1/2} \right\} \quad (35) \end{aligned}$$

Rearranging Eq. 26a gives:

$$\delta x = \frac{d_i g - u_i^2}{d_i g \sqrt{F_i^2 - 1}} \delta y \quad (36)$$

and

$$x_i = x_{i-1} + \delta x \quad (36')$$

To increase accuracy, successive approximation may be used for this and all other regions of the numerical computations.

(II) Points JNP + J, along the sidewall constitute the second region.

From the geometry of the channel,

$$\delta x = \frac{y_{i-NP} - \frac{B}{2}}{\tan \alpha} - x_{i-NP} + \frac{\delta y}{\tan \alpha} \quad (37)$$

with B representing the width of the channel where the divergent transition initiates.

Using Eq. 26b', the +c characteristic, we have,

$$\frac{\delta y}{\delta x} = \left\{ -u_{i-NP} v_{i-NP} d_{i-NP} g \sqrt{F_{i-NP}^2 - 1 + \frac{q_1^2 v_{i-NP}^2}{16 d_{i-NP}^4 g^2 \delta y^2} + \frac{q_1 u_{i-NP}}{2 d_{i-NP}^2 g \delta y}} \right. \\ \left. + \frac{q_1 v_{i-NP}}{4 d_{i-NP} \delta y} \right\} \div \left\{ d_{i-NP} g - u_{i-NP}^2 - \frac{q_1 u_{i-NP}}{2 d_{i-NP} \delta y} \right\} \quad (38)$$

Substituting Eq. 37 into Eq. 38 gives:

$$\delta y = \left\{ -u_{i-NP} v_{i-NP} \left( \frac{y_{i-NP} - \frac{B}{2}}{\tan \alpha} - x_{i-NP} + \frac{\delta y}{\tan \alpha} \right) \right. \\ \left. - g d_{i-NP} \left( \frac{y_{i-NP} - \frac{B}{2}}{\tan \alpha} - x_{i-NP} + \frac{\delta y}{\tan \alpha} \right) \right. \\ \left. \times \left( \sqrt{F_{i-NP}^2 - 1 + \frac{q_1^2 v_{i-NP}^2}{16 d_{i-NP}^4 g^2 \delta y^2} + \frac{q_1 u_{i-NP}}{2 d_{i-NP}^2 g \delta y}} \right) \right. \\ \left. + \frac{q_1 v_{i-NP}}{4 d_{i-NP} \delta y} \left( \frac{y_{i-NP} - \frac{B}{2}}{\tan \alpha} - x_{i-NP} + \frac{\delta y}{\tan \alpha} \right) \right\} \div \\ \left\{ d_{i-NP} g - u_{i-NP}^2 - \frac{q_1 u_{i-NP}}{2 d_{i-NP} \delta y} \right\} \quad (39)$$

which is solved using interval halving trial and error for the value of  $\delta y$ . Then

$$y_i = y_{i-NP} + \delta y \quad (40)$$

and

$$x_i = x_{i-NP} + \delta x \quad (40')$$

Along the sidewall, it is also known that:

$$v_i = u_i \tan \alpha \quad (41)$$

therefore

$$(v_{i-NP} + \delta v) = (u_{i-NP} + \delta u) \tan \alpha \quad (41')$$

From Eq. 28' we have

$$\frac{\delta v}{\delta u} = \frac{1}{d_{i-NP} - \frac{v_{i-NP}^2}{g}} \left\{ \frac{y_i - y_{i-NP}}{\delta u} - \left\{ d_{i-NP} - \frac{u_{i-NP}^2}{g} - \frac{q_1 u_{i-NP}}{2 d_{i-NP} g (y_i - y_{i-NP})} \right\} \right. \\ \left. \left\{ \frac{y_i - y_{i-NP}}{x_i - x_{i-NP}} \right\} \right\} \quad (42)$$

where

$$\Phi = \frac{q_1 + q_2}{(x_i - x_{i-NP}) (y_i - y_{i-NP})} + \frac{q_2}{d_{i-NP} g (x_i - x_{i-NP}) (y_i - y_{i-NP})} \\ - \left\{ u_{i-NP}^2 + v_{i-NP}^2 \right\} - u_{i-NP} \tan \theta \quad (43)$$

Equation 41' gives

$$\delta v = (u_{i-NP} + \delta u) \tan \alpha - v_{i-NP} \quad (41'')$$

Substituting this into Eq. 42 and solving for  $u_i$  yields:

$$\begin{aligned}
u_i = & \left\{ \phi (y_i - y_{i-NP}) + v_{i-NP} \left( d_{i-NP} - \frac{v_{i-NP}^2}{g} \right) + u_{i-NP} \left( d_{i-NP} - \frac{u_{i-NP}^2}{g} \right) \right. \\
& \left. - \frac{q_1 u_{i-NP}}{2d_{i-NP}g (y_i - y_{i-NP})} \right) \frac{y_i - y_{i-NP}}{x_i - x_{i-NP}} \Bigg\} \div \\
& \left\{ \frac{y_i - y_{i-NP}}{x_i - x_{i-NP}} \left( d_{i-NP} - \frac{u_{i-NP}^2}{g} - \frac{q_1 u_{i-NP}}{2d_{i-NP}g (y_i - y_{i-NP})} \right) \right. \\
& \left. + \left( d_{i-NP} - \frac{v_{i-NP}^2}{g} \right) \tan \alpha \right\} \quad (44)
\end{aligned}$$

The momentum equation along the positive characteristic line can be written as

$$\begin{aligned}
\rho (v'_{i-NP})^2 d_{i-NP} \cos \theta + \frac{1}{2} \rho g d_{i-NP}^2 \cos \theta + \frac{1}{2} \rho g (d_{i-NP} + d_i) \\
\sqrt{(\delta x)^2 + (\delta y)^2} \sin \theta \cos \gamma - \rho (v'_i)^2 d_i \cos \theta \\
- \frac{1}{2} \rho g d_i^2 \cos \theta = 0 \quad (45)
\end{aligned}$$

where

$$v'_{i-NP} = \sqrt{(u_{i-NP})^2 + (v_{i-NP})^2} \cos \left( \gamma - \tan^{-1} \left( \frac{v_{i-NP}}{u_{i-NP}} \right) \right) \quad (46)$$

Solving Eq. 45 for  $d_i$  results in:



$$\begin{aligned}
d_i = \frac{1}{2} \left\{ - \left[ \frac{2}{g} v_i'^2 - \tan \theta \cos \gamma \sqrt{\delta x^2 + \delta y^2} \right] \right. \\
+ \left\{ \left[ \frac{2}{g} v_i'^2 - \tan \theta \cos \gamma \sqrt{\delta x^2 + \delta y^2} \right]^2 + \right. \\
4 d_{i-NP} \left[ \frac{2}{g} v_{i-NP}'^2 + \tan \theta \cos \gamma \sqrt{\delta x^2 + \delta y^2} + \right. \\
\left. \left. \left. d_{i-NP} \right] \right\}^{1/2} \right\} \quad (47)
\end{aligned}$$

(III) The third region contains those points along the centerline of the channel where  $y_i = 0$ . Because the flow is symmetrical,  $v_i = 0$ , everywhere along this line.

From Eq. 26a:

$$\delta x = \frac{dg - u^2}{-uv + dg \sqrt{F^2 - 1}} \delta y \quad (48)$$

or

$$\delta x = -y_{i-1} \left( \frac{d_{i-1} g - u_{i-1}^2}{-u_{i-1} v_{i-1} + d_{i-1} g \sqrt{F_{i-1}^2 - 1}} \right) \quad (48')$$

then

$$x_i = x_{i-1} + \delta x \quad (49)$$

Since, along the centerline,  $v_i = 0$ ,  $\delta v = -v_{i-1}$ .

Solving Eq. 28a for  $\delta u$  yields:

$$\delta u = \frac{-v_{i-1} (d - \frac{v^2}{g}) - y_{i-1} u \tan \theta}{\frac{uv}{g} - d \sqrt{F^2 - 1}} \quad (50)$$

The depth along the centerline can now be found by using Eq. 35.

(IV) Region four contains all of the remaining points in the flow field.

For the -c characteristic  $\delta y = y_i - y_{i-1}$  and  $\delta x = x_i - x_{i-1}$ . For the +c characteristic  $\delta y = y_i - y_{i-NP}$  and  $\delta x = x_i - x_{i-NP}$ .

Substituting these values into Eqs. 26a and 26b gives:

$$\frac{y_i - y_{i-1}}{x_i - x_{i-1}} = \frac{-u_{i-1} v_{i-1} + d_{i-1} g \sqrt{F_{i-1}^2 - 1}}{d_{i-1} g - u_{i-1}^2} = G^- \quad (52)$$

and

$$\frac{y_i - y_{i-NP}}{x_i - x_{i-NP}} = \frac{-u_{i-NP} v_{i-NP} - d_{i-NP} g \sqrt{F_{i-NP}^2 - 1}}{d_{i-NP} g - u_{i-NP}^2} = G^+ \quad (53)$$

from Eq. 52

$$y_i = G^- (x_i - x_{i-1}) + y_{i-1} \quad (54)$$

Substituting Eq. 54 into Eq. 53 and rearranging yields:

$$x_i = \frac{G^- x_{i-1} - G^+ x_{i-NP} - y_{i-1} + y_{i-NP}}{G^- - G^+} \quad (55)$$

By substituting this value of  $x_i$  into Eq. 54,  $y_i$  can be determined.

Along the  $-c$  characteristic,  $\delta u)_n = u_i - u_{i-1}$  and  $\delta v)_n = v_i - v_{i-1}$  and along the  $+c$  characteristic  $\delta u)_p = u_i - u_{i-NP}$  and  $\delta v)_p = v_i - v_{i-NP}$ .

therefore

$$\delta u)_n - \delta u)_p = u_{i-NP} - u_{i-1} = G1 \quad (56)$$

and

$$\delta v)_n - \delta v)_p = v_{i-NP} - v_{i-1} = G2 \quad (56')$$

Let

$$\frac{-u_{i-1} \tan \theta (y_i - y_{i-1})}{d_{i-1} - \frac{v_{i-1}^2}{g}} = G3 \quad (57)$$

$$\frac{-u_{i-NP} \tan \theta (y_i - y_{i-NP})}{d_{i-NP} - \frac{v_{i-NP}^2}{g}} = G5 \quad (57')$$

$$\frac{1}{d_{i-1} - \frac{v_{i-1}^2}{g}} \left\{ \frac{u_{i-1} v_{i-1}}{g} - d_{i-1} \sqrt{F_{i-1}^2 - 1} \right\} = G4 \quad (58)$$

and

$$\frac{1}{d_{i-NP} - \frac{v_{i-NP}^2}{g}} \left\{ \frac{u_{i-NP} v_{i-NP}}{g} + d_{i-NP} \sqrt{F_{i-NP}^2 - 1} \right\} = G6 \quad (58')$$

Eqs. 11a' and 11b' become:

$$\frac{\delta v)_n}{\delta u)_n} = \frac{G3}{\delta u)_n} + G4 \quad (59)$$

and

$$\frac{\delta v)_p}{\delta u)_p} = \frac{G5}{\delta u)_p} + G6 \quad (60)$$

Combining Eqs. 56, 56', 59, and 60 yields:

$$\delta u)_p = \frac{G5 + G2 - G3 - (G1)(G4)}{G4 - G6} \quad (61)$$

then

$$u_i = u_{i-NP} + \delta u)_p \quad (62)$$

From Eq. 60  $\delta v)_p$  can be found.

Then

$$v_i = v_{i-NP} + \delta v)_p \quad (63)$$

An equation similar to Eq. 32 can be written along the +c characteristic, resulting in

$$\begin{aligned}
d_i = \frac{1}{2} \left\{ - \left[ \frac{2}{g} (V'_i)^2 - \tan \theta \cos \gamma \sqrt{(\delta x)^2 + (\delta y)^2} \right] \right. \\
+ \left\{ \left[ \frac{2}{g} (V'_i)^2 - \tan \theta \cos \gamma \sqrt{(\delta x)^2 + (\delta y)^2} \right]^2 + \right. \\
4 d_{i-NP} \left[ \frac{2}{g} (V'_{i-NP})^2 + \tan \theta \cos \gamma \sqrt{(\delta x)^2 + (\delta y)^2} \right. \\
\left. \left. + d_{i-NP} \right] \right\}^{1/2} \left. \right\} \quad (64)
\end{aligned}$$

#### DETERMINATION OF BOUNDARY SHEAR IN OPEN CHANNEL FLUMES

The expression for the boundary shear stress,  $\tau$ , was determined by combining several other equations which relate frictional resistance to the flow characteristics.

From the Chezy equation (8) we have:

$$\bar{V} = C \sqrt{R S} \quad (65)$$

where  $\bar{V}$  is the mean velocity,  $C$  is the friction factor,  $R$  is the hydraulic radius and  $S$  is the slope of the energy grade line.

Modern fluid dynamics and especially boundary layer theory (15) suggest Chezy's formula to be used in the form

$$\bar{V} = \sqrt{\frac{8}{f}} \sqrt{g R S} \quad (66)$$

where  $f$  is the Darcy-Weisbach friction factor, and  $g$  is the acceleration due to gravity.

Setting Eq. 65 equal to Eq. 66 yields:

$$C = \sqrt{\frac{8g}{f}} \quad (67)$$

The relationship between Manning's roughness factor,  $n$ , and Chezy's  $C$  (9) is known as:

$$C = \frac{1.49}{n} R^{1/6} \quad (68)$$

By equating Eqs. 67 and 68 we have

$$f = \frac{3.603 \text{ } g n^2}{R^{1/3}} \quad (69)$$

The relationship (16) between shear stress, friction factor and mean velocity is:

$$\sqrt{\frac{\tau}{\rho}} = \sqrt{\frac{f}{8}} \bar{v} \quad (70)$$

in which  $\rho$  is the mass density of the fluid.

Substituting Eq. 69 into Eq. 70 and solving for  $\tau$  yields:

$$\tau = \frac{0.45 \gamma n^2 v^2}{R^{1/3}} \quad (71)$$

in which  $\gamma$  is the specific weight of the fluid.

The above expression is used to determine the average boundary shear stress,  $\tau$ , when the Manning roughness coefficient,  $n$ , is precalibrated for the flume used in the experimental work.

## CHAPTER III

### EXPERIMENTAL FACILITY

The experimental facility used in this study consists of five major parts: main flow channel, convergent-divergent test section, plexiglas overflow devices for providing uniform lateral inflow to the divergent test section, flow supply systems, and measuring devices.

A seventy-two feet long glass flume with a two feet by two feet cross section is used as the main flow channel. This flume consists of three separate sections. Four pairs of electric motor operated gear jacks are used to support and control the slope of each section. One pair of gear jacks are used for each end section and two for the middle section. A sluice gate at the beginning of the flume is used to regulate the inflow to the main channel. The constant flowrate is supplied by a constant head storage tank behind the sluice gate. A schematic drawing of the flume and experimental setup is shown in Fig. 4.

To gradually reduce the width of the main flow channel from two feet to one foot, two pieces of sheet metal are used to form the convergent section. The divergent test section is formed by using two boards,

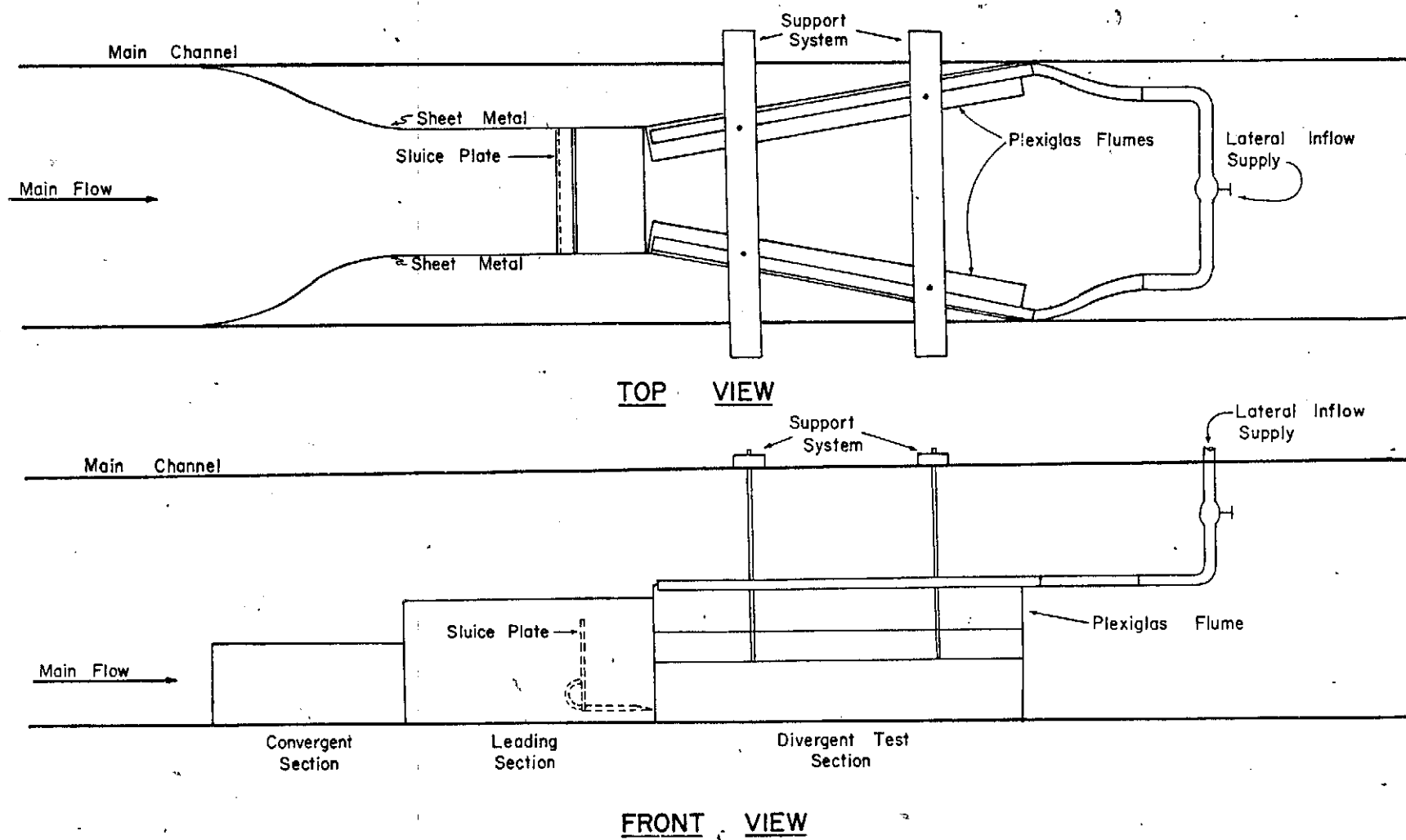


Fig. 4 - Main Channel with Experimental Converging-Diverging Apparatus



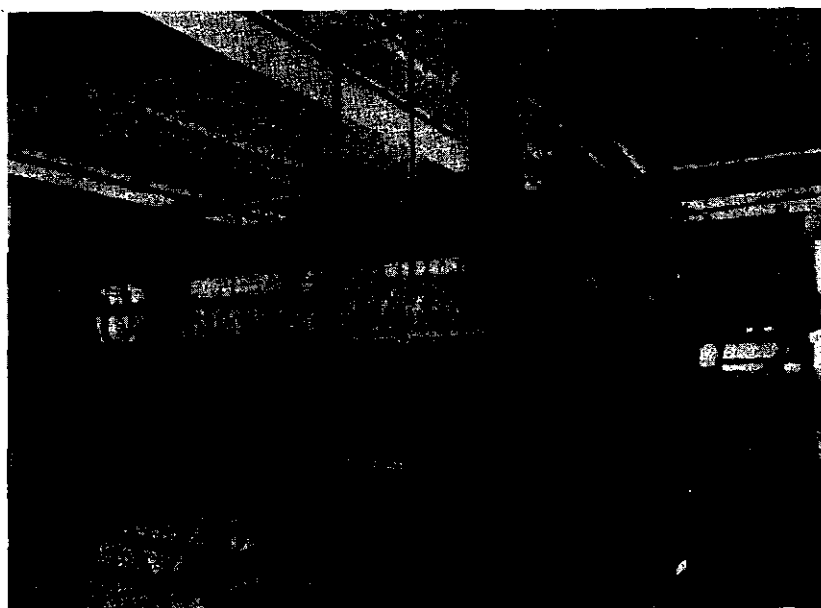
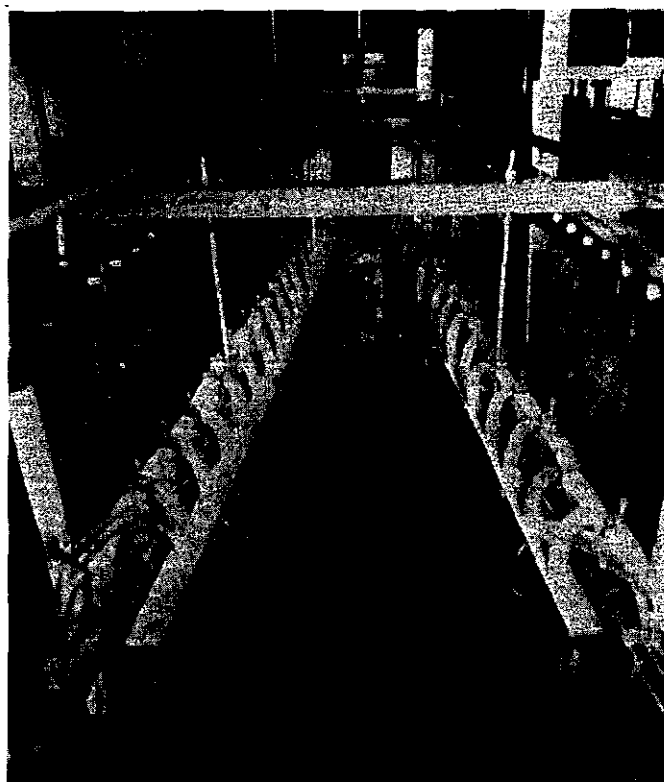


Fig. 5 Experimental Apparatus

six feet long, leading from the constricted width to the normal flume width of two feet. Between the convergent section and the test section, a four feet parallel wall section is inserted to form uniform approaching flow to the test section. In order to obtain nearly uniform velocity distribution at the entrance of the test section, a sluice plate is used at various locations until the velocity measurements indicate the velocity throughout the entrance section varies no more than one percent from its mean value. Figure 4 shows the general arrangement of the convergent-divergent section and the lateral flow supply devices.

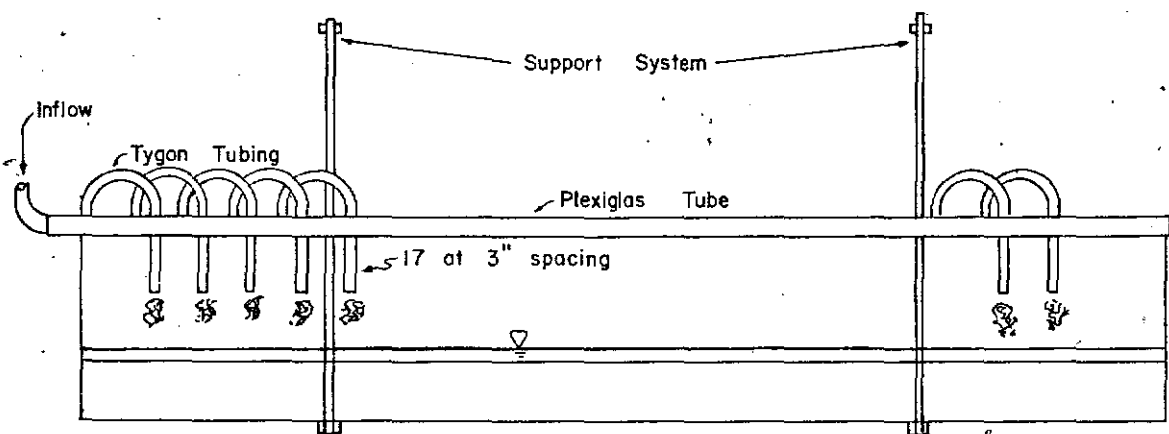
The lateral flow supply devices are plexiglas flumes, constructed so as to provide uniform sheet flow along the side walls of the divergent test section. A knife edged overflow weir along the entire front of the flume permits water to flow over and form a water sheet on an inclined plate set at fifteen degrees from the vertical. The lower edge of the inclined plate is placed at a uniform gap from the side wall to allow the sheet flow to enter the test section. A one-eighth inch plexiglas partition was inserted three-quarters of an inch from the back of the flume to separate the flume into two compartments. This partition was placed one-eighth inch from the bottom to produce a head in the back compartment

and to reduce turbulence in the front compartment. To further reduce the turbulence, a baffle strip was placed in the front compartment along the front wall. Figure 6 shows the plexiglas flume and its cross section.

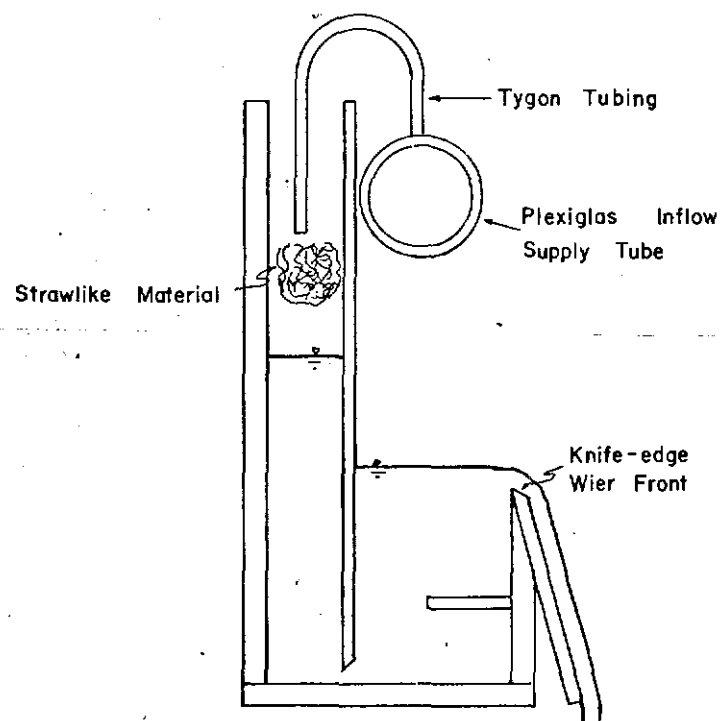
Each plexiglas flume is suspended from the main channel side walls by two, one-half inch stainless steel rods, threaded at each end. This allows adjustment of the flumes up and down to maintain their level position while the main channel slope is varied.

The lateral flow discharge is supplied through one inch galvanized pipe to the plexiglas flumes. A valve in the system regulates the flow to the flumes. To measure lateral flowrate, a pre-calibrated elbow meter was installed in the line. A mercury manometer is used to measure the differential pressure in the elbow meter. The galvanized pipe is then branched to two plexiglas tubes connected with tygon tubing. In the top of each plexiglas tube are distribution holes set at approximately three inches apart. Tygon tubing from each of these holes is used to carry the water into the back compartment of each plexiglas flume. Strawlike material was placed in the back compartment under each jet to dissipate the turbulence caused by the water jets.

An electronic point gage was used to measure the water depth. The point gage is mounted on a carriage



FRONT VIEW



CROSS SECTION

Fig. 6 - Uniform Lateral Inflow Plexiglas Flume

which slides on two pieces of tubular conduit. The conduit is mounted on each side of the main channel. A scale on one conduit determines the longitudinal location whereas a scale on the carriage determines the lateral location of the point gage. The point gage is equipped with a vernier scale to produce readings of  $\pm 5 \times 10^{-4}$  feet accuracy.

## CHAPTER IV

### EXPERIMENTAL PROCEDURE

For the experimental data collection, the constant head storage tank and its associated valves were adjusted such that a given flowrate is provided in the main channel. For each main channel flowrate, a maximum lateral inflow of 0.0242 cfs/ft. was first supplied to the diverging zone. This maximum value provides a total lateral inflow over the test divergent section of approximately one half the magnitude of the main channel flow. The lateral inflow was then reduced to 50% of the maximum for a second set of data gathering. The third data set was taken for the water surface profile of the same flowrate without lateral inflow. The main channel flowrate was then readjusted. The above procedure was repeated using the new flow. A slope of 1.5% was used for the various trials in subcritical flow region.

A uniform transverse water surface was assumed for subcritical flow conditions. Therefore, only centerline measurements were taken when the flow is subcritical.

A similar procedure was followed for supercritical flow measurements. However, the presence of standing waves

in supercritical flow makes the assumption of a constant transverse water surface invalid. Therefore, a two dimensional coordinate system, as shown in Figure 3, was selected to record these wave patterns on an x - y plane. Detailed centerline measurements were also recorded.

To study the effect of slope, two different slopes were tried. With a minimum slope of 1.0%, the described procedure was followed; then repeated, using a slope of 4.0%.

In order to measure the water depth, elevation of the channel floor was first determined. This was done by the use of an electronic point gage, which can be moved freely in the x-y plane, set along the top of the main channel. This elevation was then subtracted from the water surface elevation measurement to give the net water depth at each desired point.

Flowrates for both the main channel and the plexiglas flumes were determined using mercury-water manometers. For the main channel, the manometer is attached to a Venturi-Meter and for the lateral inflow supply flumes, it is connected to an elbow meter.

## CHAPTER V

### DATA ANALYSIS AND PRESENTATION

The direct measurements taken during the course of this study include the channel floor elevation; the water surface elevation along the centerline of the divergent test section; the head difference on the manometers attached to the Venturi and elbow meters,  $\Delta h_Q$  and  $\Delta h_{q_*}$ ; and the downstream distance of each measurement from the entrance to the divergent test section. The precalibrated flowrate curves for the Venturi and elbow meters were used to determine the main channel flowrate,  $Q$ , and the lateral inflow rate,  $q_*$ . The water depth was determined by subtracting the channel floor elevation from the water surface elevation.

#### ANALYSIS OF SUBCRITICAL SPATIALLY VARIED FLOW

For the case of subcritical spatially varied flow, a constant transverse water surface was assumed. Thus, only the analytical and experimental centerline profiles are compared. With the aid of a digital computer, the analytical water surface profile is determined for each group of initial conditions. The program used in the computations was written using Fortran IV language and is listed in Appendix III. A flow chart corresponding to this program is shown



in Fig. A-1. For each data set there are two corresponding plots. These plots were produced by the Calcomp Plotter with OS/360.

The analytical profile was computed from Eq. 14. The initial depth used in the analytical computations is the initial experimental depth and the incremental downstream distance used is 0.1 feet. Six sets of data were taken and the results are presented in Tables I and II, and graphically shown in Figures 7-10.

Table I shows the results for the first three data sets. For these data sets, a main channel flowrate of 0.368 cfs was used. Other parameters held constant were the channel slope, 1.5%; the divergent angle,  $4.17^\circ$ ; and the total downstream distance, 6 feet.

With these parameters constant, the three sets of computations shown in each Table are (A)  $q_* = 0.0$  cfs/ft, (B)  $q_* = 0.0125$  cfs/ft, and (C)  $q_* = 0.0242$  cfs/ft. Listed in each group are the analytical and experimental depths at each 0.5 foot interval. Also listed is the percent difference between the analytical and experimental depth.

The corresponding plots for these data sets are shown in Figs. 7 and 8. Figure 7 shows the relationship between water depth and downstream distance. This and all subsequent plots are plotted on arithmetic scales. The

normalized results, by dividing the water depth by the initial depth and dividing the downstream distance by the initial width, are shown in Fig. 8. For Figs. 7 and 8, (A), (B), and (C) correspond to those results listed in Table I.

Table II lists the results for the second three data sets. For these sets, all initial parameters were kept the same as used in previous sets except the main channel flow-rate which is changed to 0.211 cfs. The same lateral inflow rates as listed in Table I apply to Table II, (A), (B), and (C).

Figure 9 shows the relationship between water depth and downstream distance and the corresponding dimensionless plot is shown in Fig. 10.

Figures 7 through 10 indicate the largest difference between the analytical and experimental centerline profiles occurs near the end of the test section. Tables I and II verify this, showing the largest percent difference occurring at a downstream distance of 6 feet in all cases.

#### ANALYSIS OF SUPERCRITICAL SPATIALLY VARIED FLOW

The method of characteristics, which is used widely in analyzing supersonic gas flow, is used for the analysis of supercritical spatially varied flow. In applying this method, incremental changes along the characteristic curves are computed so that the flow information at various points along the curves can be obtained. The computed results for

each data set are presented in Tables III through XIV. Listed in each table are the points of interest and their corresponding location in the x-y coordinate system used; the velocities in both the x and y directions; and the water depth at each point.

A digital computer program (see Appendix III), written also in Fortran IV, is used for the analytical computations. Also used is the Calcomp Plotter to display the results in graphical form. The graphical results are shown in Figures 12 through 19. For each data set, there are two plots. They are the analytical and experimental centerline profiles and the analytical cross wave patterns. Experimental values measured at the entrance of the test section are used as the initial conditions in the computational analysis.

Table III shows the results for the first supercritical data set. For this set, the main channel flowrate is 0.3632 cfs, the lateral inflow is zero, and the channel slope is 1%. Holding the main channel flowrate and the slope constant, the lateral inflow is increased to 0.0236 cfs/ft for the results presented in Table V, and then decreased to 0.0125 cfs/ft in Table IV. The corresponding centerline profiles are shown in Figure 12 and the analytical cross wave patterns in Figure 13. Holding all parameters constant except the channel slope, which is changed to 4%, the results in Tables VI, VII and VIII are

produced. The corresponding centerline profiles and cross wave patterns are shown in Figures 14 and 15, respectively.

The same channel slopes and lateral inflow combinations were used for a 0.1967 cfs main channel flowrate for further experimental observations. These results are listed in Tables IX - XIV. The corresponding plots of centerline profiles and cross wave patterns are displayed in Figures 16-19.

The results for the supercritical data sets show that the analytical and experimental centerline profiles follow closely the same general trend. As can be seen from Figures 12, 14, 16, and 18, the largest difference is for the case of a 1% channel slope and the maximum lateral inflow rate.

TABLE I ANALYTICAL RESULTS FOR SUBCRITICAL FLOW

MAIN CHANNEL FLOWRATE: 0.368 CFS

(A) LATERAL INFLOW: 0.0 CFS/FT			
DOWNSTREAM	DEPTH (FT)		PERCENT
DISTANCE (FT)	ANALYTICAL	EXPERIMENTAL	DIFFERENCE
0.0	0.2730	0.273	0.0
0.50	0.2861	0.285	0.385
1.00	0.2976	0.296	0.534
1.50	0.3081	0.306	0.668
2.00	0.3178	0.314	1.205
2.50	0.3271	0.324	0.952
3.00	0.3360	0.331	1.499
3.50	0.3447	0.340	1.360
4.00	0.3531	0.349	1.170
4.50	0.3614	0.357	1.220
5.00	0.3696	0.364	1.505
5.50	0.3776	0.371	1.750
6.00	0.3856	0.378	1.964

(B) LATERAL INFLOW: 0.0125 CFS/FT			
DOWNSTREAM	DEPTH (FT)		PERCENT
DISTANCE (FT)	ANALYTICAL	EXPERIMENTAL	DIFFERENCE
0.0	0.3060	0.306	0.0
0.50	0.3177	0.317	0.212
1.00	0.3284	0.325	1.028
1.50	0.3384	0.334	1.301
2.00	0.3479	0.340	2.282
2.50	0.3571	0.348	2.551
3.00	0.3660	0.358	2.186
3.50	0.3747	0.366	2.314
4.00	0.3832	0.371	3.174
4.50	0.3915	0.381	2.686
5.00	0.3998	0.388	2.940
5.50	0.4079	0.394	3.407
6.00	0.4160	0.401	3.596

(C) LATERAL INFLOW: 0.0242 CFS/FT			
DOWNSTREAM	DEPTH (FT)		PERCENT
DISTANCE (FT)	ANALYTICAL	EXPERIMENTAL	DIFFERENCE
0.0	0.3120	0.312	0.0
0.50	0.3235	0.321	0.779
1.00	0.3342	0.328	1.862
1.50	0.3443	0.335	2.713
2.00	0.3540	0.341	3.676
2.50	0.3634	0.350	3.674
3.00	0.3724	0.358	3.871
3.50	0.3813	0.365	4.268
4.00	0.3900	0.373	4.347
4.50	0.3985	0.381	4.388
5.00	0.4069	0.387	4.891
5.50	0.4152	0.393	5.350
6.00	0.4234	0.400	5.536

TABLE II ANALYTICAL RESULTS FOR SUBCRITICAL FLOW

MAIN CHANNEL FLOWRATE: 0.211 CFS

(A) LATERAL INFLOW: 0.0 CFS/FT			
DOWNSTREAM	DEPTH (FT)		PERCENT
DISTANCE (FT)	ANALYTICAL	EXPERIMENTAL	DIFFERENCE
0.0	0.2130	0.213	0.0
0.50	0.2235	0.224	0.220
1.00	0.2332	0.231	0.935
1.50	0.2423	0.238	1.776
2.00	0.2510	0.245	2.408
2.50	0.2595	0.253	2.510
3.00	0.2678	0.261	2.533
3.50	0.2759	0.268	2.864
4.00	0.2839	0.276	2.784
4.50	0.2918	0.282	3.363
5.00	0.2997	0.289	3.556
5.50	0.3074	0.295	4.046
6.00	0.3152	0.301	4.497

(B) LATERAL INFLOW: 0.0125 CFS/FT			
DOWNSTREAM	DEPTH (FT)		PERCENT
DISTANCE (FT)	ANALYTICAL	EXPERIMENTAL	DIFFERENCE
0.0	0.2790	0.279	0.0
0.50	0.2881	0.287	0.373
1.00	0.2968	0.295	0.622
1.50	0.3054	0.300	1.767
2.00	0.3138	0.306	2.476
2.50	0.3220	0.314	2.487
3.00	0.3301	0.322	2.465
3.50	0.3382	0.328	3.011
4.00	0.3462	0.335	3.222
4.50	0.3541	0.342	3.407
5.00	0.3619	0.348	3.847
5.50	0.3697	0.354	4.258
6.00	0.3775	0.361	4.378

(C) LATERAL INFLOW: 0.0242 CFS/FT			
DOWNSTREAM	DEPTH (FT)		PERCENT
DISTANCE (FT)	ANALYTICAL	EXPERIMENTAL	DIFFERENCE
0.0	0.3260	0.326	0.0
0.50	0.3346	0.334	0.181
1.00	0.3431	0.341	0.602
1.50	0.3514	0.347	1.253
2.00	0.3596	0.354	1.570
2.50	0.3678	0.361	1.850
3.00	0.3759	0.368	2.099
3.50	0.3839	0.375	2.323
4.00	0.3919	0.382	2.526
4.50	0.3998	0.387	3.209
5.00	0.4077	0.393	3.612
5.50	0.4156	0.399	3.991
6.00	0.4234	0.405	4.350

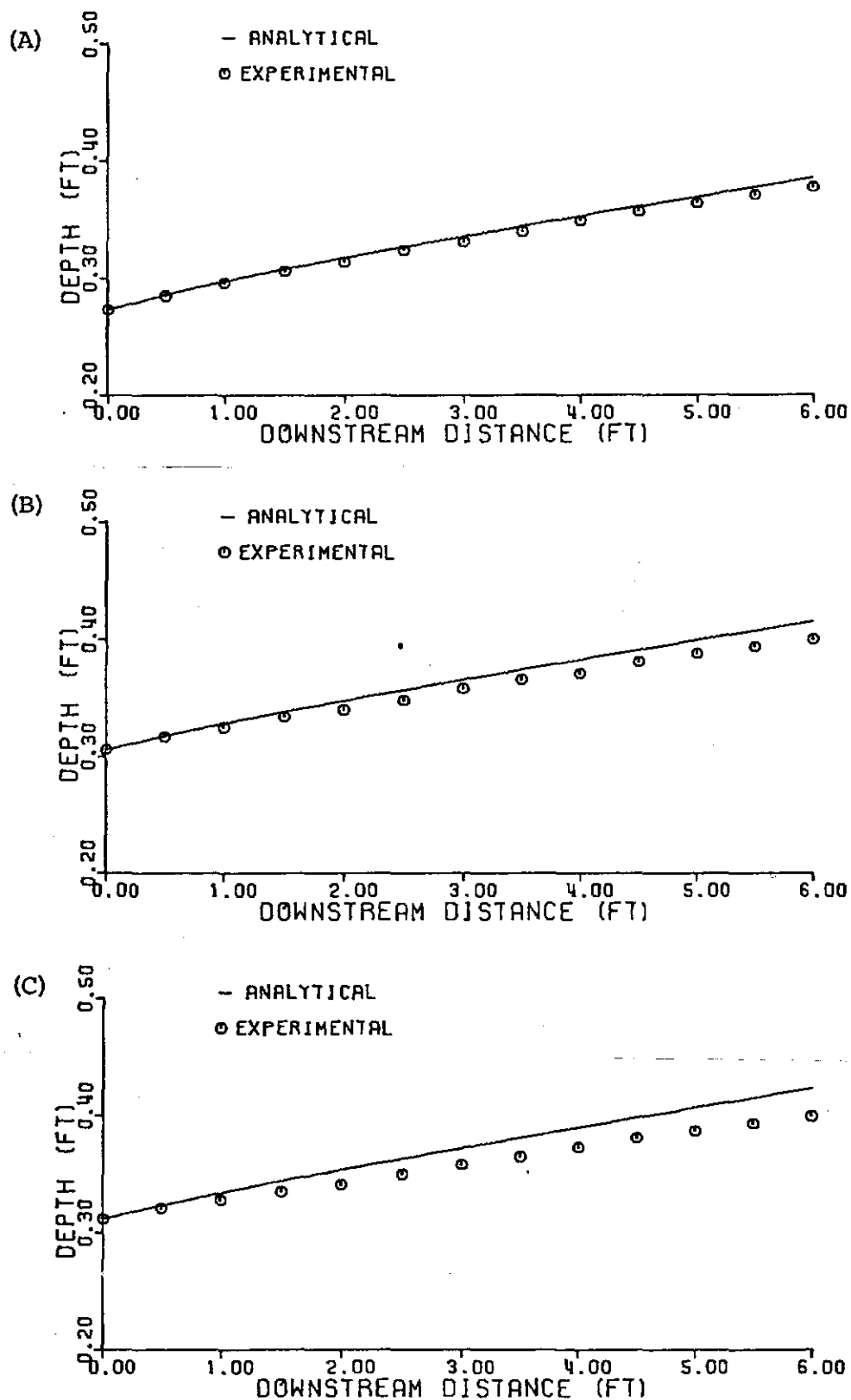


Fig. 7 Relationship Between Depth and Downstream Distance for Subcritical Flow;  $Q = 0.368$  cfs: (A)  $q_* = 0.0$  cfs/ft (B)  $q_* = 0.0125$  cfs/ft (C)  $q_* = 0.0242$  cfs/ft

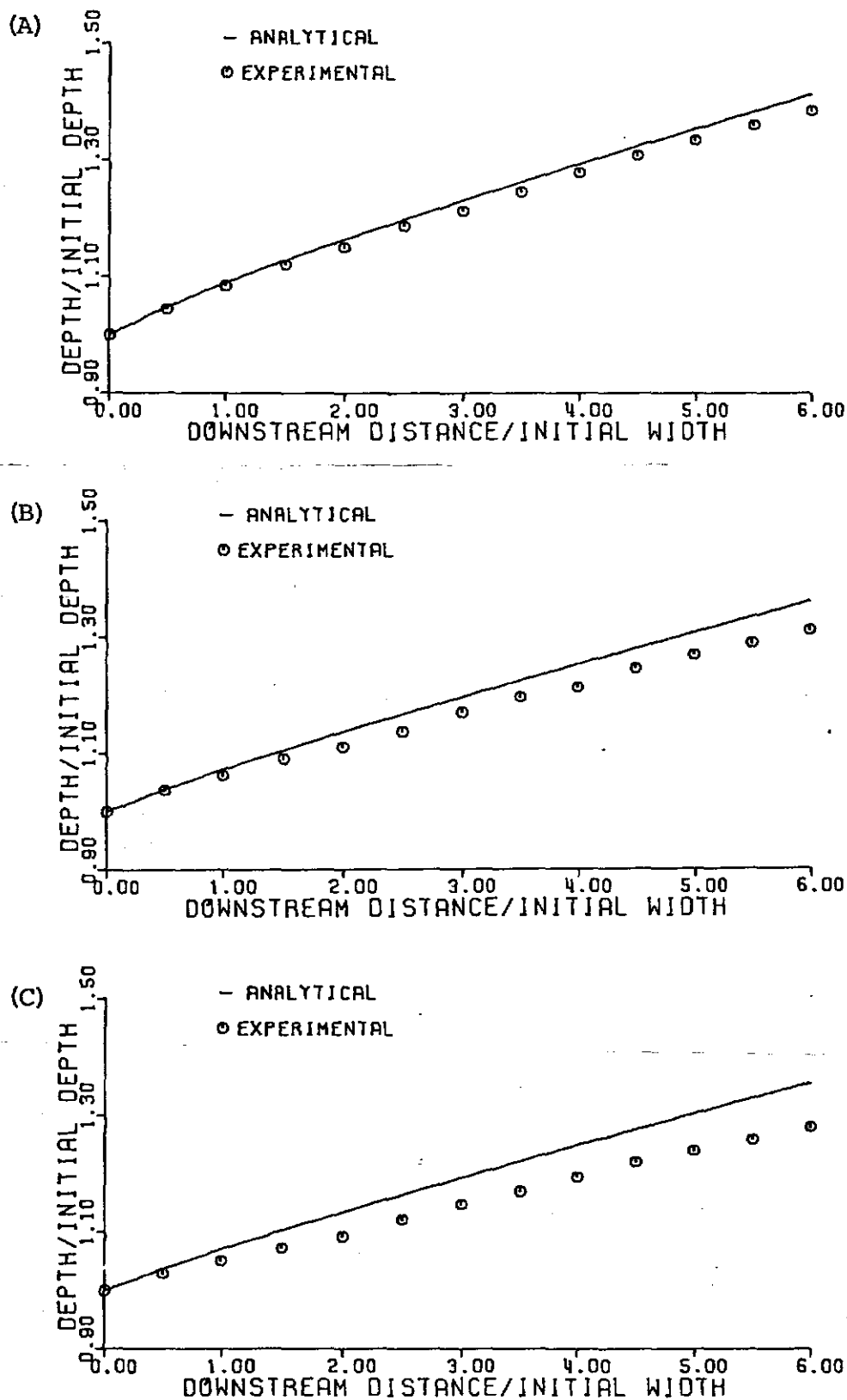


Fig. 8 Dimensionless Relationship Between Depth and Downstream Distance for Subcritical Flow;  $Q = 0.368$  cfs: (A)  $q_* = 0.0$  cfs/ft (B)  $q_* = 0.0125$  cfs/ft (C)  $q_* = 0.0242$  cfs/ft



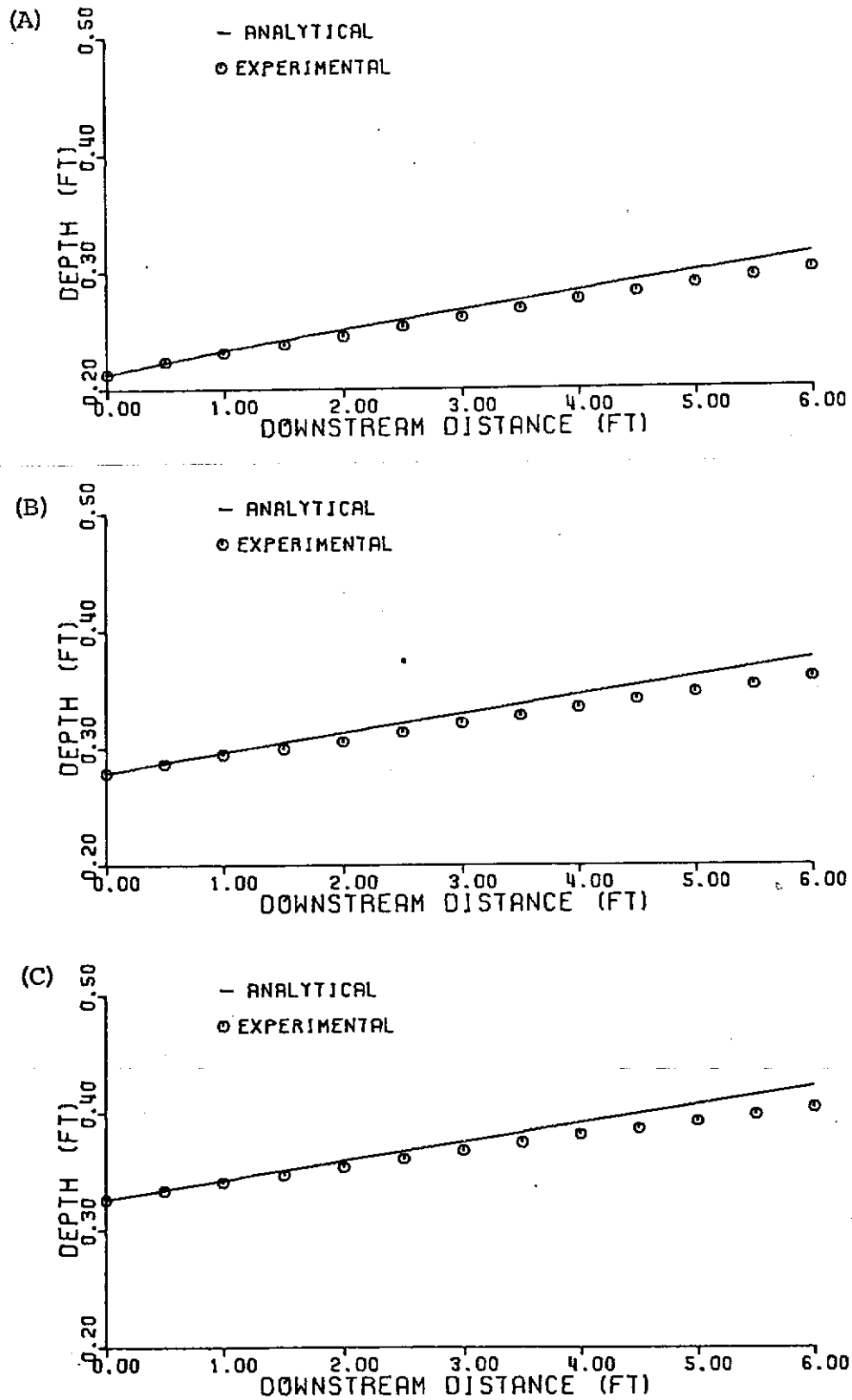


Fig. 9 Relationship Between Depth and Downstream Distance for Subcritical Flow;  $Q = 0.211$  cfs: (A)  $q_* = 0.0$  cfs/ft (B)  $q_* = 0.0125$  cfs/ft (C)  $q_* = 0.0242$  cfs/ft

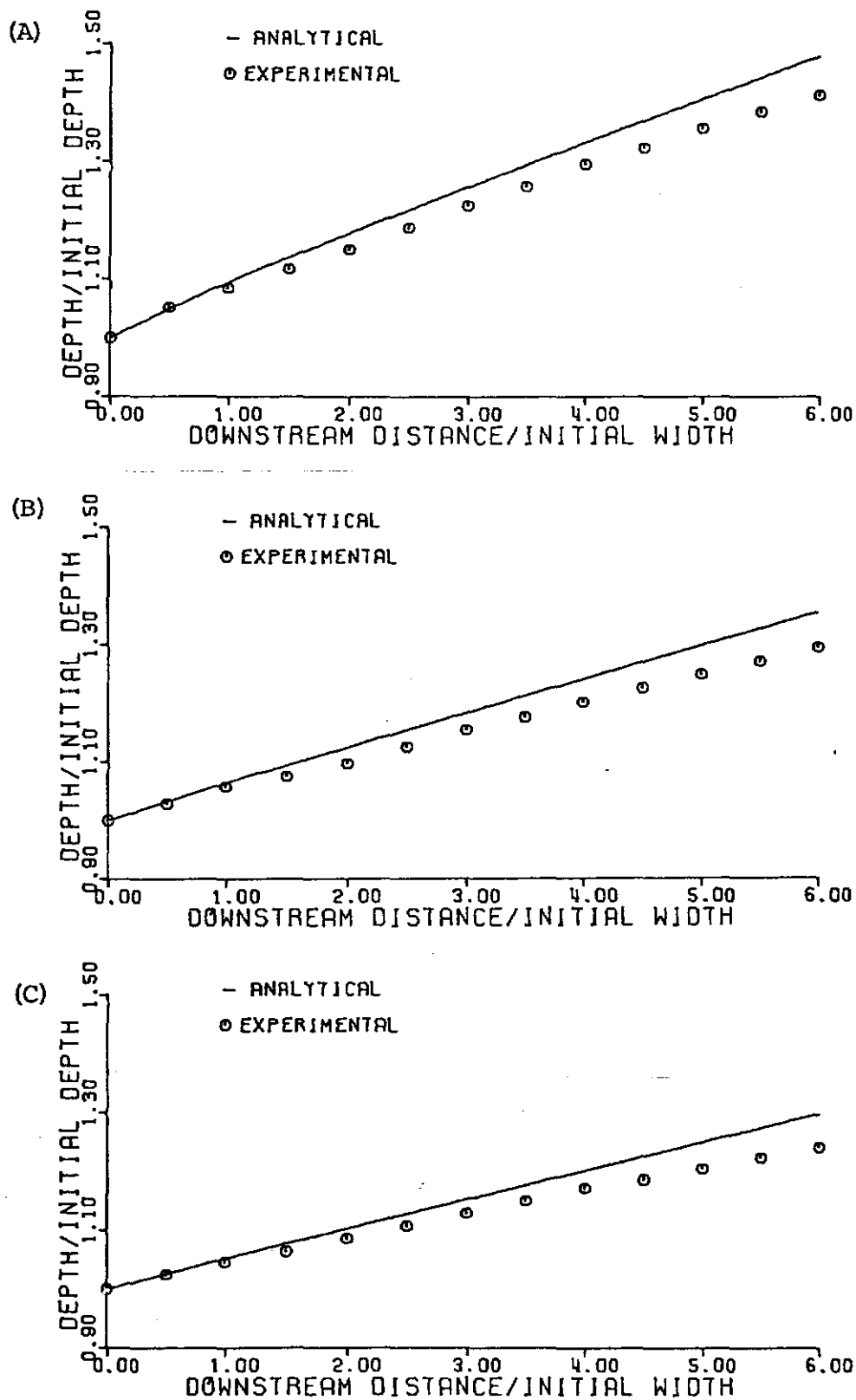


Fig. 10 Dimensionless Relationship Between Depth and Downstream Distance for Subcritical Flow;  $Q = 0.211$  cfs: (A)  $q_* = 0.0$  cfs/ft (B)  $q_* = 0.0125$  cfs/ft (C)  $q_* = 0.0242$  cfs/ft



(A)  $q_{\star} = 0.0$  cfs/ft



(B)  $q_{\star} = 0.0242$  cfs/ft

Fig 11 Typical Cross Waves of Supercritical Spatially Varied Flow  
(A) Without Lateral Inflow (B) With Lateral Inflow

TABLE III ANALYTICAL RESULTS FOR SUPERCRITICAL FLOW

MAIN CHANNEL FLOWRATE: 0.3632 CFS LATERAL INFLOW: 0.0 CFS/FT SLOPE: 1.00 %

POINT	DOWNSTREAM DISTANCE (FT)	TRANSVERSE DISTANCE (FT)	VELOCITY (FPS)		DEPTH (FT)
			X-DIRECTION	Y-DIRECTION	
0	0.0	0.500	2.9770	0.0	0.1220
1	0.025	0.478	2.9818	0.0	0.1219
2	0.161	0.359	3.0077	0.0	0.1213
3	0.299	0.239	3.0335	0.0	0.1207
4	0.440	0.120	3.0590	0.0	0.1201
5	0.584	0.000	3.0845	0.0	0.1195
6	0.056	0.505	3.1773	0.2648	0.1036
7	0.221	0.409	3.2037	0.2628	0.1033
8	0.389	0.313	3.2299	0.2610	0.1030
9	0.560	0.217	3.2560	0.2593	0.1027
10	0.734	0.120	3.2821	0.2576	0.1024
11	0.950	0.0	3.4800	0.0	0.0886
12	0.371	0.531	3.2293	0.2691	0.1025
13	0.542	0.435	3.2555	0.2672	0.1023
14	0.716	0.239	3.2816	0.2655	0.1020
15	0.893	0.243	3.3077	0.2638	0.1017
16	1.143	0.107	3.5070	0.0070	0.0879
17	1.341	0.0	3.5342	0.0	0.0871
18	0.697	0.558	3.2810	0.2734	0.1015
19	0.874	0.463	3.3071	0.2716	0.1012
20	1.054	0.367	3.3332	0.2699	0.1009
21	1.340	0.214	3.5340	0.0139	0.0872
22	1.541	0.107	3.5612	0.0069	0.0864
23	1.746	0.0	3.5884	0.0	0.0857
24	1.036	0.560	3.3326	0.2777	0.1005
25	1.219	0.491	3.3586	0.2759	0.1002
26	1.541	0.323	3.5610	0.0207	0.0864
27	1.746	0.216	3.5883	0.0127	0.0857
28	1.955	0.108	3.6156	0.0069	0.0850
29	2.168	0.0	3.6429	0.0	0.0843
30	1.386	0.615	3.3840	0.2820	0.0994
31	1.745	0.432	3.5880	0.0276	0.0857
32	1.954	0.325	3.6154	0.0206	0.0850
33	2.167	0.218	3.6428	0.0137	0.0843
34	2.384	0.109	3.6702	0.0068	0.0836
35	2.605	0.0	3.6976	0.0	0.0829
36	2.208	0.684	3.7612	0.3134	0.0753
37	2.459	0.595	3.7911	0.3059	0.0747
38	2.715	0.505	3.8210	0.2985	0.0742
39	2.975	0.414	3.8510	0.2912	0.0737
40	3.241	0.322	3.8810	0.2840	0.0731
41	4.130	0.0	4.0908	0.0	0.0649
42	2.697	0.725	3.8196	0.3183	0.0740
43	2.958	0.635	3.8496	0.3109	0.0735
44	3.224	0.545	3.8798	0.3036	0.0730
45	3.496	0.453	3.9101	0.2963	0.0724
46	4.444	0.118	4.1235	0.0125	0.0643
47	4.766	0.0	4.1567	0.0	0.0637
48	3.206	0.767	3.6783	0.3232	0.0728
49	3.478	0.677	3.9087	0.3159	0.0723
50	3.755	0.586	3.9391	0.3086	0.0718
51	4.765	0.238	4.1564	0.0250	0.0637
52	5.095	0.120	4.1898	0.0124	0.0630
53	5.431	0.0	4.2233	0.0	0.0624
54	3.736	0.811	3.9376	0.3281	0.0716
55	4.019	0.721	3.9693	0.3208	0.0711
56	5.092	0.360	4.1894	0.0374	0.0630
57	5.430	0.242	4.2232	0.0249	0.0624
58	5.774	0.122	4.2570	0.0125	0.0618
59	6.126	0.0	4.2911	0.0	0.0612
60	4.288	0.857	3.9975	0.3331	0.0705
61	5.426	0.484	4.2226	0.0500	0.0624
62	5.772	0.366	4.2567	0.0374	0.0618
63	6.125	0.246	4.2909	0.0250	0.0612
64	6.485	0.124	4.3253	0.0125	0.0606
65	6.853	0.0	4.3600	0.0	0.0600
66	6.950	1.079	4.4389	0.3699	0.0558

TABLE IV ANALYTICAL RESULTS FOR SUPERCRITICAL FLOW

MAIN CHANNEL FLOWRATE: 0.3632 CFS LATERAL INFLOW: 0.01250 CFS/FT SLOPE: 1.00 %

POINT	DOWNSTREAM DISTANCE (FT)	TRANSVERSE DISTANCE (FT)	VELOCITY (FPS)		DEPTH (FT)
			X-DIRECTION	Y-DIRECTION	
0	0.0	0.500	2.9770	0.0	0.1220
1	0.025	0.478	2.9818	0.0	0.1219
2	0.161	0.359	3.0077	0.0	0.1213
3	0.299	0.239	3.0335	0.0	0.1207
4	0.440	0.120	3.0590	0.0	0.1201
5	0.584	0.000	3.0845	0.0	0.1195
6	0.654	0.504	3.0032	0.2503	0.1111
7	0.208	0.399	3.1258	0.1418	0.1108
8	0.364	0.293	3.1515	0.1408	0.1104
9	0.522	0.186	3.1773	0.1398	0.1100
10	0.683	0.080	3.2029	0.1389	0.1096
11	0.805	0.0	3.3195	0.0	0.1007
12	0.359	0.530	3.0448	0.2537	0.1107
13	0.522	0.422	3.1732	0.1359	0.1102
14	0.683	0.315	3.1989	0.1349	0.1098
15	0.846	0.207	3.2244	0.1340	0.1093
16	0.987	0.116	3.3418	-0.0042	0.1004
17	1.170	0.0	3.2638	0.0	0.1001
18	0.684	0.557	3.0981	0.2582	0.1096
19	0.853	0.446	3.2260	0.1368	0.1091
20	1.019	0.341	3.2515	0.1359	0.1087
21	1.180	0.239	3.3695	-0.0017	0.0997
22	1.366	0.123	3.3914	0.0025	0.0994
23	1.566	0.0	3.4190	0.0	0.0987
24	1.022	0.585	3.1504	0.2625	0.1085
25	1.197	0.476	3.2783	0.1371	0.1081
26	1.379	0.362	3.3969	0.0003	0.0991
27	1.567	0.247	3.4188	0.0044	0.0988
28	1.770	0.124	3.4464	0.0019	0.0981
29	1.978	0.0	3.4737	0.0	0.0975
30	1.372	0.614	3.2024	0.2669	0.1075
31	1.583	0.487	3.4231	-0.0002	0.0985
32	1.773	0.372	3.4449	0.0040	0.0982
33	1.980	0.249	3.4725	0.0015	0.0976
34	2.191	0.125	3.4999	-0.0004	0.0969
35	2.406	0.0	3.5259	0.0	0.0964
36	1.839	0.653	3.4079	0.2840	0.0924
37	2.059	0.544	3.5430	0.1173	0.0922
38	2.284	0.430	3.5713	0.1144	0.0917
39	2.514	0.313	3.5994	0.1122	0.0911
40	2.748	0.197	3.6262	0.1123	0.0907
41	3.146	0.0	3.7302	0.0	0.0854
42	2.290	0.691	3.4485	0.2874	0.0923
43	2.530	0.574	3.5942	0.1030	0.0916
44	2.762	0.457	3.6222	0.1008	0.0910
45	2.998	0.339	3.6489	0.1009	0.0906
46	3.415	0.133	3.7535	-0.0111	0.0853
47	3.685	0.0	3.7767	0.0	0.0852
48	2.786	0.732	3.5071	0.2923	0.0911
49	3.035	0.614	3.6538	0.1012	0.0904
50	3.278	0.496	3.6805	-0.1013	0.0900
51	3.721	0.281	3.7862	-0.0103	0.0847
52	3.993	0.149	3.8093	0.0007	0.0846
53	4.306	0.0	3.8419	0.0	0.0840
54	3.310	0.776	3.5650	0.2971	0.0900
55	3.569	0.657	3.7121	0.1003	0.0894
56	4.037	0.432	3.8188	-0.0111	0.0841
57	4.312	0.301	3.8418	-0.0001	0.0840
58	4.629	0.152	3.8744	-0.0008	0.0834
59	4.957	0.0	3.9070	0.0	0.0828
60	3.850	0.821	3.6211	0.3018	0.0891
61	4.368	0.587	3.8505	-0.0159	0.0837
62	4.644	0.457	3.8733	-0.0049	0.0836
63	4.965	0.307	3.9060	-0.0056	0.0830
64	5.297	0.155	3.9365	-0.0048	0.0824
65	5.640	0.0	3.9700	0.0	0.0820
66	5.019	0.918	3.8170	0.3181	0.0801
67	5.354	0.787	3.9772	0.0708	0.0800
68	5.699	0.643	4.0106	0.0700	0.0794
69	6.054	0.497	4.0440	0.0707	0.0789
70	6.420	0.349	4.0762	0.0753	0.0786
71	7.289	0.0	4.1872	0.0	0.0753
72	5.736	0.578	3.8690	0.3224	0.0800
73	6.117	0.431	4.0420	0.0502	0.0794
74	6.474	0.683	4.0752	0.0509	0.0789
75	6.841	0.534	4.1072	0.0556	0.0785
76	7.732	0.175	4.2186	-0.0196	0.0752
77	8.173	0.0	4.2496	0.0	0.0751
78	8.561	1.047	3.9419	0.3285	0.0789

TABLE V ANALYTICAL RESULTS FOR SUPERCRITICAL FLOW

MAIN CHANNEL FLOWRATE: 0.3622 CFS LATERAL INFLOW: 0.02360 CFS/FT SLOPE: 1.00 %

POINT	DOWNSTREAM DISTANCE (FT)	TRANSVERSE DISTANCE (FT)	VELOCITY (FPS)		DEPTH (FT)
			X-DIRECTION	Y-DIRECTION	
0	0.0	0.500	2.9770	0.0	0.1220
1	0.025	0.478	2.9818	0.0	0.1219
2	0.161	0.359	3.0077	0.0	0.1213
3	0.294	0.239	3.0335	0.0	0.1207
4	0.440	0.120	3.0590	0.0	0.1201
5	0.584	0.000	3.0845	0.0	0.1195
6	0.052	0.504	2.8463	0.2372	0.1179
7	0.197	0.390	3.0554	0.0494	0.1173
8	0.342	0.275	3.0811	0.0490	0.1168
9	0.489	0.160	3.1067	0.0466	0.1163
10	0.640	0.045	3.1321	0.0483	0.1158
11	0.700	0.0	3.1793	0.0	0.1122
12	0.347	0.529	2.8925	0.2410	0.1173
13	0.503	0.409	3.1049	0.0440	0.1166
14	0.653	0.294	3.1303	0.0437	0.1160
15	0.806	0.178	3.1557	0.0434	0.1155
16	0.873	0.128	3.2029	-0.0046	0.1119
17	1.046	0.0	3.2265	0.0	0.1115
18	0.667	0.556	2.9477	0.2456	0.1162
19	0.830	0.435	3.1585	0.0424	0.1155
20	0.986	0.320	3.1837	0.0421	0.1149
21	1.061	0.265	3.2310	-0.0055	0.1113
22	1.239	0.137	3.2545	-0.0010	0.1110
23	1.432	0.0	3.2824	0.0	0.1104
24	1.003	0.584	3.0015	0.2501	0.1152
25	1.171	0.463	3.2114	0.0401	0.1144
26	1.255	0.403	3.2589	-0.0072	0.1107
27	1.435	0.276	3.2822	-0.0027	0.1104
28	1.632	0.139	3.3100	-0.0017	0.1098
29	1.834	0.0	3.3376	0.0	0.1093
30	1.351	0.613	3.0548	0.2546	0.1141
31	1.454	0.542	3.2657	-0.0106	0.1103
32	1.636	0.415	3.3089	-0.0061	0.1100
33	1.835	0.278	3.3367	-0.0051	0.1094
34	2.040	0.139	3.3642	-0.0034	0.1089
35	2.249	0.0	3.3906	0.0	0.1084
36	1.570	0.631	3.1372	0.2614	0.1081
37	1.768	0.505	3.3464	0.0248	0.1077
38	1.973	0.271	3.3762	0.0256	0.1071
39	2.185	0.235	3.4038	0.0271	0.1066
40	2.400	0.099	3.4303	0.0303	0.1062
41	2.558	0.0	3.4703	0.0	0.1041
42	1.983	0.665	3.1839	0.2653	0.1078
43	2.207	0.526	3.4021	0.0165	0.1070
44	2.421	0.389	3.4296	0.0181	0.1065
45	2.636	0.253	3.4560	0.0213	0.1061
46	2.803	0.151	3.4960	-0.0089	0.1039
47	3.049	0.0	3.5216	0.0	0.1037
48	2.456	0.705	3.2436	0.2703	0.1067
49	2.691	0.563	3.4621	0.0134	0.1059
50	2.911	0.427	3.4884	0.0167	0.1055
51	3.084	0.321	3.5266	-0.0133	0.1034
52	3.333	0.171	3.5540	-0.0045	0.1032
53	3.620	0.0	3.5864	0.0	0.1027
54	2.954	0.746	3.3028	-0.2752	0.1057
55	3.197	0.604	3.5208	0.0104	0.1051
56	3.378	0.495	3.5617	-0.0194	0.1029
57	3.629	0.345	3.5865	-0.0106	0.1027
58	3.920	0.175	3.6167	-0.0061	0.1022
59	4.223	0.0	3.6509	0.0	0.1017
60	3.470	0.789	3.3601	0.2800	0.1049
61	3.660	0.670	3.5927	-0.0278	0.1025
62	3.932	0.521	3.6178	-0.0190	0.1024
63	4.226	0.350	3.6499	-0.0145	0.1018
64	4.532	0.175	3.6820	-0.0084	0.1014
65	4.844	0.0	3.7129	0.0	0.1010
66	3.926	0.827	3.4354	0.2863	0.1014
67	4.206	0.676	3.6579	-0.0054	0.1010
68	4.507	0.507	3.6900	-0.0010	0.1005
69	4.819	0.334	3.7221	0.0050	0.1001
70	5.137	0.161	3.7530	0.0134	0.0998
71	5.438	0.0	3.7934	0.0	0.0985
72	4.528	0.877	3.4910	0.2909	0.1011
73	4.861	0.702	3.7224	-0.0149	0.1003
74	5.175	0.529	3.7543	-0.0089	0.0999
75	5.495	0.356	3.7851	-0.0005	0.0996
76	5.803	0.192	3.8254	-0.0138	0.0983
77	6.168	0.0	3.8572	0.0	0.0981
78	5.249	0.937	3.5623	0.2969	0.1001
79	5.603	0.757	3.7954	-0.0199	0.0994
80	5.926	0.584	3.8259	-0.0116	0.0991
81	6.242	0.417	3.8663	-0.0248	0.0978
82	6.610	0.226	3.8979	-0.0110	0.0976
83	7.055	0.0	3.9383	0.0	0.0971
84	6.020	1.002	3.6339	0.3028	0.0992

TABLE VI ANALYTICAL RESULTS FOR SUPERCRITICAL FLOW

MAIN CHANNEL FLOWRATE: 0.3632 CFS      LATERAL INFLOW: 0.0      CFS/FT      SLOPE: 4.00 %

POINT	DOWNSTREAM DISTANCE (FT)	TRANSVERSE DISTANCE (FT)	VELOCITY (FPS)		DEPTH (FT)
			X-DIRECTION	Y-DIRECTION	
0	0.0	0.500	3.4923	0.0	0.1040
1	0.036	0.478	3.5105	0.0	0.1036
2	0.237	0.359	3.6089	0.0	0.1015
3	0.449	0.239	3.7071	0.0	0.0995
4	0.671	0.120	3.8053	0.0	0.0975
5	0.904	0.000	3.9034	0.0	0.0955
6	0.083	0.507	3.6880	0.3073	0.0895
7	0.323	0.409	3.7942	0.3038	0.0881
8	0.577	0.311	3.9005	0.3008	0.0868
9	0.842	0.211	4.0069	0.2964	0.0854
10	1.120	0.111	4.1138	0.2962	0.0840
11	1.424	0.0	4.3542	0.0	0.0744
12	0.558	0.546	3.8991	0.3249	0.0858
13	0.825	0.449	4.0062	0.3217	0.0845
14	1.104	0.352	4.1137	0.3189	0.0832
15	1.397	0.253	4.2215	0.3166	0.0819
16	1.764	0.127	4.4746	0.0211	0.0723
17	2.125	0.0	4.5976	0.0	0.0703
18	1.086	0.590	4.1123	0.3427	0.0823
19	1.379	0.494	4.2207	0.3397	0.0811
20	1.686	0.397	4.3296	0.3371	0.0798
21	2.122	0.257	4.5963	0.0425	0.0703
22	2.506	0.130	4.7219	0.0214	0.0683
23	2.910	0.0	4.8489	0.0	0.0665
24	1.667	0.639	4.3283	0.3607	0.0790
25	1.989	0.544	4.4384	0.3579	0.0778
26	2.498	0.389	4.7193	0.0641	0.0684
27	2.906	0.262	4.8476	0.0429	0.0665
28	3.335	0.133	4.9775	0.0216	0.0646
29	3.786	0.0	5.1091	0.0	0.0629
30	2.306	0.692	4.5477	0.3790	0.0759
31	2.894	0.524	4.8437	0.0858	0.0665
32	3.327	0.397	4.9749	0.0647	0.0647
33	3.782	0.268	5.1078	0.0433	0.0629
34	4.260	0.136	5.2426	0.0218	0.0612
35	4.762	0.0	5.3793	0.0	0.0596
36	3.697	0.808	5.1516	0.4293	0.0594
37	4.248	0.705	5.3048	0.4086	0.0578
38	4.831	0.599	5.4607	0.3877	0.0562
39	5.449	0.490	5.6197	0.3667	0.0547
40	6.102	0.377	5.7820	0.3456	0.0533
41	6.140	0.0	6.3202	0.0	0.0473
42	4.815	0.901	5.4575	0.4548	0.0559
43	5.441	0.799	5.6189	0.4339	0.0544
44	6.104	0.693	5.7837	0.4130	0.0530
45	6.807	0.584	5.9520	0.3919	0.0516
46	9.126	0.194	6.5335	0.0454	0.0456
47	10.206	0.0	6.7592	0.0	0.0440
48	6.087	1.007	5.7804	0.4817	0.0527

TABLE VII ANALYTICAL RESULTS FOR SUPERCRITICAL FLOW

MAIN CHANNEL FLOWRATE: 0.3632 CFS      LATERAL INFLOW: 0.01250 CFS/FT      SLOPE: 4.00 %

POINT	DOWNSTREAM DISTANCE (FT)	TRANSVERSE DISTANCE (FT)	VELOCITY (FPS)		DEPTH (FT)
			X-DIRECTION	Y-DIRECTION	
0	0.0	0.500	3.4923	0.0	0.1040
1	0.036	0.478	3.5105	0.0	0.1036
2	0.237	0.359	3.6089	0.0	0.1015
3	0.449	0.239	3.7071	0.0	0.0995
4	0.671	0.120	3.8053	0.0	0.0975
5	0.904	0.000	3.9034	0.0	0.0955
6	0.080	0.507	3.4984	0.2915	0.0968
7	0.305	0.398	3.7083	0.1275	0.0951
8	0.536	0.287	3.8096	0.1262	0.0934
9	0.778	0.176	3.9110	0.1251	0.0917
10	1.031	0.064	4.0126	0.1242	0.0900
11	1.180	0.0	4.1276	0.0	0.0850
12	0.552	0.546	3.6997	0.3083	0.0934
13	0.808	0.434	3.9189	0.1180	0.0916
14	1.061	0.322	4.0203	0.1169	0.0900
15	1.326	0.210	4.1219	0.1160	0.0883
16	1.501	0.137	4.2412	-0.0075	0.0832
17	1.835	0.0	4.3548	0.0	0.0815
18	1.096	0.591	3.9114	0.3260	0.0899
19	1.380	0.478	4.1377	0.1072	0.0881
20	1.657	0.365	4.2394	0.1063	0.0865
21	1.862	0.283	4.3634	-0.0166	0.0814
22	2.209	0.146	4.4771	-0.0090	0.0797
23	2.598	0.0	4.5995	0.0	0.0780
24	1.707	0.642	4.1267	0.3439	0.0865
25	2.021	0.528	4.3617	0.0917	0.0848
26	2.259	0.436	4.4909	-0.0305	0.0796
27	2.620	0.298	4.6045	-0.0230	0.0780
28	3.023	0.152	4.7268	-0.0139	0.0764
29	3.462	0.0	4.8540	0.0	0.0748
30	2.392	0.699	4.3472	0.3623	0.0833
31	2.696	0.594	4.6234	-0.0520	0.0780
32	3.070	0.456	4.7368	-0.0445	0.0764
33	3.487	0.309	4.8588	-0.0355	0.0748
34	3.940	0.157	4.9855	-0.0215	0.0733
35	4.430	0.0	5.1162	0.0	0.0718
36	3.112	0.759	4.6158	0.3847	0.0751
37	3.568	0.623	4.9020	0.0042	0.0734
38	4.014	0.480	5.0267	0.0132	0.0719
39	4.496	0.332	5.1559	0.0271	0.0705
40	5.016	0.180	5.2889	0.0487	0.0692
41	5.657	0.0	5.4689	0.0	0.0666
42	4.175	0.848	4.8918	0.4076	0.0721
43	4.724	0.697	5.2049	-0.0422	0.0703
44	5.218	0.547	5.3324	-0.0284	0.0689
45	5.749	0.394	5.4632	-0.0068	0.0677
46	6.426	0.205	5.6448	-0.0557	0.0651
47	7.199	0.0	5.8160	0.0	0.0638
48	5.499	0.958	5.2059	0.4338	0.0690
49	6.141	0.796	5.5449	-0.1070	0.0672
50	6.681	0.640	5.6723	-0.0855	0.0660
51	7.399	0.439	5.8553	-0.1348	0.0635
52	8.171	0.234	6.0200	-0.0791	0.0623
53	9.131	0.0	6.2153	0.0	0.0610
54	7.122	1.094	5.5552	0.4629	0.0659



TABLE VIII ANALYTICAL RESULTS FOR SUPERCRITICAL FLOW

MAIN CHANNEL FLOWRATE: 0.3632 CFS      LATERAL INFLOW: 0.02360 CFS/FT      SLOPE: 4.00 %

POINT	DOWNSTREAM DISTANCE (FT)	TRANSVERSE DISTANCE (FT)	VELOCITY (FPS)		DEPTH (FT)
			X-DIRECTION	Y-DIRECTION	
0	0.0	0.500	3.4923	0.0	0.1040
1	0.036	0.478	3.5105	0.0	0.1036
2	0.237	0.359	3.6089	0.0	0.1015
3	0.449	0.239	3.7071	0.0	0.0995
4	0.671	0.120	3.8053	0.0	0.0975
5	0.904	0.000	3.9034	0.0	0.0955
6	0.078	0.507	3.3385	0.2782	0.1034
7	0.290	0.389	3.6323	-0.0027	0.1011
8	0.504	0.269	3.7305	-0.0027	0.0991
9	0.729	0.150	3.8286	-0.0026	0.0971
10	0.964	0.030	3.9267	-0.0026	0.0952
11	1.024	0.0	3.9499	0.0	0.0948
12	0.542	0.545	3.5440	0.2953	0.0997
13	0.791	0.420	3.8458	-0.0205	0.0973
14	1.026	0.300	3.9435	-0.0203	0.0953
15	1.272	0.179	4.0413	-0.0201	0.0934
16	1.335	0.149	4.0644	-0.0175	0.0931
17	1.656	0.0	4.1780	0.0	0.0914
18	1.095	0.591	3.7548	0.3129	0.0961
19	1.373	0.464	4.0662	-0.0505	0.0938
20	1.630	0.341	4.1635	-0.0502	0.0919
21	1.695	0.311	4.1865	-0.0476	0.0916
22	2.026	0.161	4.2989	-0.0300	0.0900
23	2.405	0.0	4.4182	0.0	0.0886
24	1.726	0.644	3.9701	0.3306	0.0928
25	2.036	0.513	4.2935	-0.0890	0.0905
26	2.103	0.483	4.3162	-0.0863	0.0901
27	2.444	0.332	4.4273	-0.0687	0.0886
28	2.831	0.170	4.5447	-0.0387	0.0872
29	3.264	0.0	4.6690	0.0	0.0859
30	2.446	0.704	4.1917	0.3493	0.0895
31	2.557	0.660	4.4513	-0.1345	0.0888
32	2.907	0.508	4.5607	-0.1168	0.0872
33	3.300	0.345	4.6759	-0.0868	0.0859
34	3.738	0.175	4.7977	-0.0481	0.0847
35	4.216	0.0	4.9235	0.0	0.0836
36	2.706	0.725	4.2559	0.3547	0.0889
37	3.096	0.576	4.6086	-0.1486	0.0870
38	3.490	0.412	4.7226	-0.1185	0.0858
39	3.927	0.241	4.8429	-0.0798	0.0846
40	4.403	0.065	4.9670	-0.0317	0.0834
41	4.589	0.0	5.0098	0.0	0.0833
42	3.648	0.804	4.5164	0.3764	0.0859
43	4.145	0.629	4.8951	-0.1840	0.0841
44	4.588	0.457	5.0121	-0.1453	0.0830
45	5.066	0.282	5.1323	-0.0972	0.0820
46	5.248	0.218	5.1730	-0.0656	0.0819
47	5.909	0.0	5.3310	0.0	0.0806
48	4.882	0.907	4.8126	0.4010	0.0833
49	5.469	0.715	5.2171	-0.2554	0.0815
50	5.943	0.539	5.3316	-0.2074	0.0806
51	6.119	0.477	5.3693	-0.1757	0.0806
52	6.770	0.257	5.5196	-0.1102	0.0794
53	7.608	0.0	5.6972	0.0	0.0784
54	6.406	1.034	5.1425	0.4285	0.0807

TABLE IX ANALYTICAL RESULTS FOR SUPERCRITICAL FLOW

MAIN CHANNEL FLOWRATE: 0.1967 CFS      LATERAL INFLOW: 0.0      CFS/FT      SLOPE: 1.00 %

POINT	DOWNSTREAM DISTANCE (FT)	TRANSVERSE DISTANCE (FT)	VELOCITY (FPS)		DEPTH (FT)
			X-DIRECTION	Y-DIRECTION	
0	0.0	0.500	2.8097	0.0	0.0700
1	0.035	0.478	2.8153	0.0	0.0699
2	0.227	0.359	2.8456	0.0	0.0694
3	0.422	0.239	2.8758	0.0	0.0688
4	0.622	0.120	2.9059	0.0	0.0683
5	0.825	0.000	2.9361	0.0	0.0678
6	0.080	0.507	2.9494	0.2458	0.0605
7	0.308	0.409	2.9830	0.2424	0.0602
8	0.539	0.310	3.0153	0.2412	0.0598
9	0.776	0.211	3.0476	0.2400	0.0595
10	1.017	0.112	3.0799	0.2389	0.0591
11	1.284	0.0	3.2349	0.0	0.0521
12	0.522	0.544	3.0160	0.2513	0.0595
13	0.760	0.446	3.0486	0.2502	0.0591
14	1.002	0.349	3.0811	0.2491	0.0588
15	1.249	0.251	3.1137	0.2480	0.0585
16	1.566	0.123	3.2727	0.0113	0.0514
17	1.857	0.0	3.3111	0.0	0.0507
18	0.983	0.582	3.0806	0.2567	0.0585
19	1.230	0.485	3.1132	0.2556	0.0582
20	1.482	0.387	3.1458	0.2545	0.0579
21	1.847	0.244	3.3080	0.0185	0.0509
22	2.148	0.121	3.3469	0.0070	0.0502
23	2.445	0.0	3.3829	0.0	0.0496
24	1.463	0.622	3.1452	0.2621	0.0576
25	1.720	0.525	3.1780	0.2610	0.0573
26	2.135	0.366	3.3434	0.0256	0.0503
27	2.444	0.242	3.3827	0.0140	0.0496
28	2.749	0.122	3.4190	0.0070	0.0490
29	3.061	0.0	3.4554	0.0	0.0485
30	1.962	0.664	3.2102	0.2675	0.0567
31	2.428	0.489	3.3789	0.0328	0.0497
32	2.747	0.365	3.4187	0.0210	0.0490
33	3.060	0.244	3.4553	0.0140	0.0485
34	3.380	0.123	3.4919	0.0070	0.0480
35	3.706	0.0	3.5288	0.0	0.0474
36	3.037	0.753	3.5284	0.2940	0.0444
37	3.425	0.648	3.5743	0.2797	0.0438
38	3.803	0.548	3.6154	0.2723	0.0434
39	4.190	0.446	3.6566	0.2650	0.0429
40	4.586	0.342	3.6981	0.2576	0.0425
41	5.828	0.0	3.9031	0.0	0.0382
42	3.809	0.817	3.6185	0.3015	0.0431
43	4.202	0.719	3.6604	0.2943	0.0427
44	4.603	0.619	3.7024	0.2871	0.0423
45	5.015	0.518	3.7448	0.2799	0.0418
46	6.380	0.165	3.9592	0.0252	0.0376
47	6.965	0.0	4.0175	0.0	0.0369
48	4.584	0.882	3.7009	0.3084	0.0421
49	4.997	0.783	3.7435	0.3012	0.0417
50	5.419	0.683	3.7863	0.2940	0.0413
51	6.890	0.317	4.0076	0.0397	0.0370
52	7.501	0.150	4.0674	0.0142	0.0363
53	8.056	0.0	4.1181	0.0	0.0358
54	5.399	0.950	3.7848	0.3154	0.0412
55	5.834	0.851	3.8282	0.3082	0.0408
56	7.414	0.471	4.0564	0.0541	0.0365
57	8.052	0.304	4.1177	0.0284	0.0358
58	8.626	0.154	4.1664	0.0142	0.0353
59	9.217	0.0	4.2215	0.0	0.0348
60	6.259	1.022	3.8702	0.3225	0.0402

TABLE X ANALYTICAL RESULTS FOR SUPERCRITICAL FLOW

MAIN CHANNEL FLOWRATE: 0.1967 CFS      LATERAL INFLOW: 0.01250 CFS/FT      SLOPE: 1.00 %

POINT	DOWNSTREAM DISTANCE (FT)	TRANSVERSE DISTANCE (FT)	VELOCITY (FPS)		DEPTH (FT)
			X-DIRECTION	Y-DIRECTION	
0	0.0	0.500	2.8097	0.0	0.0700
1	0.035	0.476	2.8153	0.0	0.0699
2	0.227	0.359	2.8456	0.0	0.0694
3	0.422	0.229	2.8758	0.0	0.0688
4	0.622	0.120	2.9059	0.0	0.0683
5	0.825	0.000	2.9361	0.0	0.0678
6	0.075	0.506	2.6773	0.2231	0.0694
7	0.278	0.390	2.8594	0.0098	0.0688
8	0.476	0.271	2.8897	0.0097	0.0683
9	0.678	0.153	2.9200	0.0094	0.0678
10	0.884	0.034	2.9502	0.0096	0.0673
11	0.944	0.0	2.9644	0.0	0.0667
12	0.503	0.542	2.7362	0.2280	0.0686
13	0.725	0.420	2.9724	0.0022	0.0679
14	0.931	0.300	2.9527	0.0021	0.0674
15	1.140	0.181	2.9828	0.0021	0.0669
16	1.203	0.146	2.9970	-0.0074	0.0664
17	1.465	0.0	3.0295	0.0	0.0661
18	0.974	0.581	2.8021	0.2335	0.0676
19	1.207	0.458	2.9892	-0.0030	0.0670
20	1.421	0.338	3.0194	-0.0031	0.0664
21	1.487	0.301	3.0337	-0.0126	0.0659
22	1.753	0.156	3.0660	-0.0052	0.0656
23	2.046	0.0	3.1024	0.0	0.0651
24	1.472	0.623	2.8668	0.2389	0.0667
25	1.715	0.499	3.0559	-0.0102	0.0660
26	1.785	0.461	3.0704	-0.0197	0.0655
27	2.054	0.315	3.1025	-0.0123	0.0652
28	2.251	0.154	3.1388	-0.0071	0.0647
29	2.661	0.0	3.1750	0.0	0.0643
30	1.995	0.666	2.9318	0.2443	0.0658
31	2.089	0.620	3.1067	-0.0275	0.0651
32	2.362	0.474	3.1388	-0.0202	0.0648
33	2.663	0.318	3.1749	-0.0150	0.0643
34	2.977	0.159	3.2110	-0.0079	0.0639
35	3.296	0.0	3.2467	0.0	0.0635
36	2.198	0.683	2.9616	0.2465	0.0649
37	2.494	0.541	3.1565	-0.0187	0.0644
38	2.798	0.385	3.1927	-0.0136	0.0640
39	3.114	0.226	3.2287	-0.0065	0.0636
40	3.436	0.068	3.2645	0.0013	0.0632
41	3.577	0.0	3.2822	0.0	0.0629
42	2.839	0.737	3.0313	0.2526	0.0643
43	3.186	0.576	3.2339	-0.0279	0.0637
44	3.506	0.417	3.2698	-0.0209	0.0633
45	3.832	0.258	3.3053	-0.0130	0.0629
46	3.476	0.189	3.3230	-0.0143	0.0626
47	4.377	0.0	3.3634	0.0	0.0623
48	3.598	0.800	3.1133	0.2594	0.0634
49	3.970	0.635	3.3183	-0.0352	0.0628
50	4.301	0.475	3.3537	-0.0275	0.0625
51	4.448	0.406	3.3714	-0.0268	0.0622
52	4.852	0.217	3.4114	-0.0145	0.0619
53	5.333	0.0	3.4590	0.0	0.0614
54	4.417	0.868	3.1956	0.2663	0.0626
55	4.805	0.702	3.4034	-0.0454	0.0621
56	4.956	0.631	3.4212	-0.0466	0.0618
57	5.364	0.443	3.4607	-0.0325	0.0615
58	5.848	0.225	3.5079	-0.0180	0.0611
59	6.366	0.0	3.5561	0.0	0.0607
60	5.278	0.940	3.2783	0.2732	0.0619
61	5.479	0.856	3.4706	-0.0662	0.0614
62	5.891	0.667	3.5099	-0.0520	0.0611
63	6.378	0.449	3.5566	-0.0376	0.0607
64	6.899	0.224	3.6043	-0.0195	0.0604
65	7.434	0.0	3.6519	0.0	0.0600
66	5.728	0.477	3.3219	0.2768	0.0613
67	6.189	0.791	3.5383	-0.0607	0.0609
68	6.680	0.573	3.5849	-0.0463	0.0605
69	7.203	0.348	3.6323	-0.0282	0.0601
70	7.740	0.125	3.6796	-0.0087	0.0598
71	8.047	0.0	3.7072	0.0	0.0596
72	8.766	1.064	3.4132	0.2844	0.0607

TABLE XI ANALYTICAL RESULTS FOR SUPERCRITICAL FLOW

MAIN CHANNEL FLOWPATE: 0.1967 CFS LATERAL INFLOW: 0.02360 CFS/FT SLOPE: 1.00 %

POINT	DOWNSTREAM DISTANCE (FT)	TRANSVERSE DISTANCE (FT)	VELOCITY (FPS)		DEPTH (FT)
			X-DIRECTION	Y-DIRECTION	
0	0.0	0.500	2.8097	0.0	0.0700
1	0.210	0.369	2.8430	0.0	0.0694
2	0.361	0.276	2.8663	0.0	0.0690
3	0.513	0.184	2.8896	0.0	0.0686
4	0.668	0.092	2.9128	0.0	0.0682
5	0.825	0.0	2.9361	0.0	0.0678
6	0.438	0.537	2.5072	0.2069	0.0767
7	0.605	0.423	2.8055	-0.1523	0.0753
8	0.744	0.320	2.8264	-0.1492	0.0748
9	0.884	0.217	2.8488	-0.1487	0.0742
10	1.027	0.115	2.8711	-0.1482	0.0737
11	1.191	0.0	2.8049	0.0	0.0805
12	0.805	0.567	2.5880	0.2157	0.0742
13	0.979	0.455	2.8689	-0.1416	0.0737
14	1.125	0.353	2.8916	-0.1410	0.0732
15	1.272	0.252	2.9140	-0.1411	0.0727
16	1.415	0.155	2.8464	0.0058	0.0795
17	1.647	0.0	2.8880	0.0	0.0785
18	1.185	0.599	2.6339	0.2195	0.0737
19	1.365	0.486	2.9186	-0.1556	0.0731
20	1.514	0.384	2.9410	-0.1552	0.0726
21	1.634	0.303	2.8722	-0.0092	0.0796
22	1.670	0.145	2.9136	-0.0149	0.0786
23	2.093	0.0	2.9368	0.0	0.0786
24	1.589	0.632	2.6691	0.2224	0.0739
25	1.771	0.520	2.9635	-0.1782	0.0729
26	1.866	0.455	2.8933	-0.0332	0.0801
27	2.105	0.295	2.9345	-0.0387	0.0790
28	2.326	0.146	2.9543	-0.0238	0.0791
29	2.557	0.0	2.9744	0.0	0.0796
30	2.605	0.667	2.7213	0.2268	0.0731
31	2.103	0.607	2.9271	-0.0385	0.0797
32	2.347	0.445	2.9682	-0.0440	0.0786
33	2.571	0.300	2.9929	-0.0292	0.0787
34	2.801	0.154	3.0127	-0.0055	0.0792
35	3.050	0.0	3.0457	0.0	0.0787
36	2.204	0.684	2.6534	0.2211	0.0829
37	2.460	0.514	2.9474	-0.1089	0.0814
38	2.674	0.363	2.9660	-0.0929	0.0815
39	2.695	0.211	2.9852	-0.0689	0.0820
40	3.132	0.051	3.0177	-0.0630	0.0815
41	3.210	0.0	2.9895	0.0	0.0844
42	2.765	0.730	2.7493	0.2291	0.0806
43	3.021	0.571	3.0179	-0.0931	0.0805
44	3.243	0.423	3.0371	-0.0698	0.0810
45	3.488	0.263	3.0694	-0.0639	0.0805
46	3.552	0.222	3.0404	-0.0015	0.0835
47	3.904	0.0	3.0911	0.0	0.0826
48	3.319	0.777	2.8096	0.2341	0.0807
49	3.579	0.619	3.0730	-0.0892	0.0810
50	3.826	0.458	3.1052	-0.0835	0.0805
51	3.876	0.426	3.0755	-0.0215	0.0835
52	4.233	0.201	3.1258	-0.0199	0.0826
53	4.563	0.0	3.1600	0.0	0.0826
54	3.879	0.823	2.8642	0.2387	0.0813
55	4.170	0.651	3.1385	-0.1064	0.0806
56	4.206	0.628	3.1082	-0.0451	0.0838
57	4.567	0.400	3.1581	-0.0432	0.0828
58	4.896	0.198	3.1918	-0.0233	0.0828
59	5.228	0.0	3.2230	0.0	0.0830
60	4.516	0.876	2.9397	0.2450	0.0805
61	4.571	0.844	3.1516	-0.0576	0.0834
62	4.940	0.614	3.2013	-0.0560	0.0824
63	5.271	0.414	3.2346	-0.0362	0.0824
64	5.603	0.218	3.2653	-0.0130	0.0827
65	5.993	0.0	3.3072	0.0	0.0823
66	4.631	0.886	2.9052	0.2421	0.0851
67	5.017	0.658	3.1892	-0.0927	0.0839
68	5.340	0.453	3.2218	-0.0723	0.0839
69	5.665	0.253	3.2522	-0.0489	0.0841
70	6.037	0.031	3.2936	-0.0358	0.0837
71	6.090	0.0	3.2800	0.0	0.0852
72	5.480	0.957	3.0106	0.2509	0.0835
73	5.863	0.742	3.2819	-0.0868	0.0832
74	6.191	0.544	3.3119	-0.0639	0.0834
75	6.569	0.323	3.3529	-0.0507	0.0830
76	6.811	0.298	3.3387	-0.0152	0.0845
77	7.140	0.0	3.3967	0.0	0.0839
78	8.317	1.026	3.0967	0.2581	0.0832

TABLE XII ANALYTICAL RESULTS FOR SUPERCRITICAL FLOW

MAIN CHANNEL FLOWRATE: 0.1967 CFS LATERAL INFLOW: 0.0 CFS/FT SLOPE: 4.00 %

POINT	DOWNSTREAM DISTANCE (FT)	TRANSVERSE DISTANCE (FT)	VELOCITY (FPS)		DEPTH (FT)
			X-DIRECTION	Y-DIRECTION	
0	0.0	0.500	3.3336	0.0	0.0590
1	0.049	0.478	3.3561	0.0	0.0587
2	0.323	0.359	3.4791	0.0	0.0569
3	0.615	0.239	3.6029	0.0	0.0552
4	0.924	0.120	3.7275	0.0	0.0536
5	1.250	0.000	3.8531	0.0	0.0521
6	0.116	0.510	3.4934	0.2911	0.0517
7	0.445	0.412	3.6316	0.2869	0.0504
8	0.795	0.314	3.7699	0.2853	0.0492
9	1.166	0.216	3.9097	0.2840	0.0479
10	1.563	0.117	4.0511	0.2830	0.0466
11	2.012	0.0	4.2954	0.0	0.0419
12	0.781	0.565	3.7709	0.3142	0.0485
13	1.158	0.470	3.9126	0.3128	0.0473
14	1.558	0.375	4.0559	0.3116	0.0461
15	1.963	0.279	4.2009	0.3112	0.0449
16	2.546	0.148	4.4715	0.0318	0.0401
17	3.137	0.0	4.6572	0.0	0.0384
18	1.540	0.628	4.0548	0.3379	0.0456
19	1.968	0.536	4.2010	0.3366	0.0445
20	2.421	0.443	4.3491	0.3360	0.0424
21	3.104	0.297	4.6450	0.0575	0.0386
22	3.753	0.148	4.8393	0.0247	0.0369
23	4.423	0.0	5.0285	0.0	0.0355
24	2.403	0.700	4.3480	0.3623	0.0429
25	2.885	0.610	4.4993	0.3615	0.0419
26	3.702	0.452	4.8222	0.0838	0.0371
27	4.414	0.302	5.0259	0.0500	0.0355
28	5.143	0.154	5.2226	0.0252	0.0341
29	5.927	0.0	5.4245	0.0	0.0328
30	3.378	0.781	4.6517	0.3876	0.0405
31	4.341	0.612	5.0034	0.1110	0.0357
32	5.124	0.461	5.2173	0.0759	0.0342
33	5.917	0.313	5.4219	0.0511	0.0328
34	6.769	0.160	5.6323	0.0259	0.0316
35	7.687	0.0	5.8490	0.0	0.0304
36	5.751	0.979	5.4165	0.4514	0.0318
37	6.858	0.860	5.6899	0.4148	0.0304
38	7.960	0.743	5.9461	0.3877	0.0291
39	9.156	0.618	6.2107	0.3604	0.0279
40	10.460	0.486	6.4855	0.3317	0.0268
41	15.047	0.0	7.4009	0.0	0.0231
42	8.127	1.177	5.9851	0.4988	0.0287

TABLE XIII ANALYTICAL RESULTS FOR SUPERCRITICAL FLOW

MAIN CHANNEL FLOWRATE: 0.1967 CFS      LATERAL INFLOW: 0.01250 CFS/FT      SLOPE: 4.00 %

POINT	DOWNSTREAM DISTANCE (FT)	TRANSVERSE DISTANCE (FT)	VELOCITY (FPS)		DEPTH (FT)
			X-DIRECTION	Y-DIRECTION	
0	0.0	0.500	3.3336	0.0	0.0590
1	0.049	0.478	3.3561	0.0	0.0587
2	0.323	0.359	3.4791	0.0	0.0569
3	0.615	0.239	3.6029	0.0	0.0552
4	0.924	0.120	3.7275	0.0	0.0536
5	1.250	0.000	3.8531	0.0	0.0521
6	0.109	0.509	3.1760	0.2647	0.0604
7	0.399	0.390	3.4794	-0.0768	0.0583
8	0.682	0.265	3.5997	-0.0757	0.0565
9	0.982	0.141	3.7210	-0.0755	0.0548
10	1.297	0.017	3.8431	-0.0754	0.0532
11	1.341	0.0	3.8331	0.0	0.0543
12	0.784	0.565	3.4375	0.2865	0.0572
13	1.146	0.433	3.7645	-0.1256	0.0551
14	1.463	0.304	3.8860	-0.1261	0.0534
15	1.794	0.177	4.0071	-0.1258	0.0518
16	1.820	0.167	3.9923	-0.0505	0.0530
17	2.306	0.0	4.1468	0.0	0.0519
18	1.658	0.638	3.7272	0.3106	0.0541
19	2.093	0.496	4.0814	-0.2069	0.0520
20	2.445	0.361	4.2026	-0.2074	0.0504
21	2.446	0.361	4.1622	-0.1320	0.0517
22	2.933	0.193	4.3298	-0.0816	0.0507
23	3.553	0.0	4.5033	0.0	0.0497
24	2.768	0.731	4.0478	0.3373	0.0512
25	3.298	0.565	4.4347	-0.3303	0.0490
26	3.268	0.577	4.4081	-0.2550	0.0504
27	3.748	0.407	4.5462	-0.2047	0.0495
28	4.348	0.214	4.7067	-0.1231	0.0487
29	5.104	0.0	4.8929	0.0	0.0479
30	4.290	0.857	4.4189	0.3662	0.0483
31	4.413	0.823	4.6883	-0.4470	0.0491
32	4.891	0.645	4.8185	-0.3952	0.0482
33	5.449	0.453	4.9606	-0.3136	0.0476
34	6.136	0.241	5.1230	-0.1905	0.0471
35	7.058	0.0	5.3215	0.0	0.0466
36	4.646	0.887	4.4588	0.3716	0.0498
37	5.259	0.706	4.8761	-0.5229	0.0485
38	5.787	0.513	5.0102	-0.4422	0.0479
39	6.432	0.299	5.1628	-0.3203	0.0475
40	7.293	0.053	5.3487	-0.1314	0.0471
41	7.505	0.0	5.3729	0.0	0.0477
42	6.676	1.056	4.9130	0.4094	0.0472

TABLE XIV ANALYTICAL RESULTS FOR SUPERCRITICAL FLOW

MAIN CHANNEL FLOWRATE: 0.1967 CFS LATERAL INFLOW: 0.02360 CFS/FT SLOPE: 4.00 %

POINT	DOWNSTREAM DISTANCE (FT)	TRANSVERSE DISTANCE (FT)	VELOCITY (FPS)		DEPTH (FT)
			X-DIRECTION	Y-DIRECTION	
0	0.0	0.500	3.3336	0.0	0.0590
1	0.307	0.366	3.4719	0.0	0.0570
2	0.527	0.274	3.5664	0.0	0.0557
3	0.758	0.183	3.6614	0.0	0.0545
4	0.999	0.091	3.7570	0.0	0.0533
5	1.250	0.000	3.8531	0.0	0.0521
6	0.693	0.558	3.1602	0.2634	0.0651
7	0.959	0.428	3.5694	-0.3738	0.0620
8	1.158	0.318	3.6518	-0.3700	0.0604
9	1.362	0.209	3.7347	-0.3695	0.0589
10	1.574	0.101	3.8178	-0.3693	0.0575
11	1.798	0.0	3.7797	0.0	0.0642
12	1.408	0.617	3.4026	0.2836	0.0616
13	1.730	0.474	3.8285	-0.4667	0.0592
14	1.946	0.361	3.9107	-0.4661	0.0577
15	2.169	0.249	3.9928	-0.4656	0.0563
16	2.293	0.193	3.9304	-0.1000	0.0638
17	2.778	0.0	4.0724	0.0	0.0634
18	2.324	0.694	3.6565	0.3047	0.0593
19	2.724	0.525	4.1133	-0.6197	0.0568
20	2.954	0.407	4.1930	-0.6192	0.0554
21	2.946	0.410	4.1029	-0.2554	0.0637
22	3.405	0.216	4.2226	-0.1551	0.0635
23	3.984	0.0	4.3759	0.0	0.0638
24	3.608	0.801	3.9389	0.3282	0.0577
25	4.163	0.573	4.4517	-0.8861	0.0546
26	3.964	0.675	4.3294	-0.5232	0.0640
27	4.372	0.482	4.4406	-0.4220	0.0641
28	4.867	0.270	4.5545	-0.2670	0.0648
29	5.611	0.0	4.7093	0.0	0.0664
30	5.794	0.983	4.3950	0.3662	0.0545
31	5.806	0.978	4.7203	-0.8981	0.0627
32	6.148	0.799	4.8096	-0.7937	0.0630
33	6.516	0.621	4.8943	-0.6385	0.0644
34	7.050	0.392	4.9948	-0.3713	0.0670
35	8.192	0.0	5.2118	0.0	0.0687
36	5.837	0.986	4.3400	0.3617	0.0640
37	6.277	0.816	4.8045	-0.8697	0.0637
38	6.633	0.640	4.8922	-0.7162	0.0652
39	7.147	0.414	4.9901	-0.4519	0.0679
40	8.251	0.017	5.2023	-0.0839	0.0697
41	8.307	0.0	5.1929	0.0	0.0708
42	7.462	1.122	4.7367	0.3947	0.0617

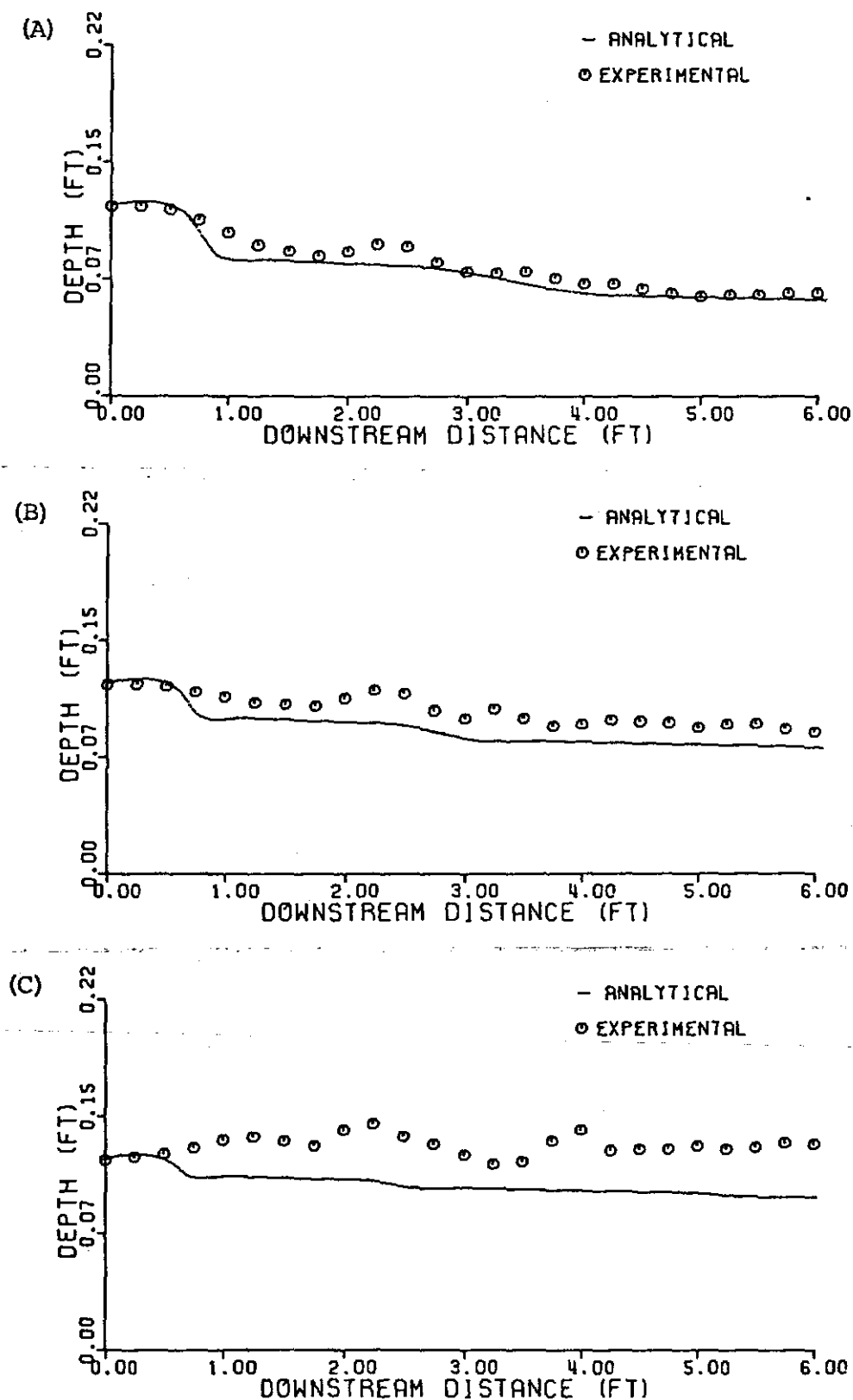


Fig. 12 Relationship Between Depth and Downstream Distance for Supercritical Flow;  $Q = 0.3632$  cfs,  $S = 1\%$ : (A)  $q_* = 0.0$  cfs/ft (B)  $q_* = 0.0125$  cfs/ft (C)  $q_* = 0.0236$  cfs/ft



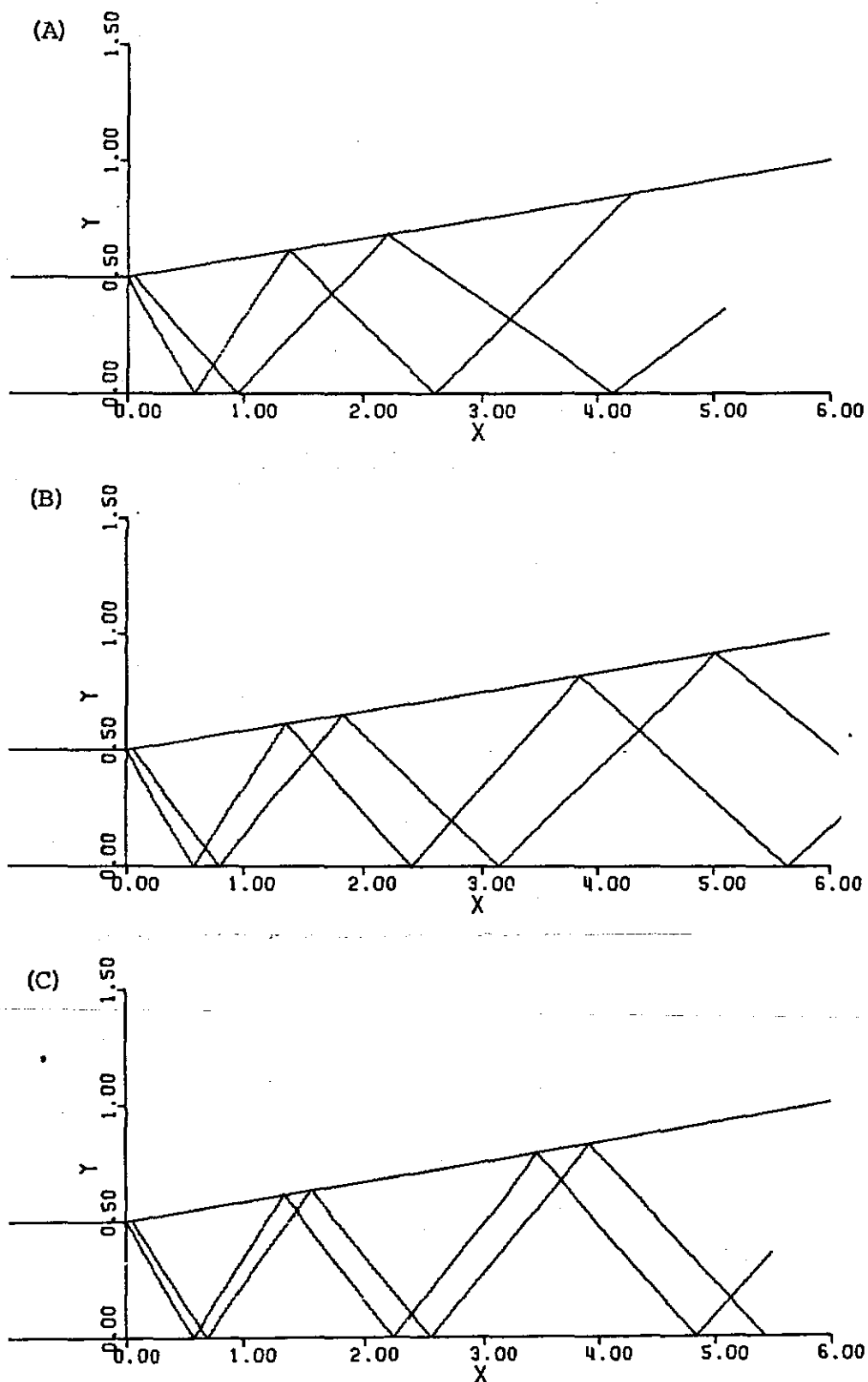


Fig. 13 Cross Wave Patterns for Supercritical Flow;  $Q = 0.3632$  cfs,  $S_o = 1\%$ : (A)  $q_* = 0.0$  cfs/ft (B)  $q_* = 0.0125$  cfs/ft (C)  $q_* = 0.0236$  cfs/ft

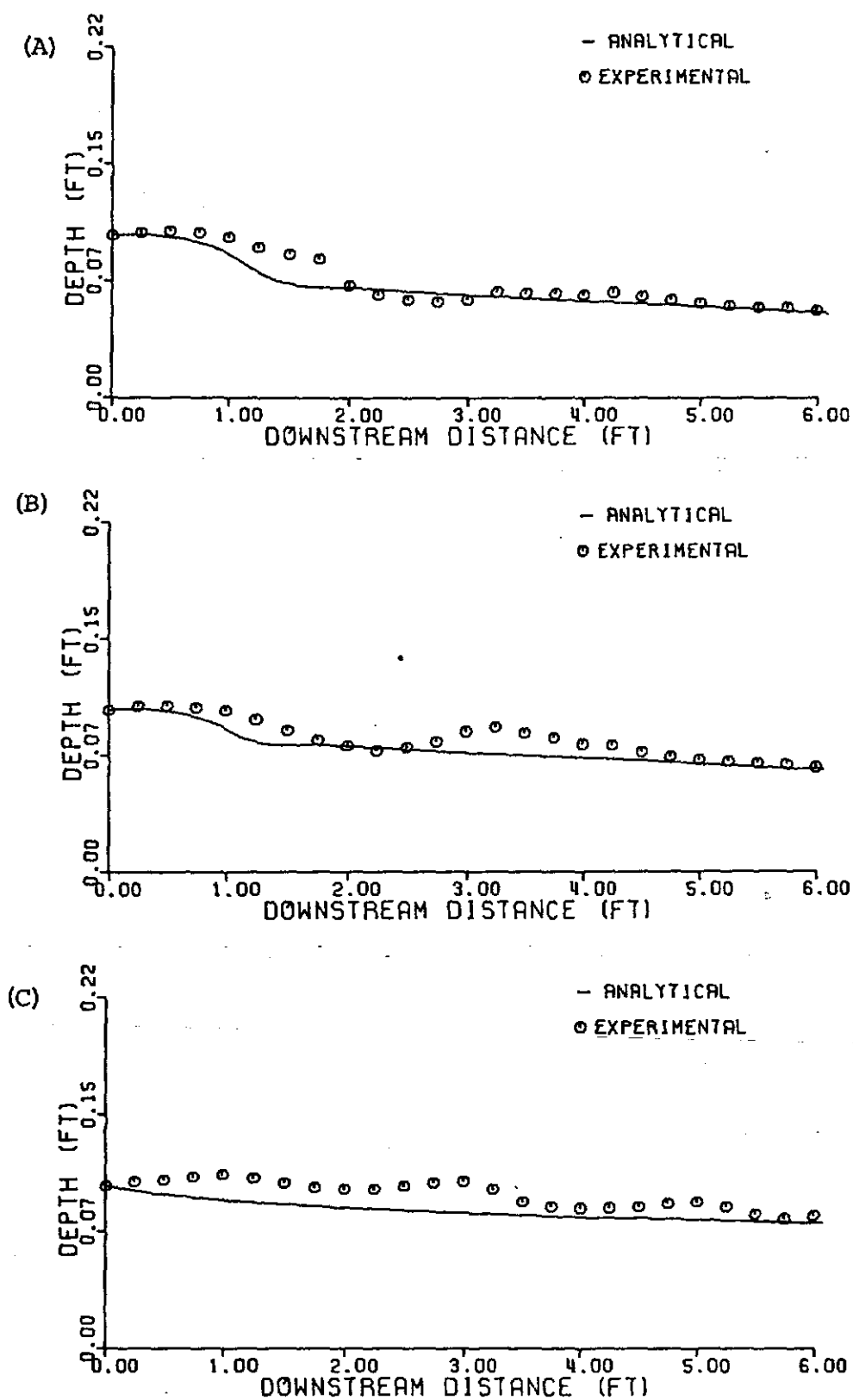


Fig. 14 Relationship Between Depth and Downstream Distance for Supercritical Flow;  $Q = 0.3632$  cfs,  $S_o = 4\%$ : (A)  $q_* = 0.0$  cfs/ft (B)  $q_* = 0.0125$  cfs/ft (C)  $q_* = 0.0236$  cfs/ft

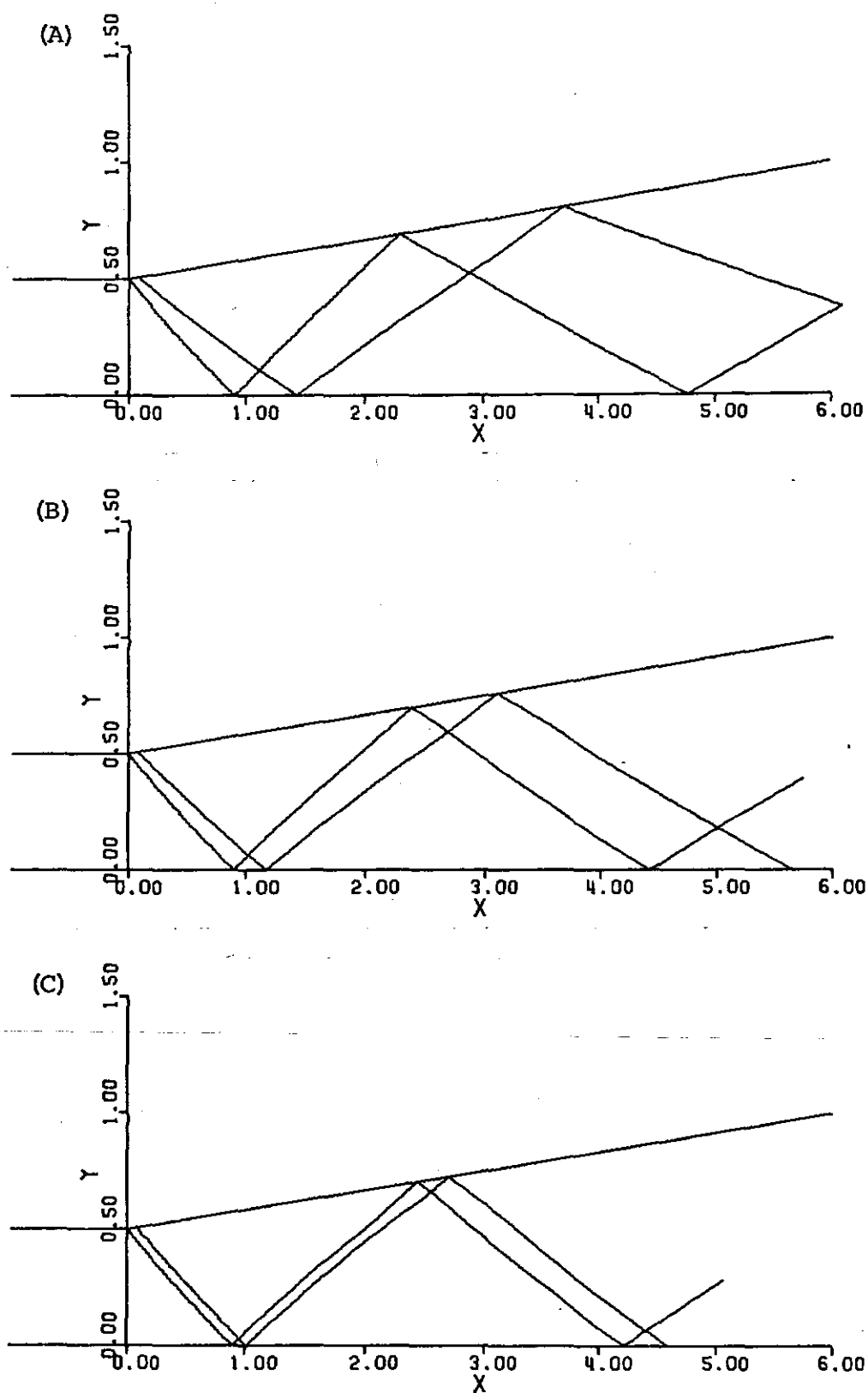


Fig. 15 Cross Wave Patterns for Supercritical Flow;  $Q = 0.3632$  cfs,  
 $S_0 = 4\%$ : (A)  $q_* = 0.0$  cfs/ft (B)  $q_* = 0.0125$  cfs/ft  
 (C)  $q_* = 0.0236$  cfs/ft

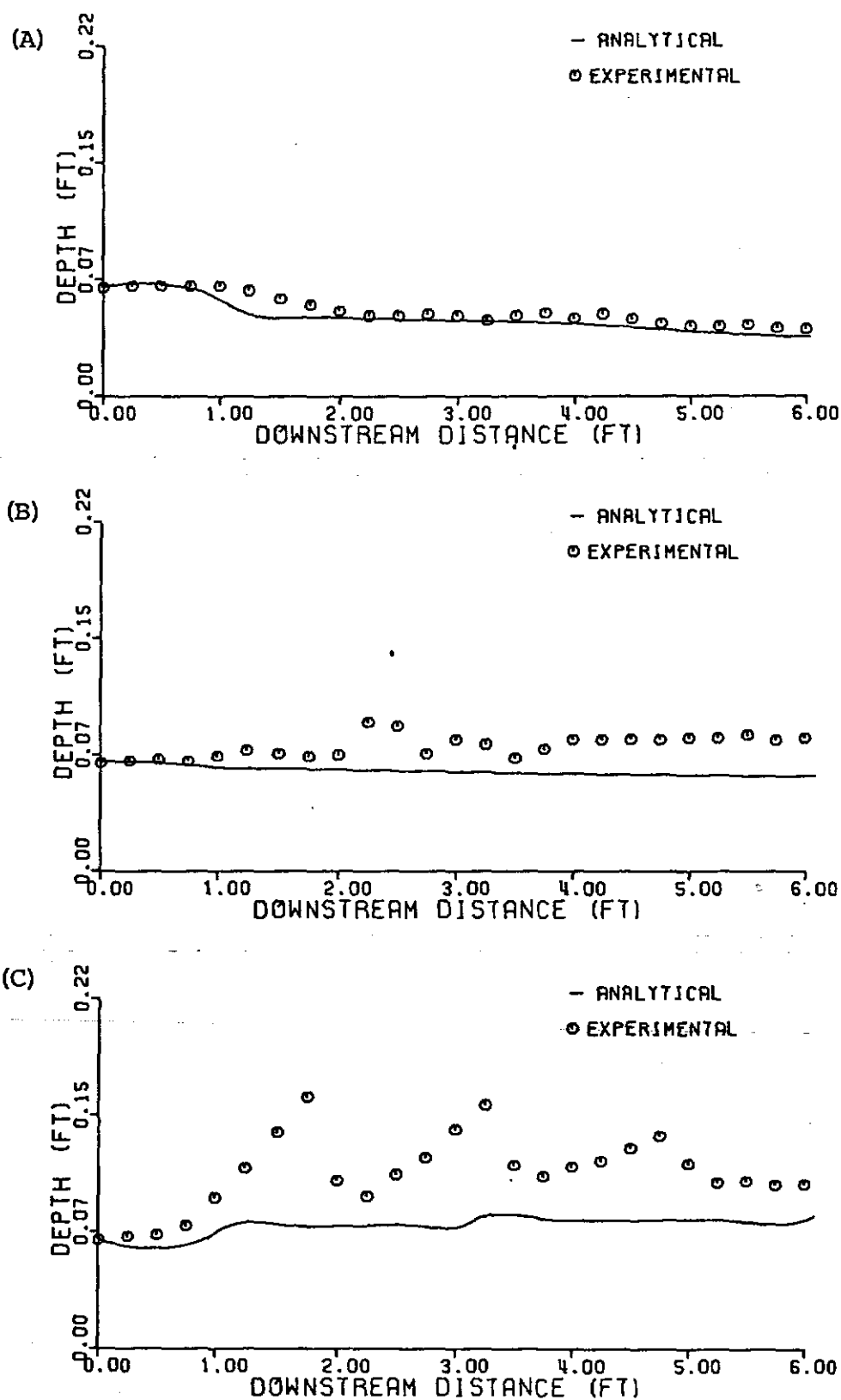


Fig. 16 Relationship Between Depth and Downstream Distance for Supercritical Flow;  $Q = 0.1967$  cfs,  $S_o = 1\%$ : (A)  $q_* = 0.0$  cfs/ft (B)  $q_* = 0.0125$  cfs/ft (C)  $q_* = 0.0236$  cfs/ft

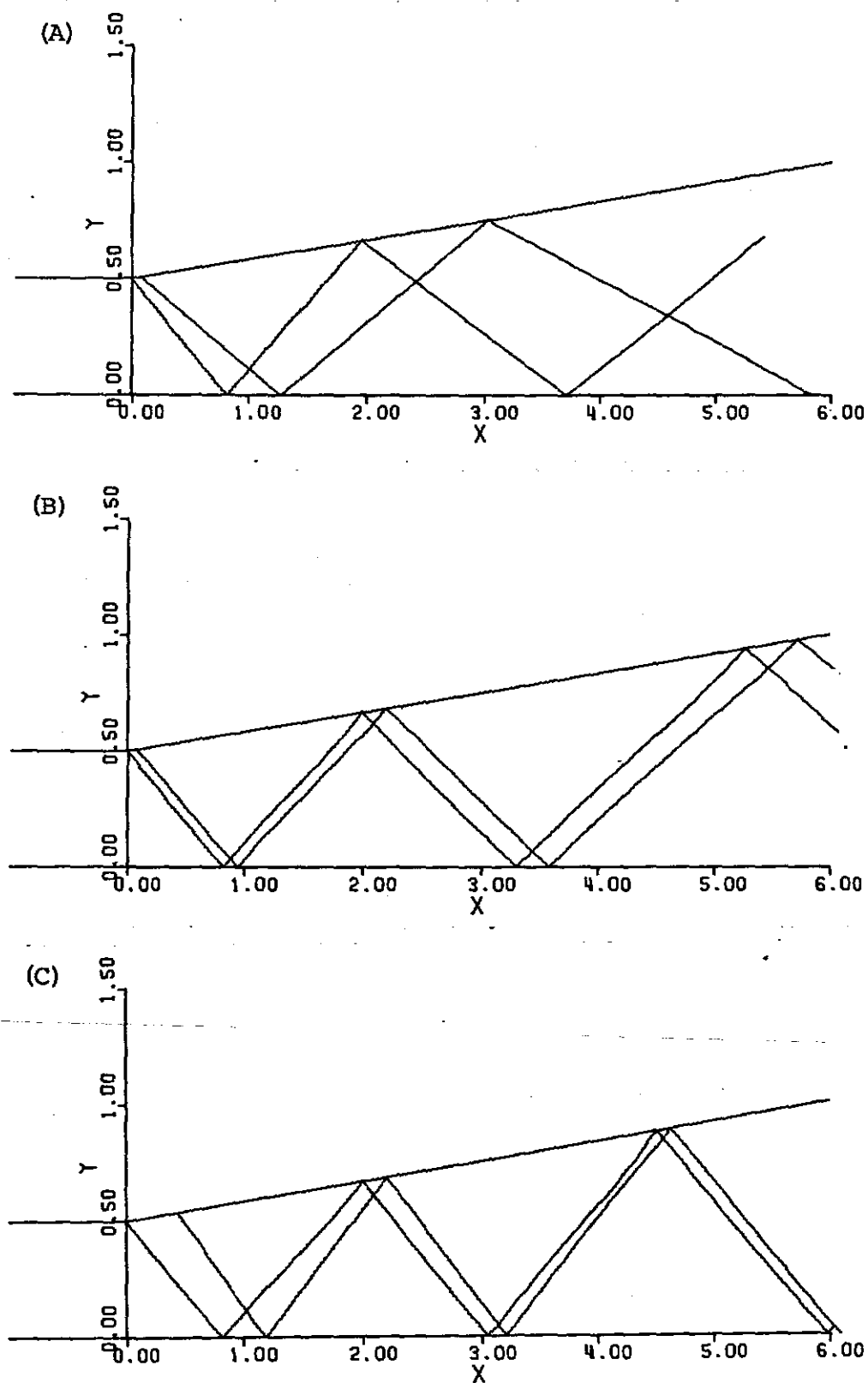


Fig. 17 Cross Wave Patterns for Supercritical Flow;  $Q = 0.1967$  cfs,  $S_o = 1\%$ : (A)  $q_* = 0.0$  cfs/ft (B)  $q_* = 0.0125$  cfs/ft (C)  $q_* = 0.0236$  cfs/ft

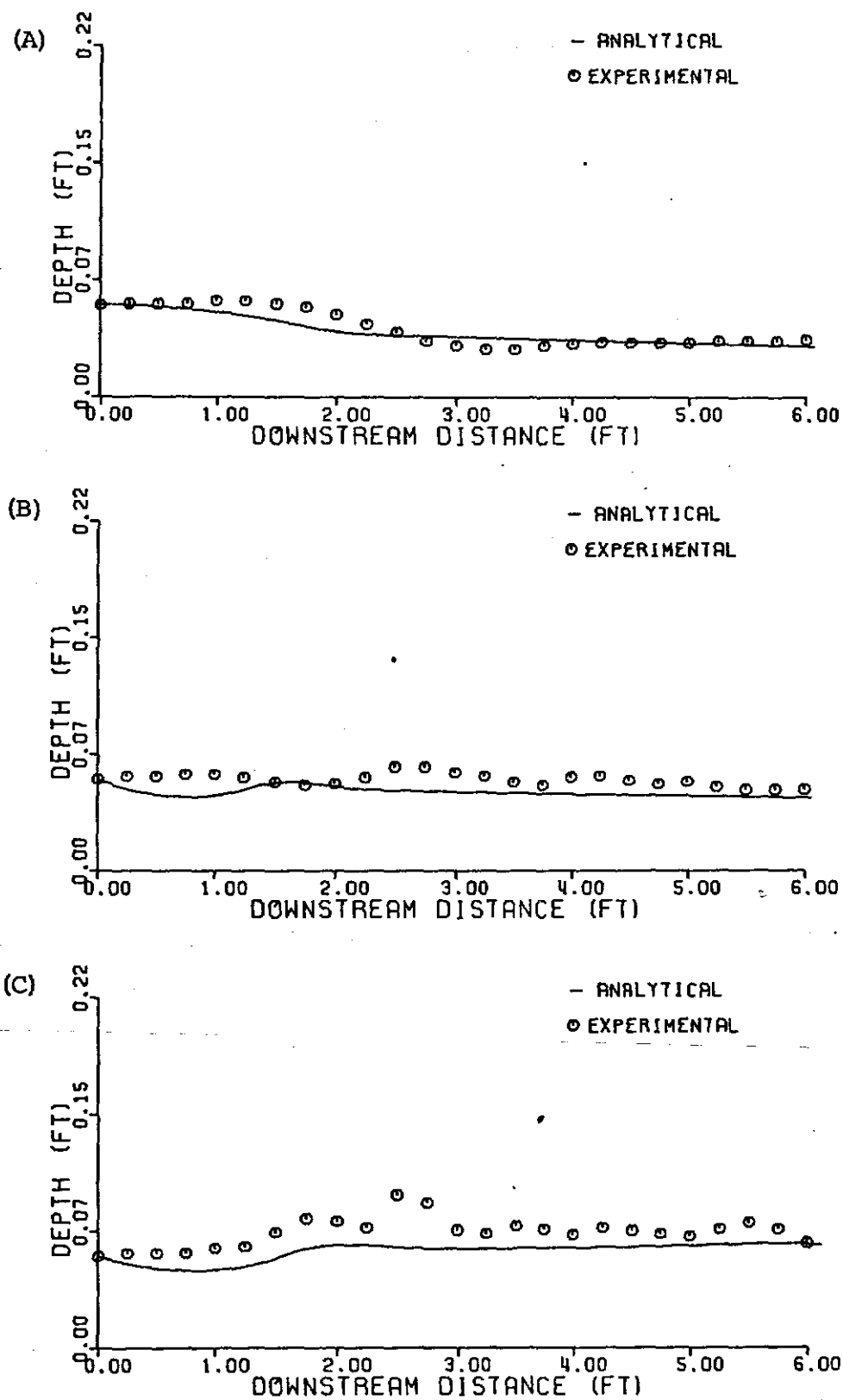
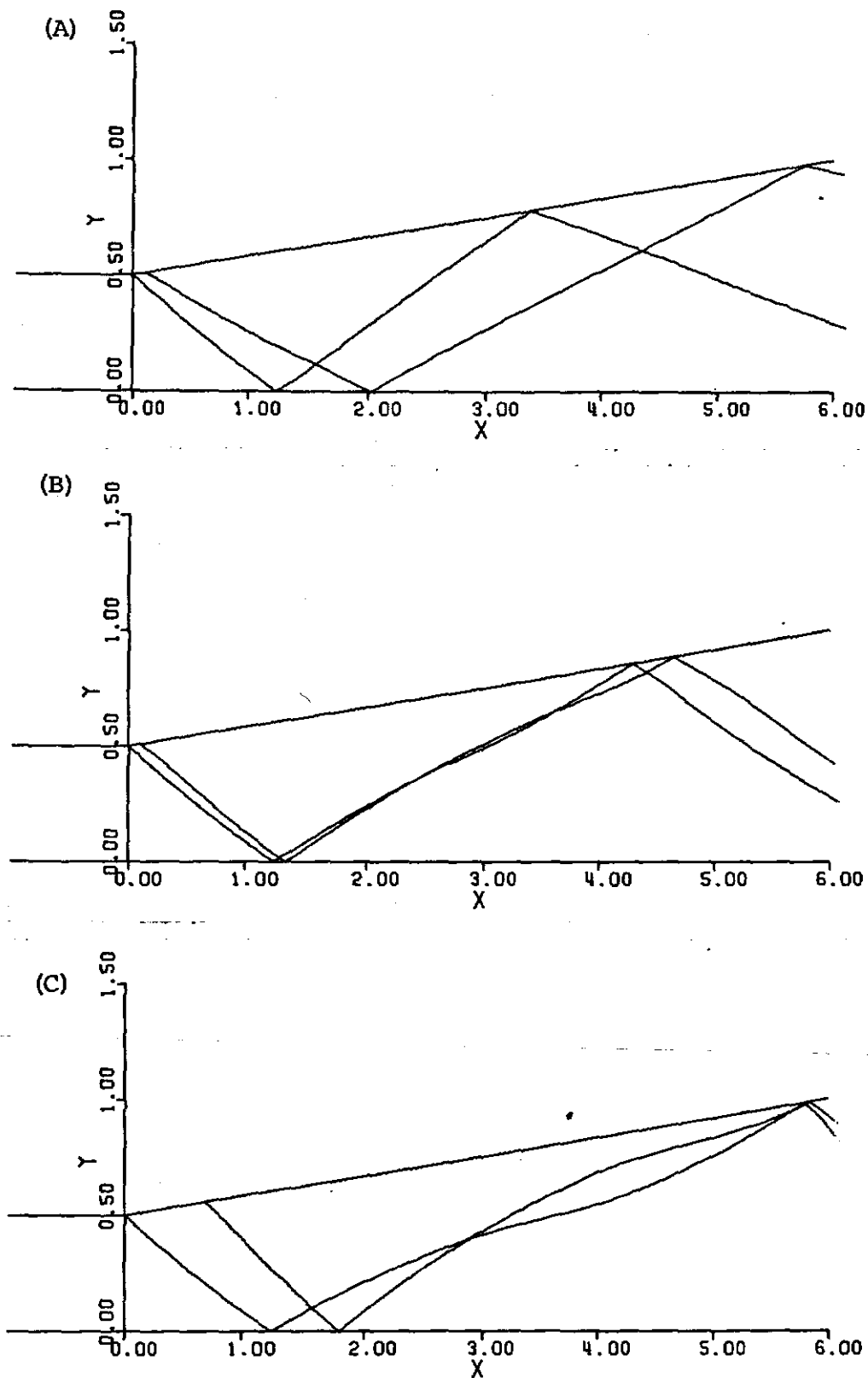


Fig. 18 Relationship Between Depth and Downstream Distance for Supercritical Flow;  $Q = 0.1967$  cfs,  $S_o = 4\%$ : (A)  $q_* = 0.0$  cfs/ft (B)  $q_* = 0.0125$  cfs/ft (C)  $q_* = 0.0236$  cfs/ft



Fig, 19 Cross Wave Patterns for Supercritical Flow;  $Q = 0.1967$  cfs,  
 $S_o = 4\%$ : (A)  $q_* = 0.0$  cfs/ft (B)  $q_* = 0.0125$  cfs/ft  
 (C)  $q_* = 0.0236$  cfs/ft

## CHAPTER VI

### CONCLUSIONS

The ability to accurately predict the flow conditions for spatially varied flow in rectangular expansions is of great importance in the design or analysis of systems where this type of flow occurs. Not only is the centerline profile important, but also the sidewall profile and the general properties and conditions of the flow system.

This project was performed to establish mathematical models that can be used to determine various flow conditions. The results obtained from this study indicate that the flow conditions for both subcritical and supercritical spatially varied flow in rectangular expansions can be determined with good accuracy. This is confirmed by comparing the results computed using the developed mathematical models to ~~that obtained from experimental analysis.~~ This further indicates that the basic assumptions made for the analytical analysis are justified and introduce negligible error in the results.

For subcritical spatially varied flow, the following conclusions are noted:

1. The analytical and experimental centerline profiles



follow very closely for the beginning portion of the test section. The analytical profile levels off further downstream than the experimentally measured water surface profile.

2. For the same main channel flow conditions, the largest percentage increase in water depth from the point of divergence occurs when there is no lateral inflow. This is due to the fact that added lateral inflow causes an increase in downstream momentum which results in a much larger initial flow depth in the test section.

3. The discrepancies between the analytical and experimental results, demonstrated in the case when lateral inflow is added to the test section, is believed to be the result of inaccurate boundary shear calculations. In which, the effect of the lateral inflow on the shear stress computation was not taken into consideration.

For spatially varied supercritical flow through a transition, it is concluded that:

1. The characteristic method derived, based on the momentum approach, is an accurate method for analyzing such flow phenomena.

2. The analytical model developed in this study provides accurate predictions of the flow profile in the expansion section as long as the main channel flow has the dominate effect on the flow characteristics. That is to

say, if the lateral inflow is too large, the effect of the added discharge tends to cause great disturbances on the standing waves, which are used as the characteristic lines for the analytical computations. Such disturbances are believed to be responsible for the discrepancies observed between the analytical and experimental results. This is shown in Figs. 12(c) and 16(c).

3. The prevailingness of the main channel flow of the supercritical flow characteristics is determined not only by the rate of the main channel discharge, but also by the magnitude of the channel slope. It is noted in this study that larger main channel flowrates and/or channel slopes often yield better results. This can readily be seen by comparing Figs. 12(c) and 14(c); 16(c) and 18(c) for the effect of slope and Figs. 12(c) and 16(c); 14(c) and 18(c) for the effect of the rate of discharge.

4. It is also noted that the effect of a large lateral inflow is seen in the form of undular jumps along the centerline. When such phenomena occur, the characteristic method fails to predict the flow profile, since the characteristic lines, i.e. standing waves, no longer exist.

For a more complete analysis on spatially varied flow in rectangular expansions, future studies should be conducted for systems with non-linear boundaries and lateral inflow in a form other than uniform sheet flow.

## APPENDIX I

### REFERENCES

1. Hinds, J., "Side Channel Spillways," Transactions, ASCE, Vol. 89, 1926, pp. 881-927.
2. Favre, H., "Contribution à l'étude des Courants Liquides," Dunod, Paris, 1933, pp. 37-54.
3. Camp, T. F., "Lateral Spillway Channels," Transactions, ASCE, Vol. 105, 1940, pp. 606-617.
4. Li, W.-H., "Open Channels with Nonuniform Discharge," Transactions, ASCE, Vol. 120, 1955, pp. 255-274.
5. Yen, B. C. and Wenzel, H. G., "Dynamic Equations For Steady Spatially Varied Flow," Journal of the Hydraulics Division, ASCE, Vol. 96, No. HY3, Proc. Paper 7179, March 1970, pp. 801-814.
6. Ippen, A. T., "Mechanics of Supercritical Flow," High-Velocity Flow in Open Channels: A Symposium, Transactions, ASCE, Vol. 116, 1951, pp. 268-295.
7. Harrison, A. J. M., "Design of Channels for Supercritical Flow," Proceedings, Institution of Civil Engineering, Vol. 35, Great Britain, November 1966, pp. 475-490.
8. Chow, V. T., Open Channel Hydraulics, McGraw-Hill Book Company, New York, 1959.
9. Rouse, H., Bhoota, B. V. and Hsu, E.-Y., "Design of Channel Expansions," High-Velocity Flow in Open Channels: A Symposium, Transactions, ASCE, Vol. 116, 1951, pp. 347-363.
10. Hom-ma, M. and Shima, S., "On the Flow in a Gradually Diverged Open Channel," The Japan Science Review, Series I., Vol. 2, No. 3, 1952.
11. Knapp, R. T., "Design of Channel Curves for Supercritical Flow," High-Velocity Flow in Open Channels: A Symposium, Transactions, ASCE, Vol. 116, 1951, pp. 296-325.

12. Bagge, G. and Herbich, J. B., "Transitions in Supercritical Open-Channel Flow," Journal of the Hydraulics Division, ASCE, Vol. 93, No. HY5, Proc. Paper 5417, September 1967, pp. 23-41.
13. Herbich, J. B. and Walsh, P., "Supercritical Flow in Rectangular Expansions," Journal of the Hydraulics Division, ASCE, Vol. 98, No. HY9, Proc. Paper 9216, September 1972, pp. 1691-1700.
14. Blaisdell, F. W., "Flow Through Diverging Open Channel Transitions at Supercritical Velocities," U.S. Soil Conservation Service, Progress Report SCS-TP-76, April 1949.
15. Schlichting, H., Grenzschichttheorie, 5th Edition (Karlsruhe: Braun, 1965).
16. Streeter, V. L., Fluid Mechanics, McGraw-Hill Book Company, New York, 1971.

## APPENDIX II

### NOTATION

A	=	cross sectional area of a flow section, $L^2$ ;
B	=	width of channel, in y-direction, L;
C	=	Chezy friction coefficient;
d	=	depth of flow section, L;
f	=	Darcy - Weisbach friction coefficient;
F	=	Froude number;
g	=	gravitational acceleration, $LT^{-2}$ ;
$h_f$	=	friction head loss, L;
K	=	pressure correction factor;
L	=	characteristic length, L;
M	=	momentum flux of the main flow, $MLT^{-2}$
$M_L$	=	momentum flux of the lateral inflow, $MLT^{-2}$
n	=	Manning roughness coefficient;
P	=	pressure force of the main flow, $MLT^{-2}$
$P_L$	=	pressure force acting perpendicular to the side-wall, $MLT^{-2}$
Q	=	main channel flowrate, $L^3 T^{-1}$
$q_*$	=	lateral inflow per unit length, $L^2 T^{-1}$ ;
$R_f$	=	boundary resistance force, M;
R	=	hydraulic radius, L;
S	=	energy grade line slope;
$S_o$	=	channel slope;
U	=	lateral inflow velocity, $LT^{-1}$ ;

- $u$  = x - component of the main flow velocity,  $LT^{-1}$ ;  
 $V$  = resultant main flow velocity,  $LT^{-1}$ ;  
 $\bar{V}$  = mean velocity of the main flow,  $LT^{-1}$ ;  
 $v$  = y - component of the main flow velocity,  $LT^{-1}$ ;  
 $W$  = force due to the weight of the fluid,  $MLT^{-2}$   
 $w$  = z - component of the main flow velocity,  $LT^{-1}$ ;  
 $x$  = distance downstream from the origin of the divergent section,  $L$ ;  
 $\alpha$  = angle of divergence;  
 $\beta$  = momentum flux correction factor;  
 $\gamma$  = specific weight of fluid,  $ML^{-2}T^{-2}$   
 $\theta$  = angle the channel floor makes with the horizontal;  
 $\rho$  = mass density of fluid,  $ML^{-3}$   
 $\tau$  = boundary shear stress,  $ML^{-2}$ ;  
 $\phi$  = angle of the lateral inflow velocity vector with the flow direction.

## APPENDIX III

FLOW CHARTS AND COMPUTER PROGRAMS USED IN THE ANALYSIS  
OF SUBCRITICAL AND SUPERCRITICAL SPATIALLY  
VARIED FLOW IN RECTANGULAR EXPANSIONS

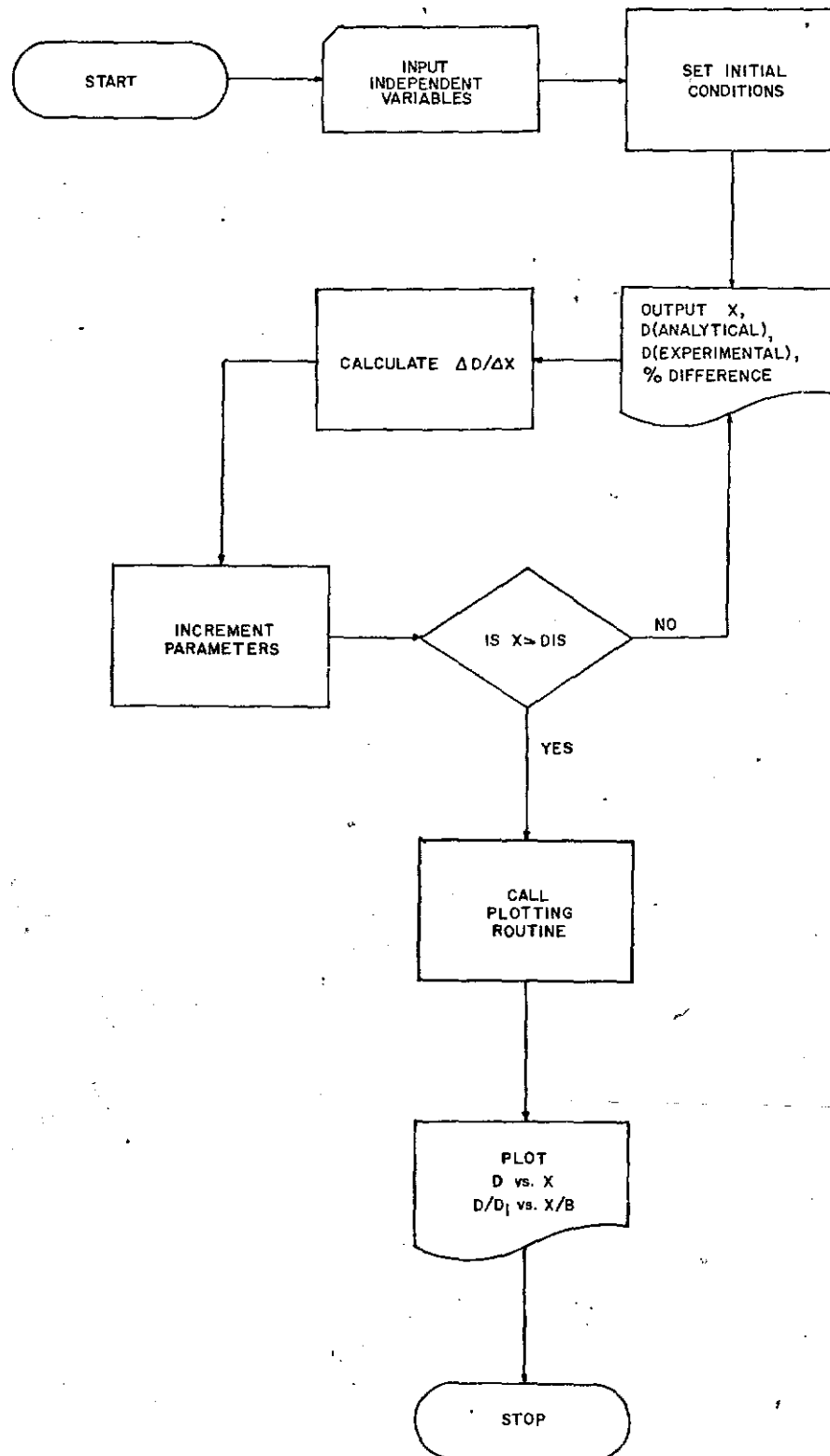


Fig. A-1 — Flow Chart for Computer Program for Subcritical Flow



Fig. A-2 COMPUTER PROGRAM FOR SUBCRITICAL FLOW

```

C THIS PROGRAM CALCULATES THE FLOW PROFILE FOR SPATIALLY
C VARIOUS SUBCRITICAL FLOW IN A RECTANGULAR EXPANSION.
C A PLOT IS MADE COMPARING THIS PROFILE WITH THE
C EXPERIMENTAL PROFILE.
C
C THE INPUT CONSISTS OF THE FOLLOWING:
C
C L NUMBER OF DATA SETS
C NEXP NUMBER OF EXPERIMENTAL POINTS PER DATA SET
C S0 CHANNEL SLOPE (FT/FT)
C BETA MOMENTUM FLUX CORRECTION FACTOR
C TANA TANGENT OF THE DIVERGENT ANGLE
C B INITIAL WIDTH OF THE CHANNEL (FT)
C QSTAR LATERAL INFLOW (CFS/FT)
C KP PRUSSKE CORRECTION FACTOR
C D(1) INITIAL DEPTH (FT)
C PI RATIO OF THE CIRCUMFERENCE OF A CIRCLE
C TO ITS DIAMETER
C HP VERTICAL DISTANCE THE LATERAL INFLOW FALLS (FT)
C G GRAVITATIONAL ACCELERATION (FT/SEC**2)
C DX INCREMENTAL CHANGE IN DOWNSTREAM DISTANCE (FT)
C X(1) INITIAL DOWNSTREAM DISTANCE (FT)
C Q MAIN CHANNEL FLOWRATE (CFS)
C N MANNING'S ROUGHNESS COEFFICIENT
C DIS TOTAL LENGTH OF CHANNEL REACH UNDER ANALYSIS (FT)
C GAMA SPECIFIC WEIGHT OF THE FLUID (LB/FT**3)
C
C THE MINIMUM VALUES ON THE PLOT ARE DENOTED BY THE
C 'MIN' PREFIX AND THE SCALE FACTORS ARE DENOTED
C BY THE 'SC' PREFIX.
C
0001 DIMENSION DATA(1024)
0002 REAL A(10),D(125),DP(125),X(125),XP(125),DDI(125),DDIP(125),
(XB(125),XBP(125),KP,EXX(25),EXD(25),EXXB(25),EXUDI(25),NUM,N,
(MINXP,MINXBP,MINDP,MINDD,MINEX,MINED,MINEXB,MINEXD
INTEGER H
0003 CALL PLOTS(DATA,4096)
0004 CALL FACTOR (0.7)
0005 READ(5,1050) L,NEXP
0006 READ(5,1060) MINXP,MINDP,MINXBP,MINDD,MINEX,MINED,MINEXB,MINEXD
0007 READ(5,1060) SCXP,SCDP,SCXBP,SCDD,SCEX,SCED,SCEXB,SCEXD
0008 DO 120 I=1,L
0009
C
C INITIALIZING THE POSITION OF THE PLOTTER PEN
C
0010 CALL PLOT(0.0,-11.0,-3)
0011 CALL PLOT(0.0,3.25,-3)
0012 READ(5,1060) S0,BETA,TANA,L,QSTAR,KP,D(1),PI
0013 READ(5,1060) HP,G,DX,X(1),Q,N,DIS,GAMA
0014 S0P=S0*100.
0015 RU=B
0016 ALFA=ATAN(TANA)
0017 ALPHA=ALFA*180./PI
0018 WRITE(6,1000) Q
0019 WRITE(6,1010) QSTAR
0020 WRITE(6,1020)

```

```

SUB 1
SUB 2
SUB 3
SUB 4
SUB 5
SUB 6
SUB 7
SUB 8
SUB 9
SUB 10
SUB 11
SUB 12
SUB 13
SUB 14
SUB 15
SUB 16
SUB 17
SUB 18
SUB 19
SUB 20
SUB 21
SUB 22
SUB 23
SUB 24
SUB 25
SUB 26
SUB 27
SUB 28
SUB 29
SUB 30
SUB 31
SUB 32
SUB 33
SUB 34
SUB 35
SUB 36
SUB 37
SUB 38
SUB 39
SUB 40
SUB 41
SUB 42
SUB 43
SUB 44
SUB 45
SUB 46
SUB 47
SUB 48
SUB 49
SUB 50
SUB 51
SUB 52
SUB 53
SUB 54
SUB 55
SUB 56
SUB 57
SUB 58

```

```

0021      WRITE(6,1030)
0022      DI=D(1)
C
C      ACCUMULATION OF THE EXPERIMENTAL DATA
C
0023      DO 10 JJ=1,NEXP
0024      READ(5,1070)EXX(JJ),EXD(JJ)
0025      EXXB(JJ)=EXX(JJ)/BO
0026      10 EXUDI(JJ)=EXD(JJ)/DI
0027      THETA=ATAN(SO)
0028      PHI=(PI/2.)-THETA
0029      J=1
0030      JJ=0
0031      20 DD(J)=D(J)/DI
0032      XB(J)=X(J)/BO
0033      IF(((J-6)/5)+5.NE.(J-6)) GO TO 30
0034      JJ=JJ+1
0035      PDIFF=ABS(D(J)-EXD(JJ))*100./DIJ)
0036      WRITE(6,1040) X(J),D(J),EXD(JJ),PDIFF
0037      30 V=L/(U(J)*B)
0038      U=SQRT(2.*G*HP)
0039      AREA=B*D(J)
0040      PERI=B+2.*D(J)
0041      RAD=AREA/PERI
0042      TAU=(U.45*GAMA*V*V*N*N)/(RAD**0.3333)
C
C      A(1) THROUGH A(8) ARE THE INDIVIDUAL TERMS IN THE
C      EXPRESSION FOR DD/DX
C
0043      A(1)=SO
0044      A(2)=(QSTAR*U*COS(PHI)*COS(ALFA))/(G*D(J)*B)
0045      A(3)=((2.)*BETA*V*V*TANA)/(G*B)
0046      A(4)=((-2.)*BETA*V*QSTAR*COS(PHI)*COS(ALFA))/(G*B*D(J))
0047      A(5)=(-1.)*TAU/(GAMA*D(J))-2.*TAU/(GAMA*B)
0048      A(6)=2.*(KP*D(J)/B)*COS(THETA)*(SIN(ALFA)-TAN(ALFA))
0049      A(7)=2.*KP*COS(THETA)
0050      A(8)=((-1.)*BETA*V*V)/(G*D(J))
0051      NUM=U.0
C
C      CALCULATION OF DD/DX
C
0052      DO 40 I=1,6
0053      40 NUM=NUM+A(I)
0054      DEN=A(7)+A(8)
0055      DDDX=NUM/DEN
0056      J=J+1
0057      H=J-1
0058      DIJ)=D(H)+DDDX*DX
0059      X(J)=X(H)+DX
0060      IF(X(J).GE.DIS) GO TO 50
0061      B=B+2.*DX*TANA
0062      C=Q+QSTAR*DX
0063      GO TO 20
C
C      EVERY FIFTH ANALYTICAL POINT IS PLOTTED
C
0064      50 K=(J/5)+1
0065      DO 60 I=2,K

```

```

SUB 59
SUB 60
SUB 61
SUB 62
SUB 63
SUB 64
SUB 65
SUB 66
SUB 67
SUB 68
SUB 69
SUB 70
SUB 71
SUB 72
SUB 73
SUB 74
SUB 75
SUB 76
SUB 77
SUB 78
SUB 79
SUB 80
SUB 81
SUB 82
SUB 83
SUB 84
SUB 85
SUB 86
SUB 87
SUB 88
SUB 89
SUB 90
SUB 91
SUB 92
SUB 93
SUB 94
SUB 95
SUB 96
SUB 97
SUB 98
SUB 99
SUB 100
SUB 101
SUB 102
SUB 103
SUB 104
SUB 105
SUB 106
SUB 107
SUB 108
SUB 109
SUB 110
SUB 111
SUB 112
SUB 113
SUB 114
SUB 115
SUB 116

```

```

0066      XP(1)=X((1-1)*5+1)
0067      DP(1)=D((1-1)*5+1)
0068      XBP(1)=XB((1-1)*5+1)
0069      60 DDIP(1)=DDI((1-1)*5+1)
0070      XP(1)=X(1)
0071      DP(1)=D(1)
0072      XBP(1)=XB(1)
0073      DDIP(1)=DDI(1)
C
C      THE SUBSCRIPT (K+1) IS A MINIMUM FOR THE PARTICULAR
C      VARIABLE TO BE PLOTTED
C
0074      XP(K+1)=MINXP
0075      DP(K+1)=MINDP
0076      XBP(K+1)=MINXBP
0077      DDIP(K+1)=MINDD
0078      EXX(K+1)=MINEX
0079      EXD(K+1)=MINED
0080      EXXB(K+1)=MINEXB
0081      EXDDI(K+1)=MINEXD
C
C      THE SUBSCRIPT (K+2) IS THE VALUE OF ONE DIVISION
C      ON THE AXIS OF THE PLOT
C
0082      XP(K+2)=SCXP
0083      DP(K+2)=SCDP
0084      XBP(K+2)=SCXBP
0085      DDIP(K+2)=SCDD
0086      EXX(K+2)=SCEX
0087      EXD(K+2)=SCED
0088      EXXB(K+2)=SCEXB
0089      EXDDI(K+2)=SCEND
C
C      SCALING OF THE VARIABLES TO BE PLOTTED
C
0090      DO 70 I=1,K
0091      XP(I)=(XP(I)-XP(K+1))/XP(K+2)
0092      DP(I)=(DP(I)-DP(K+1))/DP(K+2)
0093      XBP(I)=(XBP(I)-XBP(K+1))/XBP(K+2)
0094      DDIP(I)=(DDIP(I)-DDIP(K+1))/DDIP(K+2)
0095      EXX(I)=(EXX(I)-EXX(K+1))/EXX(K+2)
0096      EXD(I)=(EXD(I)-EXD(K+1))/EXD(K+2)
0097      EXXB(I)=(EXXB(I)-EXXB(K+1))/EXXB(K+2)
0098      70 EXDDI(I)=(EXDDI(I)-EXDDI(K+1))/EXDDI(K+2)
C
C      LOCATING AND LABELING THE AXES
C
0099      CALL AXIS(0.0,0.0,'DOWNSTREAM DISTANCE (FT)',-24.6,,0.0,XP(K+1),
0100      1XP(K+2))
0100      CALL AXIS(0.0,0.0,'DEPTH (FT)',10.3,,90.,DP(K+1),DP(K+2))
0101      CALL AXIS(0.0,5.0,'DOWNSTREAM DISTANCE/INITIAL WIDTH',-33.6,,0.0,
0102      (XBP(K+1),XBP(K+2)))
0102      CALL AXIS(0.0,5.0,'DEPTH/INITIAL DEPTH',19.3,,90.,DDIP(K+1),DDIP(
0103      (K+2)))
C
C      SUBROUTINE SMOOTH IS USED FOR THE ANALYTICAL PROFILE
C
0103      CALL SMOOTH(XP(1),DP(1),0)

```

```

SUB 117
SUB 118
SUB 119
SUB 120
SUB 121
SUB 122
SUB 123
SUB 124
SUB 125
SUB 126
SUB 127
SUB 128
SUB 129
SUB 130
SUB 131
SUB 132
SUB 133
SUB 134
SUB 135
SUB 136
SUB 137
SUB 138
SUB 139
SUB 140
SUB 141
SUB 142
SUB 143
SUB 144
SUB 145
SUB 146
SUB 147
SUB 148
SUB 149
SUB 150
SUB 151
SUB 152
SUB 153
SUB 154
SUB 155
SUB 156
SUB 157
SUB 158
SUB 159
SUB 160
SUB 161
SUB 162
SUB 163
SUB 164
SUB 165
SUB 166
SUB 167
SUB 168
SUB 169
SUB 170
SUB 171
SUB 172
SUB 173
SUB 174

```

0104	KK=K-1	SUB	175
0105	DO 80 I=2,KK	SUB	176
0106	80 CALL SMOOTH(XP(I),DP(I),-2)	SUB	177
0107	CALL SMOOTH(XP(K),DP(K),-999)	SUB	178
0108	CALL PLOT(0.0,0.0,-3)	SUB	179
	C	SUB	180
	C SUBROUTINE SYMBOL IS USED FOR THE EXPERIMENTAL RESULTS	SUB	181
	C	SUB	182
0109	DO 90 JJ=1,NEXP	SUB	183
0110	90 CALL SYMBOL(EXX(JJ),EXD(JJ),.08,1,0.0,-1)	SUB	184
0111	CALL SYMBOL(1.0,3.0,0.11,'_ ANALYTICAL',0.0,12)	SUB	185
0112	CALL SYMBOL(1.0,2.75,.157,' EXPERIMENTAL ',0.0,15)	SUB	186
0113	CALL PLOT(0.0,5.0,-3)	SUB	187
0114	CALL SMOOTH(XBP(1),DDIP(1),0)	SUB	188
0115	DO 100 I=2,KK	SUB	189
0116	100 CALL SMOOTH(XBP(I),DDIP(I),-2)	SUB	190
0117	CALL SMOOTH(XBP(K),DDIP(K),-999)	SUB	191
0118	CALL PLOT(0.0,0.0,-3)	SUB	192
0119	DO 110 JJ=1,NEXP	SUB	193
0120	110 CALL SYMBOL(EXXB(JJ),EXDDI(JJ),.08,1,0.0,-1)	SUB	194
0121	CALL SYMBOL(1.0,3.0,0.11,'_ ANALYTICAL',0.0,12)	SUB	195
0122	CALL SYMBOL(1.0,2.75,.157,' EXPERIMENTAL ',0.0,15)	SUB	196
0123	1000 FORMAT('1',////////,3HX,'MAIN CHANNEL FLOWRATE:',F6.3,' CFS'/)	SUB	197
0124	1010 FORMAT(' ',37X,'LATERAL INFLOW:',F7.4,' CFS/FT')	SUB	198
0125	1020 FORMAT(' ',37X,'DOWNSTREAM',14X,'DEPTH (FT)',13X,'PERCENT')	SUB	199
0126	1030 FORMAT(' ',37X,'DISTANCE (FT)',4X,'ANALYTICAL',2X,'EXPERIMENTAL', (4X,'DIFFERENCE')	SUB	200
0127	1040 FORMAT(' ',40X,F5.2,10X,F7.4,7X,F6.3,9X,F6.3)	SUB	202
0128	1050 FORMAT(2I3)	SUB	203
0129	1060 FORMAT(8F10.5)	SUB	204
0130	1070 FORMAT(2F10.2)	SUB	205
	C	SUB	206
	C SHIFTS PLOTTER PEN FOR ANOTHER SET OF DATA	SUB	207
	C	SUB	208
0131	120 CALL PLOT(12.0,0.0,-3)	SUB	209
0132	CALL PLOT(0.0,0.0,999)	SUB	210
0133	RETURN	SUB	211
0134	END	SUB	212

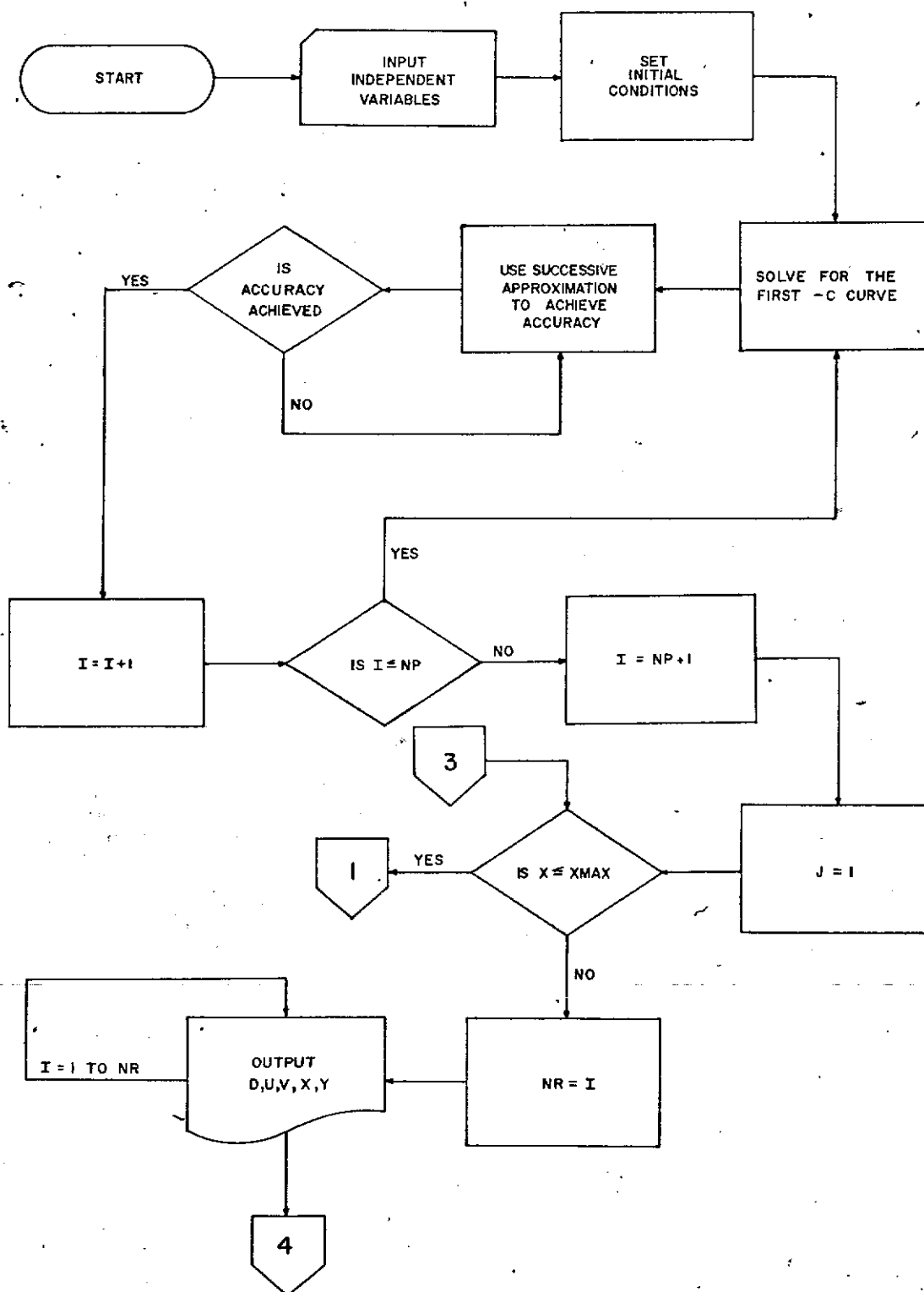


Fig. A-3a - Flow Chart for Computer Program for Supercritical Flow

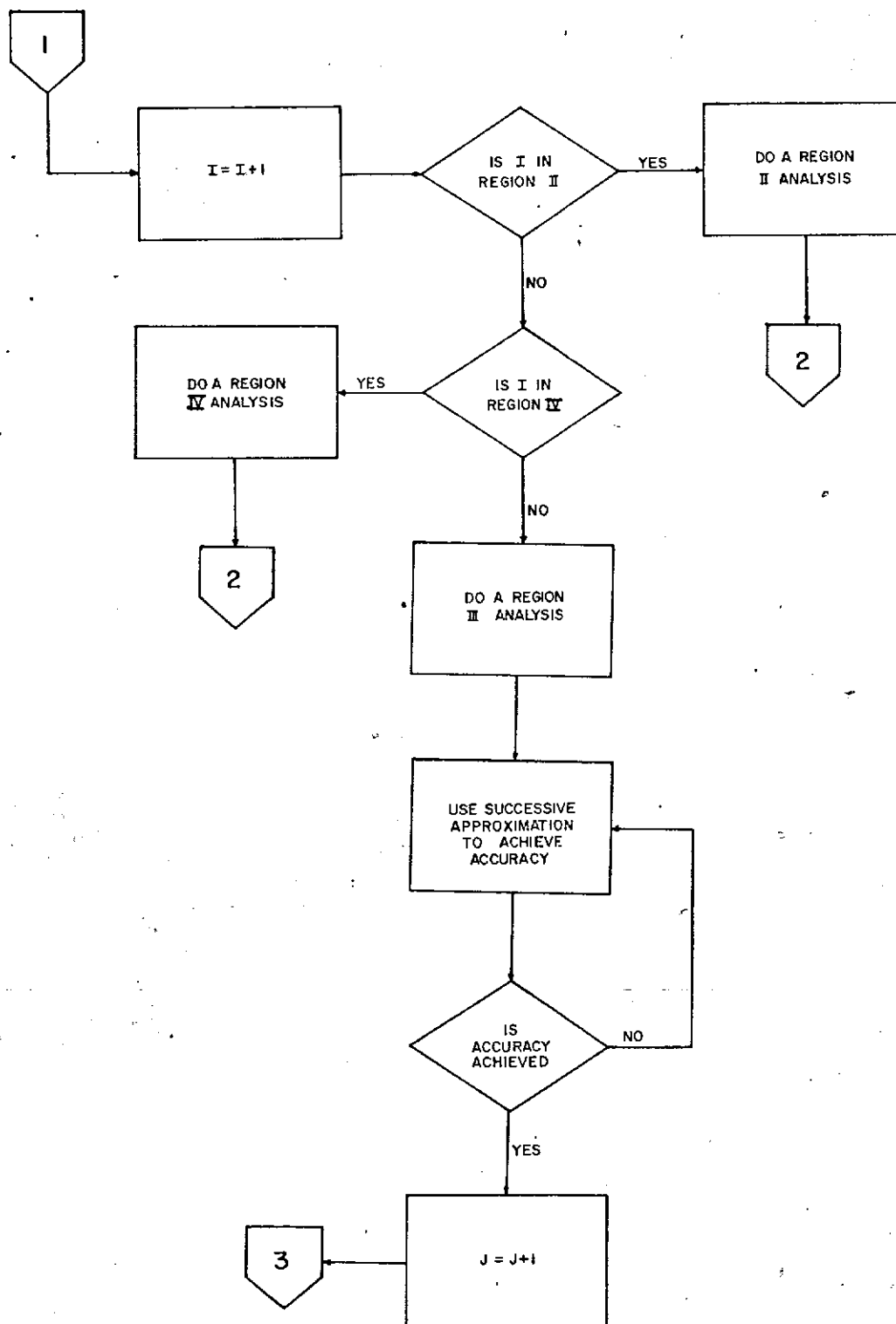


Fig. A-3b — Flow Chart for Computer Program for Supercritical Flow

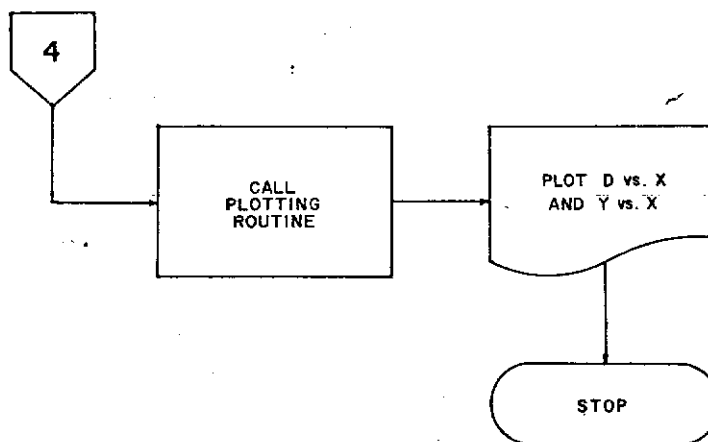
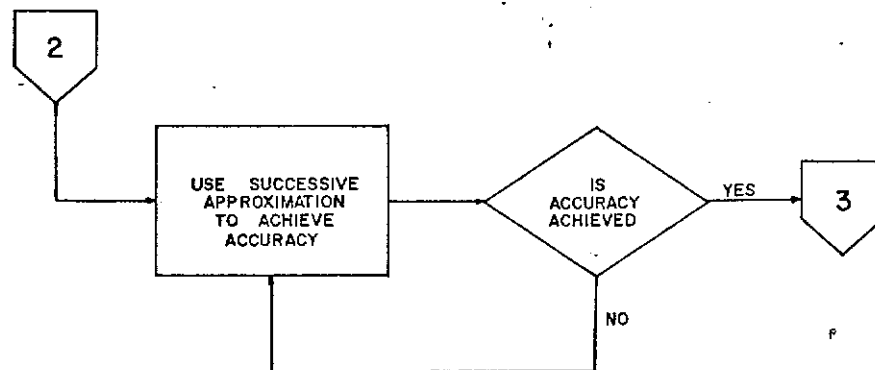


Fig. A-3c - Flow Chart for Computer Program for Supercritical Flow



Fig. A-4 COMPUTER PROGRAM FOR SUPERCRITICAL FLOW

```

C
C THIS PROGRAM CALCULATES THE FLOW PROFILE AND THE CROSS WAVE
C PATTERNS FOR SPATIALLY VARIED SUPERCRITICAL FLOW IN A REC-
C TANGULAR EXPANSION. THE METHOD OF CHARACTERISTICS IS USED
C TO DETERMINE THE FLOW CONDITIONS AT EACH POINT IN THE FLOW
C REGIME. PLOTS ARE MADE OF THE CROSS WAVE PATTERNS; AND THE
C ANALYTICAL AND EXPERIMENTAL CENTERLINE PROFILES.
C
C THE INPUT CONSISTS OF THE FOLLOWING:
C
C   UO      THE INITIAL VELOCITY IN THE X-DIRECTION (FPS)
C   DO      THE INITIAL DEPTH AT POINT 0 (FT)
C   Q       THE MAIN CHANNEL FLOWRATE (CFS)
C   THETA   BOTTOM SLOPE OF THE CHANNEL
C   ALPHA   ANGLE OF THE SIDEWALL WITH THE CENTERLINE
C   B       WIDTH OF THE INITIAL CHANNEL (FT)
C   ACC     DESIRED ACCURACY FOR THE CALCULATION OF U(II)
C   DELYO   THE CHANGE IN Y-DISTANCE FROM POINT 0 TO POINT 1
C   QSTAR   LATERAL INFLOW (CFS/FT)
C   NP      THE NUMBER OF POINTS IN THE FIRST -C CURVE
C   XMAX    THE MAXIMUM LENGTH ALONG CENTERLINE FOR WHICH ANALYSIS
C           IS DESIRED
C   IDATA   THE NUMBER OF DATA SETS
C   NEXP    THE NUMBER OF EXPERIMENTAL POINTS
C
C THE MINIMUM VALUES ON THE PLOTS ARE DENOTED BY THE 'MIN' PREFIX
C AND THE SCALE FACTORS ARE DENOTED BY THE 'SC' PREFIX.
C
C NOTE: ALPHA AND THETA ARE GIVEN IN DEGREES
C
C001      DIMENSION DATA (1024)
C002      CALL PLOTS (IDATA,4096)
C003      CALL FACTER(0.7)
C004      REAL XPT(500),YPT(500),XPI(500),DPI(500),FXXP(100),FXDP(100),
C005      (MINXT,MINXP,MINDP,MINYT
C006      COMMON U(500),D(500),V(500),X(500),Y(500),I,NP,NPP,J,THETA,
C007      (ALPHA,UMM,UNP,VMM,VNP,UMM,CNP,DELUN,DELP,DELVN,DELP,DELXN,
C008      (DELP,DELYN,DELYP,DELX,DELYD,CRAV,DELU,UD,QSTAR,YD,XD,FNP,OI,UO
C009      READ (5,1000) IDATA
C010      READ(5,1010) MINXT,MINXP,MINDP,MINYT,SCXPT,SCXP,SCDP,SCYPT
C011      DO 380 ID=1,IDATA
C
C      INITIALIZING THE POSITION OF THE PLOTTER PEN
C
C009      CALL PLOT(5.0,-11.0,-3)
C010      CALL PLOT(5.0,3.25,-3)
C011      READ(5,1000) NEXP
C012      READ(5,1010)UO,DO,THETA,ALPHA,B,ACC,Q,QSTAR
C013      READ(5,1030)NP,XMAX,DELYO
C014      THETA=THETA*6.2832/360.0
C015      ALPHA=ALPHA*6.2832/360.0
C016      SLOPE=100.*TAN(THETA)
C
C      ACCUMULATION OF THE EXPERIMENTAL POINTS
C
C017      DO 10 II=1,NEXP
C018      10 READ(5,1060) EXXP(II),EXDP(II)

```

```

SUP 1
SUP 2
SUP 3
SUP 4
SUP 5
SUP 6
SUP 7
SUP 8
SUP 9
SUP 10
SUP 11
SUP 12
SUP 13
SUP 14
SUP 15
SUP 16
SUP 17
SUP 18
SUP 19
SUP 20
SUP 21
SUP 22
SUP 23
SUP 24
SUP 25
SUP 26
SUP 27
SUP 28
SUP 29
SUP 30
SUP 31
SUP 32
SUP 33
SUP 34
SUP 35
SUP 36
SUP 37
SUP 38
SUP 39
SUP 40
SUP 41
SUP 42
SUP 43
SUP 44
SUP 45
SUP 46
SUP 47
SUP 48
SUP 49
SUP 50
SUP 51
SUP 52
SUP 53
SUP 54
SUP 55
SUP 56
SUP 57
SUP 58

```

```

0019      NPP=NP+1
0020      GRAV=32.174
0021      YD=B/2.
0022      XD=0.0
0023      VU=0.0
0024      20 DELYD=DELYD+0.1*DELYD
0025      J=0
0026      DELY=- (YD+DELYD)/(NP-1)
C
C      THE FOLLOWING EQUATIONS ARE FOR A TYPE 1 ANALYSIS. THIS TYPE
C      OF ANALYSIS IS FOR THE FIRST NP POINTS (THE POINTS ALONG THE
C      FIRST -C CURVE).
C
0027      DO 40 I=1,NP
0028      V(I)=0.0
0029      UX=100.
0030      UMM=UC
0031      IF (I.NE.1) UMM=U(I-1)
0032      ENM=DU
0033      IF (I.NE.1) ENM=D(I-1)
0034      IF (I.NE.1) DELYD=DELY
0035      30 DELU=-UMM*TAN(THETA)*DELYD/DMM/SQRT(UMM**2/GRAV/DMM-1.)
0036      U(I)=UC+DELU
0037      IF (I.NE.1) U(I)=U(I-1)+DELU
0038      Y(I)=YD+DELYD
0039      IF (I.NE.1) Y(I)=Y(I-1)+DELY
0040      DELX=DELYD*(UMM*GRAV-(UMM**2))/DMM/GRAV/SQRT(UMM**2/GRAV/DMM-1.)
0041      X(I)=XD+DELX
0042      IF (I.NE.1) X(I)=X(I-1)+DELX
0043      IF (I.NE.1) DELXN=X(I)-X(I-1)
0044      IF (I.NE.1) DELYN=Y(I)-Y(I-1)
0045      CALL DEPTH
0046      IF (ABS(UX-U(I)).LE.ACC) GO TO 40
0047      UMM=(U(I)+UC)/2.0
0048      IF (I.NE.1) ENM=(U(I)+U(I-1))/2.
0049      DMM=(D(I)+DU)/2.0
0050      IF (I.NE.1) ENM=(U(I)+U(I-1))/2.
0051      UX=U(I)
0052      GO TO 30
0053      40 CONTINUE
0054      I=NP+1
0055      J=1
0056      50 CONTINUE
0057      JN=J*(NP+1)
0058      IF (I.EQ.JN) GO TO 90
0059      JNP=(J+1)*NP+J
0060      IF (I.EQ.JNP) GO TO 120
C
C      THESE EQUATIONS ARE FOR A REGION 4 ANALYSIS. THIS TYPE OF ANALYSIS
C      IS FOR THE POINTS IN THE INTERIOR REGION OF FLOW.
C
0061      60 UMM=U(I-1)
0062      UNP=U(I-NP)
0063      VMM=V(I-1)
0064      VNP=V(I-NP)
0065      ENM=D(I-1)
0066      ENP=D(I-NP)
0067      UX=100.

```

SUP 59  
 SUP 60  
 SUP 61  
 SUP 62  
 SUP 63  
 SUP 64  
 SUP 65  
 SUP 66  
 SUP 67  
 SUP 68  
 SUP 69  
 SUP 70  
 SUP 71  
 SUP 72  
 SUP 73  
 SUP 74  
 SUP 75  
 SUP 76  
 SUP 77  
 SUP 78  
 SUP 79  
 SUP 80  
 SUP 81  
 SUP 82  
 SUP 83  
 SUP 84  
 SUP 85  
 SUP 86  
 SUP 87  
 SUP 88  
 SUP 89  
 SUP 90  
 SUP 91  
 SUP 92  
 SUP 93  
 SUP 94  
 SUP 95  
 SUP 96  
 SUP 97  
 SUP 98  
 SUP 99  
 SUP 100  
 SUP 101  
 SUP 102  
 SUP 103  
 SUP 104  
 SUP 105  
 SUP 106  
 SUP 107  
 SUP 108  
 SUP 109  
 SUP 110  
 SUP 111  
 SUP 112  
 SUP 113  
 SUP 114  
 SUP 115  
 SUP 116

```

0066      70 FNP=SQRT((UNP**2+VNP**2)/GRAV/DNP)          SUP 117
0069      FMM=SQRT((UMM**2+VMM**2)/GRAV/DMM)          SUP 118
0070      GM=(-UMM*VMM+DMM*GRAV*SQRT(FMM**2-1.))/(DMM*GRAV-UMM**2) SUP 119
0071      GP=(-UNP*VNP+DNP*GRAV*SQRT(FNP**2-1.))/(DNP*GRAV-UNP**2) SUP 120
0072      X(I)=(GM*X(I-1)-GP*X(I-NP)-Y(I-1)+Y(I-NP))/(GM-GP) SUP 121
0073      Y(I)=GY*(X(I)-X(I-1))+Y(I-1)                SUP 122
0074      G1=U(I-NP)-U(I-1)                            SUP 123
0075      G2=V(I-NP)-V(I-1)                            SUP 124
0076      G4=(UMM*VMM+DMM*GRAV*SQRT(FMM**2-1.))/(DMM*VMM**2/GRAV) SUP 125
0077      G6=(DNP*SQRT(FNP**2-1.)+UNP*VNP/GRAV)/(DNP-VNP**2/GRAV) SUP 126
0078      G7=-UMM*TAN(THETA)*(Y(I)-Y(I-1))/(DMM-VMM**2/GRAV) SUP 127
0079      G8=-UNP*TAN(THETA)*(Y(I)-Y(I-NP))/(DNP-VNP**2/GRAV) SUP 128
0080      DELUP=(G8+G2-G7-G1*G4)/(G4-G6)                SUP 129
0081      DELUN=(G2-G7+G8-G6*G1)/(G4-G6)                SUP 130
0082      DELVP=G8+DELUP*G6                            SUP 131
0083      DELVN=G7+G4*DELUN                             SUP 132
0084      U1=U(I-NP)+DELUP                             SUP 133
0085      U2=U(I-1)+DELUN                             SUP 134
0086      V1=V(I-NP)+DELVP                             SUP 135
0087      V2=V(I-1)+DELVN                             SUP 136
0088      U(I)=(U1+U2)/2.0                             SUP 137
0089      V(I)=(V1+V2)/2.0                             SUP 138
0090      DELXP=X(I)-X(I-NP)                             SUP 139
0091      DELXN=X(I)-X(I-1)                             SUP 140
0092      DELYP=Y(I)-Y(I-NP)                             SUP 141
0093      DELYN=Y(I)-Y(I-1)                             SUP 142
0094      CALL CEPTH                                     SUP 143
0095      IF(ABS(UX-U(I)).LE.ACC) GO TO 80              SUP 144
0096      UX=U(I)                                         SUP 145
0097      UMM=(U(I-1)+U(I))/2.                          SUP 146
0098      UNP=(U(I-NP)+U(I))/2.                          SUP 147
0099      VMM=(V(I-1)+V(I))/2.0                          SUP 148
0100      VNP=(V(I-NP)+V(I))/2.0                          SUP 149
0101      DMM=(U(I-1)+D(I))/2.0                          SUP 150
0102      DNP=(U(I-NP)+D(I))/2.0                          SUP 151
0103      GO TO 70                                       SUP 152
0104      80 I=I+1                                       SUP 153
0105      GO TO 50                                       SUP 154
C                                               SUP 155
C THE FOLLOWING EQUATIONS ARE FOR A REGION 2 ANALYSIS. THIS TYPE OF SUP 156
C ANALYSIS IS FOR THE POINTS ALONG THE SIDEWALL. THE NUMBER FOR SUP 157
C THESE POINTS CORRESPONDS TO THE EQUATION: I=J*(NP+1), WHERE J SUP 158
C IS THE NUMBER OF THE -C CURVE IN WHICH THIS POINT IS FOUND. SUP 159
C                                               SUP 160
0106      90 UNP=U(I-NP)                                SUP 161
0107      VNP=V(I-NP)                                SUP 162
0108      DNP=D(I-NP)                                SUP 163
0109      UX=100.                                       SUP 164
0110      100 FNP=SQRT((UNP**2+VNP**2)/GRAV/DNP)        SUP 165
0111      CALL UYDX                                     SUP 166
0112      IF(DELX.EQ.1000.) GO TO 370                  SUP 167
0113      DELXP=X(I)-X(I-NP)                            SUP 168
0114      DELYP=Y(I)-Y(I-NP)                            SUP 169
0115      C2=CSTAR*ABS(X(I)-X(I-NP))/COS(ALPHA)          SUP 170
0116      PHIN=(U1+U2)/ABS(DELXP)/ABS(DELYP)-UNP*TAN(THETA)+(UNP**2+VNP SUP 171
      (**2)*2/DNP/GRAV/ABS(DELXP)/ABS(DELYP)          SUP 172
0117      UTOP=PHIN*DELYP-(DNP-VNP**2/GRAV)*(U(I-NP)*TAN(ALPHA)-V(I-NP)) SUP 173
0118      USBT=LELYP*(DNP-UNP**2/GRAV-U1*UNP/2./DNP/GRAV/ABS(DELXP))/ SUP 174

```

```

0119      (DELXP+TAN(ALPHA))*(DNP-VNP**2/GRAV) SUP 175
0120      CELU=UTOP/UBOT SUP 176
0121      DELV=(U(I-NP)+DELU)*TAN(ALPHA)-V(I-NP) SUP 177
0122      U(I)=U(I-NP)+DELU SUP 178
0123      V(I)=V(I-NP)+DELV SUP 179
0124      DLUU=U(I)-U(I-NP) SUP 180
0125      DELVP=V(I)-V(I-NP) SUP 181
0126      CALL DEPTH SUP 182
0127      IF (ABS(U(I)-UX).LE.ACC) GO TO 110 SUP 183
0128      UX=U(I) SUP 184
0129      UNP=(U(I)+U(I-NP))/2.0 SUP 185
0130      VNP=(V(I)+V(I-NP))/2.0 SUP 186
0131      DNP=(D(I)+D(I-NP))/2.0 SUP 187
0132      GO TO 100 SUP 188
0133      110 IF (X(I).GT.XMAX) GO TO 160 SUP 189
0134      I=I+1 SUP 190
0135      GOTO 50 SUP 191
C SUP 192
C THE FOLLOWING EQUATIONS ARE FOR A REGION 3 ANALYSIS. THIS TYPE OF SUP 193
C ANALYSIS IS FOR THE POINTS ALONG THE CENTERLINE OF FLOW. THE SUP 194
C NUMBERS FOR THESE POINTS CORRESPOND TO THE EQUATION: SUP 195
C      I=(J+1)*NP+J SUP 196
C SUP 197
0136      120 VMM=V(I-1) SUP 198
0137      UMM=U(I-1) SUP 199
0138      DMM=D(I-1) SUP 200
0139      V(I)=0.0000 SUP 201
0140      Y(I)=0.0000 SUP 202
0141      UX=10. SUP 203
0142      130 UTOP=-V(I-1)*(DMM-VMM**2/GRAV)-Y(I-1)*UMM*TAN(THETA) SUP 204
0143      FMM=SQRT((UMM**2+VMM**2)/GRAV/DMM) SUP 205
0144      UBOT=UMM*VMM/GRAV-DMM*SQRT(FMM**2-1.) SUP 206
0145      DLUU=(-Y(I-1))*DMM*GRAV-UMM**2/(-UMM*VMM+DMM*GRAV*SQRT(FMM SUP 207
0146      (**2-1.)) SUP 208
0147      V(I)=X(I-1)+DLUX SUP 209
0148      U(I)=U(I-1)+UTOP/UBOT SUP 210
0149      DLUU=U(I)-U(I-1) SUP 211
0150      DELVN=V(I)-V(I-1) SUP 212
0151      DLUU=X(I)-X(I-1) SUP 213
0152      DLUU=Y(I)-Y(I-1) SUP 214
0153      CALL DEPTH SUP 215
0154      IF (ABS(UX-U(I)).LE.ACC) GO TO 140 SUP 216
0155      VMM=(V(I)+V(I-1))/2.0 SUP 217
0156      UMM=(U(I)+U(I-1))/2.0 SUP 218
0157      DMM=(D(I)+D(I-1))/2.0 SUP 219
0158      UX=U(I) SUP 220
0159      GOTO 130 SUP 221
0160      140 JNPP=2*NP+1 SUP 222
0161      IF (I.NE.JNPP) GO TO 150 SUP 223
0162      IF ((X(JNPP)-X(NP)).GT.0.03) GO TO 150 SUP 224
0163      GO TO 20 SUP 225
0164      150 J=J+1 SUP 226
0165      I=I+1 SUP 227
0166      GOTO 50 SUP 228
0167      160 NR=I SUP 229
0168      I=0 SUP 230
0169      QSTAR=2.*QSTAR SUP 231
0170      WRITE(10,1040) Q,QSTAR,SLOPE SUP 232

```

```

0169      WRITE(6,1050)
0170      WRITE(6,1070)I,X0,Y0,U0,V0,D0
0171      DO 170 I=1,NR
0172      170 WRITE(6,1070)I,X(I),Y(I),U(I),V(I),D(I)
0173      XP(1)=X0
0174      YPT(1)=Y0
0175      DP(1)=D0
0176      YPT(1)=Y0
0177      NRR=NR
0178      DO 180 I=1,NRR
0179      XP(I+1)=X(I)
0180      YPT(I+1)=Y(I)
0181      DO 190 I=1,J
0182      XP(I+1)=X(I)*NPP-1)
0183      DP(I+1)=D(I)*NPP-1)
0184      K=J+1
0185      KK=NR+1
0186      XPT(KK+1)=MINXT
0187      XP(K+1)=MINXP
0188      DP(K+1)=MINDP
0189      YPT(KK+1)=MINYT
0190      EXXP(NEXP+1)=MINXP
0191      EXDP(NEXP+1)=MINDP
0192      XPT(KK+2)=SCXPT
0193      XP(K+2)=SCXP
0194      DP(K+2)=SCDP
0195      YPT(KK+2)=SCYPT
0196      EXXP(NEXP+2)=SCXP
0197      EXDP(NEXP+2)=SCDP
C
C      SCALING OF THE VARIABLES TO BE PLOTTED
C
0198      DO 200 I=1,NEXP
0199      EXXP(I)=(EXXP(I)-EXXP(NEXP+1))/EXXP(NEXP+2)
0200      EXDP(I)=(EXDP(I)-EXDP(NEXP+1))/EXDP(NEXP+2)
0201      DO 210 I=1,K
0202      XP(I)=(XP(I)-XP(K+1))/XP(K+2)
0203      DP(I)=(DP(I)-DP(K+1))/DP(K+2)
0204      DO 220 I=1,KK
0205      XPT(I)=(XPT(I)-XPT(KK+1))/XPT(KK+2)
0206      YPT(I)=(YPT(I)-YPT(KK+1))/YPT(KK+2)
C
C      LOCATING AND LABELING OF THE AXES
C
0207      CALL AXIS (0.0,0.0,0.0,'DOWNSTREAM DISTANCE (FT)',-24.6,0.0,0.0,
0208      (XP(K+1),XP(K+2))
0209      CALL AXIS (0.0,0.0,0.0,'DEPTH (FT)',10.3,.90,DP(K+1),DP(K+2))
0210      CALL AXIS (0.0,5.0,0.0,'X',-1.6,0.0,0.0,XPT(KK+1),XPT(KK+2))
0211      CALL AXIS (0.0,5.0,0.0,'Y',1.3,0.90,YPT(KK+1),YPT(KK+2))
0212      CALL PLOT (-1.0,5.0,0.3)
0213      CALL PLOT (6.0,5.0,2)
0214      CALL PLOT (6.0,7.0,3)
0215      CALL PLOT (0.0,6.0,2)
0216      CALL PLOT (-1.0,6.0,2)
C
C      SUBROUTINE SMOOTH IS USED FOR THE ANALYTICAL RESULTS
C

```

SUP 233  
 SUP 234  
 SUP 235  
 SUP 236  
 SUP 237  
 SUP 238  
 SUP 239  
 SUP 240  
 SUP 241  
 SUP 242  
 SUP 243  
 SUP 244  
 SUP 245  
 SUP 246  
 SUP 247  
 SUP 248  
 SUP 249  
 SUP 250  
 SUP 251  
 SUP 252  
 SUP 253  
 SUP 254  
 SUP 255  
 SUP 256  
 SUP 257  
 SUP 258  
 SUP 259  
 SUP 260  
 SUP 261  
 SUP 262  
 SUP 263  
 SUP 264  
 SUP 265  
 SUP 266  
 SUP 267  
 SUP 268  
 SUP 269  
 SUP 270  
 SUP 271  
 SUP 272  
 SUP 273  
 SUP 274  
 SUP 275  
 SUP 276  
 SUP 277  
 SUP 278  
 SUP 279  
 SUP 280  
 SUP 281  
 SUP 282  
 SUP 283  
 SUP 284  
 SUP 285  
 SUP 286  
 SUP 287  
 SUP 288  
 SUP 289  
 SUP 290

```

C      PLOTS DEPTH VERSUS DOWNSTREAM DISTANCE
C
0216      CALL SMOOTH(XP(1),DP(1),0)
0217      DO 230 I=2,J
0218      230 CALL SMOOTH(XP(I),DP(I),-2)
0219      I=J+1
0220      CALL SMOOTH(XP(1),DP(1),-999)
0221      CALL SYMBOL(4.0,3.0,0.11,'_ ANALYTICAL',0.0,12)
0222      CALL SYMBOL(4.0,2.75,-.157,' EXPERIMENTAL ',0.0,15)
0223      CALL PLOT(0.0,0.0,-3)
C
C      SUBROUTINE SYMBOL IS USED FOR THE EXPERIMENTAL RESULTS
C
0224      DO 240 I=1,NEXP
0225      240 CALL SYMBOL(EXXP(I),EXDP(I),0.06,1,0.0,-1)
C
C      PLOTS FIRST -C CURVE
C
0226      CALL PLOT(0.0,5.0,-3)
0227      CALL SMOOTH(XPT(1),YPT(1),0)
0228      DO 250 I=2,NP
0229      250 CALL SMOOTH(XPT(I),YPT(I),-2)
0230      I=NP+1
0231      CALL SMOOTH(XPT(1),YPT(1),-999)
C
C      PLOTS SECOND -C CURVE
C
0232      I=NP+2
0233      CALL SMOOTH(XPT(I),YPT(I),0)
0234      II=NP+3
0235      III=2*NP+1
0236      DO 260 I=1,III
0237      260 CALL SMOOTH(XPT(I),YPT(I),-2)
0238      I=2*NP+2
0239      CALL SMOOTH(XPT(1),YPT(1),-999)
C
C      PLOTS FIRST +C CURVE
C
0240      I=NP+1
0241      IF(XPT(1).GT.XMAX) GO TO 370
0242      CALL SMOOTH(XPT(1),YPT(1),0)
0243      II=2*NP+1
0244      III=NP*(NP+1)-NP+1
0245      DO 270 I=1,III,NP
0246      IF(I.GT.NP) GO TO 370
0247      270 CALL SMOOTH(XPT(I),YPT(I),-2)
0248      I=NP*(NP+1)+1
0249      IF(I.GT.NP) GO TO 370
0250      CALL SMOOTH(XPT(1),YPT(1),-999)
C
C      PLOTS SECOND +C CURVE
C
0251      I=2*NP+2
0252      IF(XPT(1).GT.XMAX) GO TO 370
0253      CALL SMOOTH(XPT(1),YPT(1),0)
0254      II=3*NP+2
0255      III=(NP+1)**2+1-NP
0256      DO 280 I=1,III,NP

```

SUP 291  
 SUP 292  
 SUP 293  
 SUP 294  
 SUP 295  
 SUP 296  
 SUP 297  
 SUP 298  
 SUP 299  
 SUP 300  
 SUP 301  
 SUP 302  
 SUP 303  
 SUP 304  
 SUP 305  
 SUP 306  
 SUP 307  
 SUP 308  
 SUP 309  
 SUP 310  
 SUP 311  
 SUP 312  
 SUP 313  
 SUP 314  
 SUP 315  
 SUP 316  
 SUP 317  
 SUP 318  
 SUP 319  
 SUP 320  
 SUP 321  
 SUP 322  
 SUP 323  
 SUP 324  
 SUP 325  
 SUP 326  
 SUP 327  
 SUP 328  
 SUP 329  
 SUP 330  
 SUP 331  
 SUP 332  
 SUP 333  
 SUP 334  
 SUP 335  
 SUP 336  
 SUP 337  
 SUP 338  
 SUP 339  
 SUP 340  
 SUP 341  
 SUP 342  
 SUP 343  
 SUP 344  
 SUP 345  
 SUP 346  
 SUP 347  
 SUP 348

0257	IF(I.GT.NR) GO TO 370		
0258	280 CALL SMOOTH(XPT(I),YPT(I),-2)	SUP	349
0259	I=(NP+1)**2+1	SUP	350
0260	IF(I.GT.NR) GO TO 370	SUP	351
0261	CALL SMOOTH(XPT(I),YPT(I),-999)	SUP	352
	C	SUP	353
	C	SUP	354
	C	SUP	355
	PLOTS THIRD -C CURVE	SUP	356
0262	I=NP*(NP+1)+1	SUP	357
0263	IF(XPT(I).GT.XMAX) GO TO 370	SUP	358
0264	CALL SMOOTH(XPT(I),YPT(I),0)	SUP	359
0265	II=NP*(NP+1)+2	SUP	360
0266	III=(NP+1)*NP+NP	SUP	361
0267	DO 290 I=II,III	SUP	362
0268	IF(I.GT.NR) GO TO 370	SUP	363
0269	290 CALL SMOOTH(XPT(I),YPT(I),-2)	SUP	364
0270	I=(NP+1)*NP+NP+1	SUP	365
0271	IF(I.GT.NR) GO TO 370	SUP	366
0272	CALL SMOOTH(XPT(I),YPT(I),-999)	SUP	367
	C	SUP	368
	C	SUP	369
	C	SUP	370
0273	I=(NP+1)**2+1	SUP	371
0274	IF(XPT(I).GT.XMAX) GO TO 370	SUP	372
0275	CALL SMOOTH(XPT(I),YPT(I),0)	SUP	373
0276	II=(NP+1)**2+2	SUP	374
0277	III=(NP+2)*NP+NP+1	SUP	375
0278	DO 300 I=II,III	SUP	376
0279	IF(I.GT.NR) GO TO 370	SUP	377
0280	300 CALL SMOOTH(XPT(I),YPT(I),-2)	SUP	378
0281	I=(NP+2)*NP+NP+2	SUP	379
0282	IF(I.GT.NR) GO TO 370	SUP	380
0283	CALL SMOOTH(XPT(I),YPT(I),-999)	SUP	381
	C	SUP	382
	C	SUP	383
	C	SUP	384
0284	I=(NP+2)*NP+1	SUP	385
0285	IF(XPT(I).GT.XMAX) GO TO 370	SUP	386
0286	CALL SMOOTH(XPT(I),YPT(I),0)	SUP	387
0287	II=(NP+2)*NP+NP+1	SUP	388
0288	III=NP*2*NP+NP+1	SUP	389
0289	DO 310 I=II,III,NP	SUP	390
0290	IF(I.GT.NR) GO TO 370	SUP	391
0291	310 CALL SMOOTH(XPT(I),YPT(I),-2)	SUP	392
0292	I=NP*2*NP+1	SUP	393
0293	IF(I.GT.NR) GO TO 370	SUP	394
0294	CALL SMOOTH(XPT(I),YPT(I),-999)	SUP	395
	C	SUP	396
	C	SUP	397
	C	SUP	398
0295	I=(NP+3)*NP+2	SUP	399
0296	IF(XPT(I).GT.XMAX) GO TO 370	SUP	400
0297	CALL SMOOTH(XPT(I),YPT(I),0)	SUP	401
0298	II=(NP+3)*NP+NP+2	SUP	402
0299	III=(NP+1)*(2*NP+1)+NP+1	SUP	403
0300	DO 320 I=II,III,NP	SUP	404
0301	IF(I.GT.NR) GO TO 370	SUP	405
0302	320 CALL SMOOTH(XPT(I),YPT(I),-2)	SUP	406



0303	I=(NP+1)*(2*NP+1)+1	SUP	407
0304	IF(I.GT.NR) GO TO 370	SUP	408
0305	CALL SMOOTH(XPT(I),YPT(I),-999)	SUP	409
	C	SUP	410
	C	SUP	411
	C	SUP	412
0306	I=2*NP*(NP+1)+1	SUP	413
0307	IF(XPT(I).GT.XMAX) GO TO 370	SUP	414
0308	CALL SMOOTH(XPT(I),YPT(I),0)	SUP	415
0309	II=2*NP*(NP+1)+2	SUP	416
0310	III=(2*NP+3)*NP	SUP	417
0311	DO 330 I=II,III	SUP	418
0312	IF(I.GT.NR) GO TO 370	SUP	419
0313	330 CALL SMOOTH(XPT(I),YPT(I),-2)	SUP	420
0314	I=(2*NP+3)*NP+1	SUP	421
0315	IF(I.GT.NR) GO TO 370	SUP	422
0316	CALL SMOOTH(XPT(I),YPT(I),-999)	SUP	423
	C	SUP	424
	C	SUP	425
	C	SUP	426
0317	I=(2*NP+1)*(NP+1)+1	SUP	427
0318	IF(XPT(I).GT.XMAX) GO TO 370	SUP	428
0319	CALL SMOOTH(XPT(I),YPT(I),0)	SUP	429
0320	II=(2*NP+1)*(NP+1)+2	SUP	430
0321	III=2*(NP+2)*NP+1	SUP	431
0322	DO 340 I=II,III	SUP	432
0323	IF(I.GT.NR) GO TO 370	SUP	433
0324	340 CALL SMOOTH(XPT(I),YPT(I),-2)	SUP	434
0325	I=2*(NP+2)*NP+2	SUP	435
0326	IF(I.GT.NR) GO TO 370	SUP	436
0327	CALL SMOOTH(XPT(I),YPT(I),-999)	SUP	437
	C	SUP	438
	C	SUP	439
	C	SUP	440
0328	I=(2*NP+3)*NP+1	SUP	441
0329	IF(XPT(I).GT.XMAX) GO TO 370	SUP	442
0330	CALL SMOOTH(XPT(I),YPT(I),0)	SUP	443
0331	II=(2*NP+3)*NP+NP+1	SUP	444
0332	III=(2*NP+3)*NP+1+(NP-1)*NP	SUP	445
0333	DO 350 I=II,III,NP	SUP	446
0334	IF(I.GT.NR) GO TO 370	SUP	447
0335	350 CALL SMOOTH(XPT(I),YPT(I),-2)	SUP	448
0336	I=(2*NP+3)*NP+1+(NP-1)*NP	SUP	449
0337	IF(I.GT.NR) GO TO 370	SUP	450
0338	CALL SMOOTH(XPT(I),YPT(I),-999)	SUP	451
	C	SUP	452
	C	SUP	453
	C	SUP	454
0339	I=2*(NP+2)*NP+2	SUP	455
0340	IF(XPT(I).GT.XMAX) GO TO 370	SUP	456
0341	CALL SMOOTH(XPT(I),YPT(I),0)	SUP	457
0342	II=2*(NP+2)*NP+NP+2	SUP	458
0343	III=2*(NP+2)*NP+2+(NP-1)*NP	SUP	459
0344	DO 360 I=II,III,NP	SUP	460
0345	IF(I.GT.NR) GO TO 370	SUP	461
0346	360 CALL SMOOTH(XPT(I),YPT(I),-2)	SUP	462
0347	I=2*(NP+2)*NP+(NP-1)*NP+NP+2	SUP	463
0348	IF(I.GT.NR) GO TO 370	SUP	464

0349	CALL SMOOTH(XPT(I),YPT(I),-999)	SUP	465
	C	SUP	466
	C        SHIFTS PLOTTER PEN FOR ANOTHER SET OF DATA	SUP	467
	C	SUP	468
0350	370 CONTINUE	SUP	469
0351	CALL PLOT (20.0,0.0,-3)	SUP	470
0352	380 CONTINUE	SUP	471
0353	CALL PLOT (0.0,0.0,999)	SUP	472
0354	1000 FORMAT(15)	SUP	473
0355	1010 FORMAT(UP,4)	SUP	474
0356	1020 FORMAT(8F10.5)	SUP	475
0357	1030 FORMAT(15,2F10.5)	SUP	476
0358	1040 FORMAT('1',//////////,22X,'MAIN CHANNEL FLOWRATE:',F7.4,	SUP	477
	(' CFS',5X,'LATERAL INFLOW:',F8.5,' CFS/FT',4X,'SLOPE:',F5.2,	SUP	478
	(' (1/1)	SUP	479
0359	1050 FORMAT(' ',25X,'POINT',5X,'DOWNSTREAM',6X,'TRANSVERSE',12X,	SUP	480
	('VELOCITY (FPS)',4X,'DEPTH',36X,'DISTANCE (FT)',3X,'DISTANCE (FT)	SUP	481
	(' ',4X,'X-DIRECTION',2X,'Y-DIRECTION',5X,'(FT)')	SUP	482
0360	1060 FORMAT(2F10.5)	SUP	483
0361	1070 FORMAT(' ',23X,15,5X,F6.3,10X,F6.3,10X,F7.4,7X,F7.4,5X,F7.4)	SUP	484
0362	RETURN	SUP	485
0363	END	SUP	486

0001	SUBROUTINE DEPTH	DPH	1
0002	COMMON U(500),D(500),V(500),X(500),Y(500),I,NP,NPP,J,THETA,	DPH	2
	(ALPHA,UMM,UNP,VMM,VNP,DMN,ENP,DELUN,DELUP,DELYN,DELYP,DELXN,	DPH	3
	DELXP,DELYN,DELYP,DELX,DELYO,GRAV,DELU,DU,QSTAR,YO,XO,FNP,Q1,UG	DPH	4
0003	II=(J+1)*NP+J	DPH	5
0004	IF(I.NE.II) GO TO 30	DPH	6
0005	10 G11=ATAN(ABS(V(I-1))/ABS(U(I-1)))	DPH	7
0006	G21=ATAN(ABS(DELYN)/ABS(DELYN))	DPH	8
0007	G1=ATAN(ABS(V(I))/ABS(U(I)))	DPH	9
0008	G2=G21	DPH	10
0009	U=G21+G11	DPH	11
0010	IF(V(I-1).LT.0.0) U=G21-G11	DPH	12
0011	P=G2+G1	DPH	13
0012	IF(V(I).LT.0.0) P=G2-G1	DPH	14
0013	VP1=SQRT(U(I-1)**2+V(I-1)**2)*COS(C)	DPH	15
0014	VP=SQRT(U(I)**2+V(I)**2)*COS(P)	DPH	16
0015	B=2.*VP**2/GRAV-TAN(THETA)*COS(G21)*SQRT(DELYN**2+DELYN**2)	DPH	17
0016	C=(-2.*VP1**2/GRAV-TAN(THETA)*COS(G21)*SQRT(DELYN**2+DELYN**2)	DPH	18
	(**2)-B*(1-1))*U(I-1)	DPH	19
0017	GO TO 40	DPH	20
0018	20 G21=ATAN(ABS(DELYO)/ABS(DELYN))	DPH	21
0019	VP1=U(COS(G21))	DPH	22
0020	G2=G21	DPH	23
0021	VP=U(I)*COS(G2)	DPH	24
0022	B=2.*VP**2/GRAV-TAN(THETA)*COS(G2)*SQRT(DELYN**2+DELYO**2)	DPH	25
0023	C=(-2.*VP1**2/GRAV-TAN(THETA)*COS(G2)*SQRT(DELYN**2+DELYO**2)	DPH	26
	(-C)*U	DPH	27
0024	GO TO 40	DPH	28
0025	30 IF(I.GE.1) GO TO 20	DPH	29
0026	IF(I.LE.NP) GO TO 10	DPH	30
0027	G15=ATAN(ABS(V(I-NP))/ABS(U(I-NP)))	DPH	31
0028	G25=ATAN(ABS(DELYP)/ABS(DELYN))	DPH	32
0029	G1=ATAN(ABS(V(I))/ABS(U(I)))	DPH	33
0030	G2=G25	DPH	34
0031	C=G25-G15	DPH	35
0032	IF(V(I-NP).LT.0.0) U=G25+G15	DPH	36
0033	P=G2-G1	DPH	37
0034	IF(V(I).LT.0.0) P=G1+G2	DPH	38
0035	VP5=SQRT(U(I-NP)**2+V(I-NP)**2)*COS(P)	DPH	39
0036	VP=SQRT(U(I)**2+V(I)**2)*COS(P)	DPH	40
0037	B=2.*VP**2/GRAV-TAN(THETA)*COS(G2)*SQRT(DELYN**2+DELYP**2)	DPH	41
0038	C=(-2.*VP5**2/GRAV-TAN(THETA)*COS(G2)*SQRT(DELYN**2+DELYP**2)	DPH	42
	(-B*(1-NP))*U(I-NP)	DPH	43
0039	40 U(I)=(-B+SQRT(B**2-4.*C))/2.	DPH	44
0040	RETURN	DPH	45
0041	END	DPH	46

```

0001      SUBROUTINE DYDX
0002      COMMON U(500),D(500),V(500),X(500),Y(500),I,NP,NPP,J,THETA,
      (ALPHA,UMM,UNP,VMM,VNP,DMM,DNP,DELUN,DELUP,DELVN,DELVP,DELXN,
      DELXP,DELYN,DELYP,DELX,DELY,GRAV,DELU,DD,QSTAR,YO,XO,FNP,Q1,UD
0003      IF(I.EQ.NPP) GO TO 10
0004      Q1=QSTAR*ABS(X(I-NP)-X(I-NPP))/COS(ALPHA)
0005      GO TO 20
0006      10 Q1=QSTAR*ABS(X(I-NP)-XO)/COS(ALPHA)
0007      20 CONTINUE
0008      ZZ=Q1*Q1*VNP**2/10./LNP**4/GRAV**2/(Y**2+Q1*UNP/2./DNP**2/GRAV/DY
0009      Z=(Y(I-NP)-YO)/TAN(ALPHA)-X(I-NP)
0010      AAAA=-UNP*VNP*Z-GRAV*DNP*Z*SQRT(FNP**2.-1.+ZZ)+Q1*VNP/4./DNP/TAN(
      (ALPHA)
0011      BBBB=.1*VNP*Z/4./DNP
0012      CCCC=-UNP*VNP/TAN(ALPHA)-GRAV*DNP/TAN(ALPHA)*SQRT(FNP**2.-1.+ZZ)
0013      DDDD=LNP*(KAV-UNP*UNP)
0014      EEEE=-Q1*UNP/2./DNP
0015      BAC=(AAAA-EEEE)**2.+BBBB*(DDDD-CCCC)
0016      IF (BAC.LT.0.0) GO TO 30
0017      DY=(AAAA-EEEE+SQRT(BAC))/2./{DDDD-CCCC}
0018      GO TO 40
0019      30 DELX=100.
0020      WRITE(6,1000)
0021      1000 FORMAT(' ',////21X,'DELTA Y FAILS TO CONVERGE; THE CHARACTERISTIC
      ( METHOD CAN NOT BE APPLIED TO THIS SET OF DATA')
0022      40 Y(I)=Y(I-NP)+DY
0023      X(I)=(Y(I)-YO)/TAN(ALPHA)
0024      RETURN
0025      END
      DYDX 1
      DYDX 2
      DYDX 3
      DYDX 4
      DYDX 5
      DYDX 6
      DYDX 7
      DYDX 8
      DYDX 9
      DYDX 10
      DYDX 11
      DYDX 12
      DYDX 13
      DYDX 14
      DYDX 15
      DYDX 16
      DYDX 17
      DYDX 18
      DYDX 19
      DYDX 20
      DYDX 21
      DYDX 22
      DYDX 23
      DYDX 24
      DYDX 25
      DYDX 26
      DYDX 27
      DYDX 28
      DYDX 29

```



